

ANALYSIS OF VISIBILITY/AEROSOL RELATIONSHIPS AND
VISIBILITY MODELING/MONITORING ALTERNATIVES FOR CALIFORNIA

FINAL REPORT

February 1982

LIBRARY
CALIFORNIA AIR RESOURCES BOARD
P.O. BOX 2815
SACRAMENTO, CA 95812

by

John Trijonis et al.
Santa Fe Research Corporation
Santa Fe, New Mexico

Glen Cass and Gregory McRae
Consultants
Pasadena, California

Yuji Horie, Wei-Yue Lim, and Nancy Chang
Technology Service Corporation
Santa Monica, California

Thomas Cahill
University of California
Davis, California

Submitted to: California Air Resources Board
P.O. Box 2815
Sacramento, California 95812

Mr. Charles Unger, Project Officer

Contract Number A9-103-31

The statements and conclusions in this report are those of the Contractor and not necessarily those of the State Air Resources Board. The mention of commercial products, their source or their use in connection with material reported herein is not to be construed as actual or implied endorsement of such products.

ABSTRACT

This report investigates visibility/aerosol relationships in California and provides guidance for future visibility modeling and monitoring. The study includes a review of available visibility modeling methods, a statistical analysis of visibility/aerosol relationships, an approximate characterization of haze budgets, and a recommended strategy for future visibility monitoring.

The review of visibility models considers two basic modeling approaches: deterministic (source-oriented) models and empirical (receptor-oriented) models. Three deterministic dispersion models are currently available for characterizing plume blight from isolated point sources, but the development of reliable dispersion models for regional haze is problematical. Deterministic visibility models generally suffer from the lack of sufficiently detailed field data for validating and implementing the models. Several empirical visibility models, with a wide range of complexity, are currently available. The most complex of these empirical models -- those employing short-term, chemically-resolved, size-segregated aerosol data with information on aerosol humidification and light absorption -- fit observed visibilities very well, make physical sense, and help to identify the sources of visibility degradation.

Statistical analyses relating airport visibility data to Hi-Vol particulate data and relative humidity are conducted at 34 California locations. Some of the Hi-Vol variables -- benzene soluble organics, Pb (motor vehicle tracer), Hi (fuel oil tracer), and Si or Mn (soil dust tracers) -- generally lack consistent statistically significant relationships with light extinction. Good correlations (.65 to .90), however, are obtained in relating atmospheric light extinction to sulfates, nitrates, remainder of TSP, and relative humidity, especially if the regression models treat relative humidity in a physically reasonable way. In agreement with theoretical considerations and other empirical results, it is found that the extinction efficiencies for secondary aerosols (especially sulfates) are in order of magnitude greater than the extinction efficiencies for the remainder of TSP. The extinction efficiencies of sulfates and nitrates in California exhibit interesting geographical features that appear to be explainable in terms of physical aerosol properties, e.g. in terms of geographical variations in the size distribution of sulfates.

Haze budgets for the 34 study sites indicate that natural blue-sky scatter by air molecules contributes only 5% of total extinction in the haziest parts of California but up to 40% in the clearest areas of California. As a fraction of total extinction, absorption by NO_2 generally contributes a rather uniform 7-11% throughout California. Sulfates apparently account for 40-70% of total extinction in the Los Angeles and San Diego areas and about 15-35% in the remainder of California. Nitrate contributions cannot currently be adequately assessed, but the available data suggest that nitrates are more important on a percentage basis in the northern half of California where they may contribute 10-40% of total extinction. The

contribution from other (non-sulfate, non-nitrate) aerosols varies widely among locations, from 10 to 70%. The most significant component of the other aerosol category is expected to be soot (elemental carbon).

There is a potential need for two distinct types of visibility-related monitoring in California. The first type concerns a statewide network of telephotometers, nephelometers, and/or absorption monitors to collect precise instrumental data on visibility for quantifying existing conditions, spatial/temporal patterns, and future trends. The second type involves special field studies using nephelometers and dichotomous samplers to collect detailed particulate data for one year at various locations. An appropriate statistical analysis of the data from the field studies would yield very detailed and useful extinction budgets.

TABLE OF CONTENTS

1.	INTRODUCTION AND SUMMARY.	1
	1.1 Basic Concepts and Definitions	3
	1.2 Summary.	8
	1.3 References for Chapter 1	16
2.	REVIEW OF VISIBILITY AIR QUALITY MODELS	17
	2.1 Elements of the Visibility Modeling Problem.	17
	2.2 Quantifying Visibility Impairment and the Koschmieder Formula.	19
	2.3 Atmospheric Optics	22
	2.4 Modeling the Processes Responsible for Visibility Impairment	28
	2.5 Empirical Visibility Models.	34
	2.6 Empirical Extinction Model Applications.	37
	2.7 Conclusions.	54
	2.8 References for Chapter 2	56
3.	VISIBILITY/AEROSOL RELATIONSHIPS BASED ON HI-VOL DATA	61
	3.1 Description of the Data Base	61
	3.2 Statistical Modeling Approach.	66
	3.3 Data Overview.	76
	3.4 Regression Relations	78
	3.5 References for Chapter 3	98
4.	EXTINCTION BUDGETS.	103
	4.1 Extinction by Gases.	103
	4.2 Extinction Budgets	105
	4.3 References for Chapter 4	109
5.	FUTURE VISIBILITY MONITORING.	111
	5.1 Visibility Monitoring Network.	111
	5.2 Extinction Budget Field Projects	116
	5.3 References for Chapter 5	120
	APPENDIX A.	A-1
	APPENDIX B.	B-1

1. INTRODUCTION AND SUMMARY

One of the most readily apparent effects of air pollution, visibility degradation, is receiving increased attention from researchers because it may be closely related to some of the most damaging effects of air pollution. Two obvious types of damage associated with visibility impairment are aesthetic/psychological costs and hindrance of aviation. There has also been speculation, partly supported by theory and data relevant to the Northeast United States, that haze levels may play a significant role in climate modification. Also, because visibility is closely related to atmospheric sulfate and nitrate concentrations, haze is linked with other sulfate and nitrate problems, such as acid rain and, possibly, health effects.

Visibility degradation is an especially important air quality issue in California where mountain ranges frequently offer exceptional panoramas. Concern is often expressed over the intense haze that can be found in the Los Angeles basin, San Joaquin Valley, and other areas of dense emissions. It is also a common public opinion that visibility levels have deteriorated in some of the more remote areas of California and there is apprehension that future growth and development will lead to further visibility degradation.

The concerns over visibility degradation, both nationwide and in California, are reflected in the 1977 Clean Air Act Amendments wherein Congress established as a national goal "the prevention of any future and the remedying of any existing impairment of visibility in mandatory Class I Federal areas, which impairment results from manmade pollution". The Environmental Protection Agency (EPA) has recently developed regulations for the first phase of a national visibility program (Federal Register 1980). As mandated by Congress, EPA's regulations require State Implementation Plans to include best available controls for both new and existing major sources that impair visibility in mandatory Class I areas (national parks, national wilderness areas, etc. of pre-specified sizes). The regulations also require State Implementation Plans to include a 10 - 15 year strategy for making reasonable progress toward the national visibility goal.

The Federal visibility regulatory program will have significant effects on air quality planning in the state of California. Of the 156 mandatory Class I Federal areas where EPA has judged visibility to be an important

value (Federal Register 1979), 29 areas are located in California. In future State Implementation Plans, the California Air Resources Board will be faced with the problem of formulating visibility protection plans for these 29 areas (and possibly for additional areas that may be redesignated Class I).

Because visibility is an important air quality concern in California, and because technical information is needed to support visibility provisions in future State Implementation Plans, the Air Resources Board has recently funded two major studies of visibility in California. The first of these studies (Trijonis 1980, 1982) characterized various features of visibility in California by using visual range measurements at 67 weather stations in conjunction with data on particulate concentrations and meteorology. That study addressed the issues of data quality, visibility/meteorology relationships, geographical visibility patterns, seasonal visibility patterns, diurnal visibility patterns, visibility/aerosol relationships, and historical visibility trends. The second study, for which this document serves as a final report, consists of a review of visibility modeling, a comprehensive statistical analysis of visibility/aerosol relationships, and a consideration of future visibility monitoring.

The specific objectives of this report are as follows:

- To review deterministic and empirical models for visibility, and to provide guidance for model selection considering data availability.
- To conduct statistical studies of visibility/aerosol relationships at numerous (34) locations throughout California using airport visibility data and routine Hi-Vol particulate data.
- To determine approximate extinction budgets apportioning visibility impairment at the study sites among Rayleigh scatter, NO₂ absorption, sulfates, nitrates, and other aerosols.
- To recommend potential programs for future visibility monitoring in California.

The four objectives listed above are the subjects of Chapters 2 through 5, respectively. The remaining sections of the present chapter provide an introduction to the basic technical concepts of visibility and a summary of findings and conclusions.

It should be noted that this report represents the combined efforts of visibility researchers from several organizations. The Caltech

Environmental Quality Laboratory performed the visibility modeling review of Chapter 2. The statistical analysis of visibility and Hi-Vol data in Chapter 3 was conducted by Technology Service Corporation and Santa Fe Research Corporation. A special study of size segregated particulate data (Appendix A) was prepared by the University of California at Davis. Santa Fe Research Corporation was responsible for the extinction budget analysis (Chapter 4), the visibility monitoring review (Chapter 5), and the assembly of the final report.

1.1 BASIC CONCEPTS AND DEFINITIONS

Visibility refers to the clarity of the atmosphere and can be defined quantitatively in terms of discoloration (wavelength shifts produced by the atmosphere), contrast (the relative brightness of visible objects), and/or visual range (the farthest distance that one would be able to distinguish a large black object against the horizon sky). Because much of this study is based on weather-station measurements of visual range, we will define visibility as visual range and will use the two terms interchangeably. It should be noted that the concept of visual range makes most sense in situations of large-scale homogeneous haze, which is the type of visibility phenomenon being addressed in this report.

Visibility through the atmosphere is restricted by the absorption and scattering of light by both gases and particles. The sum of absorption and scattering is called total extinction which is measured by the extinction coefficient "B". The extinction coefficient represents the fraction of light that is attenuated per unit distance as a light beam traverses the atmosphere. In a homogeneous atmosphere, visibility is inversely proportional to extinction; the Koschmieder formula expressing this relationship is:

$$B = \frac{k}{V} \quad (1-1)$$

The constant in Equation (1-1) is usually chosen to be $k = 3.9$ or $k = 3.0$, depending on whether one assumes a 2% or 5% contrast detection threshold for the observer.

Examples of visibility in certain areas and corresponding extinction coefficients (for $k = 3.0$) are listed in Table 1.1. Figures 1.1 and 1.2 illustrate the geographical variations of visual range for the continental United States and California, respectively.

It is often preferable to discuss visibility in terms of extinction coefficient rather than visual range because the extinction coefficient can be linearly subdivided into contributions from various atmospheric components. In general, total extinction is a linear sum of four terms:

$$B = B_{\text{Rayleigh}} + B_{\text{Ab-Gas}} + B_{\text{Scat-Part}} + B_{\text{Ab-Part}}$$

Here, B_{Rayleigh} = light scattering by air molecules (Rayleigh or blue-sky scatter). This term is on the order of .10 to .12 $(10^4\text{m})^{-1}$ depending on altitude (i.e. depending on the density of air); it would restrict visibility to approximately 155-190 miles (for a 5% contrast) if all particles and pollutant gases were absent.

$B_{\text{Ab-Gas}}$ = light absorption by gaseous nitrogen dioxide (NO_2) is the only prevalent gaseous pollutant that is a significant light absorber. Although concentrations of NO_2 are usually not large enough to produce significant reductions in overall visual range, NO_2 can produce significant brownish discoloration because it preferentially absorbs blue light.

$B_{\text{Scat-Part}}$ = light scattering by particles (aerosols). In most cases, this is the dominant part of total extinction and therefore the main contributor to reduced visual range.

$B_{\text{Ab-Part}}$ = light absorption by particles. This term can become substantial in those areas where elemental carbon (soot) constitutes a significant fraction of the aerosol.

As noted above, light scattering by particles usually dominates total extinction in hazy air masses. The two major exceptions are remote areas

TABLE 1.1 VISIBILITIES AND EXTINCTION COEFFICIENTS
TYPICAL OF VARIOUS AREAS.

VISIBILITY (MILES)	EXTINCTION COEFFICIENT (10^{-4} m^{-1})	EXAMPLES OF AREAS EXHIBITING THIS AVERAGE VISIBILITY
8	2.34	Central/eastern part of the Los Angeles Basin.
10	1.87	Fringes of the Los Angeles Basin, or metropolitan centers in the Northeast, or large-scale haze in the Ohio Valley.
12	1.56	San Joaquin Valley of California, or large-scale haze typical of most nonurban areas east of the Mississippi and south of the Great Lakes.
20	0.93	Delta region east of San Francisco, or the Central Plains states (Minnesota, Iowa, and the eastern parts of Nebraska, Kansas, Oklahoma, and Texas).
50	0.37	Northeast plateau of California, or the area along the California-Arizona border, or the northern mountain states (Idaho and Montana).
80	0.23	Area along the California-Nevada border, or the southern mountain/desert states (Nevada, Utah, Colorado, northern New Mexico, and northern Arizona).
155	0.12	Air at sea level free of all particles and all pollutant gases.
190	0.10	Air at 5000 feet altitude free of all particles and all pollutant gases.

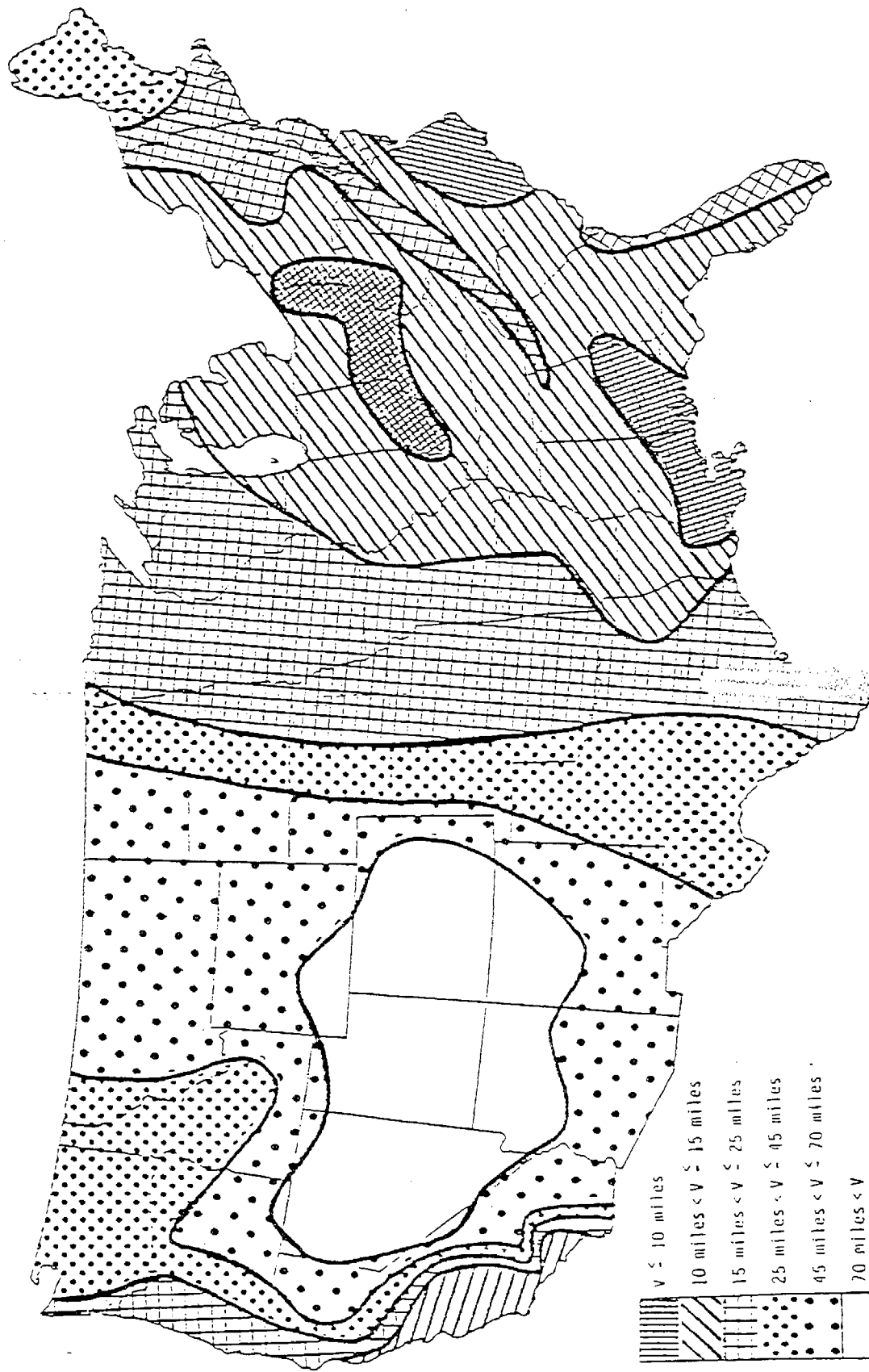


Figure 1.1 Shaded isopleth map of median mid-day visibilities for suburban/nonurban areas in the United States (Trijonis and Shapland 1979).

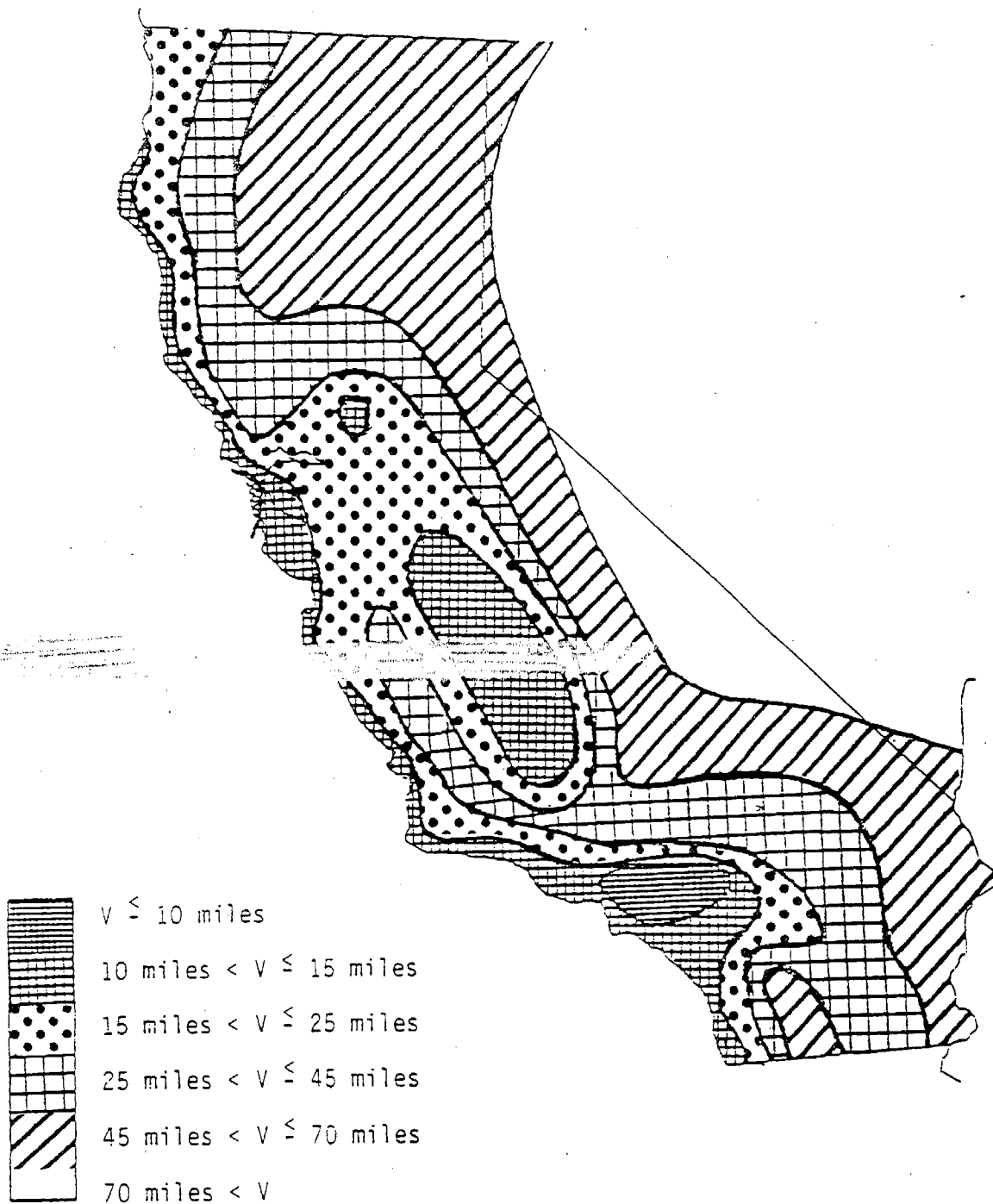


Figure 1.2 Shaded isopleth map for median 1 PM visibilities in California (Trijonis 1980, 1982).

of the desert/mountain Southwest (including the California-Nevada border region) where natural blue-sky scatter is comparable to light scattering by aerosols, and certain urban areas where absorption by elemental carbon may be comparable to light scattering by aerosols.

1.2 SUMMARY

The following sections summarize the findings and conclusions of this report. For convenient referral, the summary is organized according to the order of the chapters.

Review of Visibility Air Quality Models

Two major classes of mathematical models are available for characterizing the relationship between precursor emissions, ambient pollutant concentrations, and visibility. The first class is deterministic emissions-source-oriented models that combine atmospheric transport, diffusion, and chemical reaction with theoretical radiative transfer calculations. The other class of techniques involves the use of empirical relationships between pollutant concentrations and visual range. The latter receptor-oriented models make extensive use of atmospheric measurements and statistical inferences drawn from field observations on pollutant concentrations and atmospheric light extinction.

Three source-oriented dispersion models for visibility reduction are available at present. Each is based on a Gaussian plume air quality model, and hence each is best suited to plume blight calculations arising from single remote emission sources rather than for use on multi-source regional haze problems. Basically each of these models is composed of three elements. The first component is a procedure for calculating the concentration fields using the source emissions and atmospheric conditions as input data. Given the concentration fields and the optical characteristics of the gases and aerosols, the second element of a visibility model is the radiative transfer calculation algorithm. The final component of each model is the procedure for translating the changes in light intensity due to the presence of pollutants into measures of human visual perception. These models require large amounts of input data, including aerosol size distributions and optical properties. Since such data are seldom available, these models to

date have been subjected to a very limited set of field verification tests. In addition, since these models are usually implemented in the form of large computer programs, a potential user of these techniques must assess the availability of the computer codes and their documentation. Of the three models reviewed, only one is in the public domain with sufficient documentation to be readily usable.

More than 20 applications of empirical-statistical models are reviewed. In these models, light extinction per unit pollutant concentration for each absorbing or scattering pollutant species is estimated by regression of atmospheric extinction coefficient measurements on co-occurring fluctuations in pollutant species concentrations. Very simple empirical visibility models that try to relate 24-hour average total suspended particulate matter concentrations to visual range often show a poor ability to track changes in visibility and lend little insight into the pollutant sources responsible for visibility reduction. More advanced empirical models that combine short-term average, chemically resolved, size-segregated pollutant data with information on atmospheric humidity and aerosol light absorption, however, fit observed visibilities very well, make physical sense, and help to identify the sources responsible for visibility reduction.

One example of a third class of model also was identified that lies part-way between the empirical models and the source-oriented dispersion models. In this case, atmospheric light extinction is computed from Mie theory based on measured aerosol size distribution data, rather than from pollutant properties calculated from an atmospheric transport model. Comparisons to date show that this receptor-oriented theoretical calculation scheme yields answers comparable to an empirical visibility model applied to the same data set.

As a practical matter, the choice facing a person who must select a visibility model is frequently dictated by data availability. For example, vast amounts of information are needed by a regional scale radiative transfer model if it is to accurately characterize the simultaneous effects of emission, transport, dispersion, chemical transformation, and optical interactions. For this practical reason, the most appropriate choice of a modeling methodology for immediate application is the class of methods based on regression analysis, or the receptor-oriented theoretical calculation scheme employing measured size distribution data. Given high quality measurements,

these two types of empirical visibility models can be structured to make physical sense, to track changes in total extinction extremely well, and to yield insight into the portion of the visibility problem attributable to different pollutants and sources.

Visibility/Aerosol Relationships Based on Hi-Vol Data

Our analysis of visibility/aerosol relationships uses routine airport visibility data and routine Hi-Vol particulate data for 34 locations in California. The statistical analysis centers on multiple regression equations that relate daytime average extinction (determined from airport visibility data) to daytime average relative humidity and to 24-hour Hi-Vol data for sulfates, nitrates, and the remainder of TSP. At several sites we also include Hi-Vol data for benzene soluble organics and various elemental tracers: Pb (motor vehicle particles), Ni (fuel oil particles), and Si or Mn (soil dust particles). The coefficients in the multiple regression equations can be interpreted as "extinction coefficients per unit mass" or "extinction efficiencies" for each aer

There are several limitations to the use of regression models for quantifying visibility/aerosol relationships: (1) random errors in the data base caused by imprecision in the measurement techniques for airport visibility and aerosol concentrations; (2) incompatibilities between the airport data and the aerosol data which are collected at different locations and over different hours of the day; (3) biases in the measurement of sulfates and, especially, nitrates; and (4) statistical problems introduced by the intercorrelations among the "independent" variables (sulfates, nitrates, remainder of TSP, and relative humidity) and by correlations between these variables and other visibility-related pollutants omitted from the analysis. The most important limitations are the measurement errors for nitrates and the statistical problems. In fact, because of the difficulties associated with nitrates, it is best to regard the "nitrate" variable as a gross measure of both nitrate aerosols and related photochemical pollutants (such as secondary organic aerosols and NO_2). The above limitations must be kept in mind when interpreting the results of the regression analyses.

It is critical to treat relative humidity (water) in an adequate manner when conducting the regression analysis. Several theoretical and experimental studies suggest that, at relative humidities of 65-75%, the

mass of water associated with fine ambient aerosols is approximately equal to or slightly greater than the mass of aerosol electrolytes (e.g. sulfates and nitrates). As relative humidity increases toward 100%, the mass of aerosol water rises even more (hyperbolically). The role of aerosol water becomes even more critical when one realizes that, because of density differences, water should scatter significantly more light per unit mass than the aerosol electrolytes. These observations help to explain why many statistical studies have found that sulfate (or sometimes nitrate) is the major, if not the dominant, contributor to atmospheric light extinction. Not only do sulfates constitute a significant fraction of the fine (optically active) aerosol, but also they often carry with them a substantial volume of water. Furthermore, it should be remarked that water is an integral part of the aerosol to which it is attached. For example, if the sulfate aerosol were eliminated, the water associated with the sulfate aerosol would also be eliminated from the particulate phase.

At each of the 34 study sites, the multiple regression models are run on two data bases -- one excluding days with precipitation or any fog, and the other excluding days with precipitation or severe fog. Also, two regression forms are used -- a completely linear model, and a nonlinear relative humidity model adding the term $(1-RH)^{-1}$ or $(1-RH)^{-2/3}$ as a multiplicative factor to the aerosol variables. The nonlinear RH regression model yields higher correlation coefficients and physically more reasonable regression coefficients than the linear RH regression model. This makes sense because the nonlinear RH model represents a much better approximation to the thermodynamic behavior of hygroscopic aerosols (e.g. sulfates). Specifically, the nonlinear RH regression model treats water as an integral part of the aerosol and parallels the hyperbolic relationship between aerosol water and relative humidity.

The regression analyses reveal that some of the Hi-Vol variables generally lack consistent, statistically significant relationships with extinction (visibility). The insignificant variables are organics, Pb (motor vehicle particles), Ni (fuel oil particles), and Si or Mn (soil dust particles). The lack of statistically significant relationships does not imply that these aerosol components have zero or negligible effect on visibility. Rather, we can only conclude that the effect of these aerosol components is not overwhelming enough so that one can determine extinction

efficiencies from the (admittedly limited) airport and Hi-Vol data. For some of these variables, the lack of a statistically significant relationship reflects their small contribution to fine aerosol concentrations; for others, the lack of a statistically significant relationship may reflect data quality or statistical colinearity problems.

The regression analyses in this report, as well as similar studies found in the literature, indicate that the extinction efficiencies for secondary aerosols (nitrates and especially sulfates) are nearly one order of magnitude greater than the extinction efficiencies for the remainder of TSP. Qualitatively, this agrees with known principles of aerosol physics. Secondary aerosols tend to accumulate in the particle size range from 0.1 to 1 micron, while the remainder of TSP is usually dominated by the coarse particle mode residing in the size range above 2 microns. Light-scattering per unit mass of aerosol as a function of particle size exhibits a pronounced peak at a particle size of about 0.5 microns, and particles in the 0.1 to 1 micron size range scatter much more light per unit mass than particles ~~above 2 microns in size.~~

Some statistically significant geographical features are evident in the extinction efficiencies for sulfates and nitrates. Sulfate extinction efficiencies are greater in the southern half of California than in the northern half of California, while nitrate extinction efficiencies exhibit exactly the opposite geographical pattern. The north/south variation in the extinction efficiencies may be partly spurious -- caused by statistical problems introduced by intercorrelations between the sulfate and nitrate variables. To some extent, however, the north/south variations appear to represent physical realities. In particular, we have found a relationship between sulfate extinction efficiencies and published data on sulfate size distributions; sulfate extinction efficiencies are higher in those geographical regions where the sulfate size distribution is centered in the upper part of the accumulation mode (between 0.5 and 1.0 microns). Also, the higher nitrate extinction efficiencies in northern California may reflect the extreme temperature sensitivity of the equilibrium between particulate ammonium nitrate and gaseous ammonia and nitric acid. Specifically, in northern California relatively more of the Hi-Vol nitrate may represent real nitrate aerosol, while in southern California relatively more of the Hi-Vol nitrate may represent collection of gaseous nitric acid (artifact nitrate).

Extinction Budgets

For each of the 34 study locations, average extinction budgets are calculated which apportion visibility reduction among five components: light scattering by air molecules (Rayleigh scatter), light absorption by NO_2 , extinction by sulfates, extinction by nitrates; and extinction by other (non-sulfate, non-nitrate) particles. The contributions from Rayleigh scatter and NO_2 absorption are computed from known physical constants (and measured NO_2 concentrations). The contributions from sulfates and nitrates are computed from extinction efficiencies for sulfates and nitrates. The extinction efficiencies for sulfates and nitrates are based on our regression results as well as on other theoretical and empirical considerations. We do not explicitly include the nitrate term for sites in southern California because our regressions failed to yield consistent, physically reasonable coefficients for nitrates in southern California. The contribution from "other" particles is calculated by simply subtracting the air molecule, NO_2 , sulfate, and nitrate components from total average extinction.

Because Rayleigh scatter is nearly constant, the percentage contribution from Rayleigh scatter is inversely proportional to total average extinction. The average percentage contribution from Rayleigh scatter varies from about 5% in the haziest parts of California (e.g. the central Los Angeles basin) to about 40% in the clearest areas of California (e.g. along the Nevada border). At most of our specific study locations, Rayleigh scatter constitutes 5 to 15% of average total extinction.

The percentage contributions from NO_2 are fairly uniform among the study locations -- typically 7-11%. This reflects the phenomenon that locations with higher pollutant aerosol levels and resulting higher average extinction levels also tend to have higher NO_2 levels.

Our results indicate that sulfate aerosol is the predominant visibility reducing pollutant in the Los Angeles and San Diego areas; in these areas, sulfates apparently account for about 40 to 70% of total extinction. Sulfates are also significant in the remainder of California, typically contributing about 15-35% of total extinction. As discussed previously, sulfates are critical to visibility not only because they constitute a significant fraction of the fine aerosol but also because they attract a large volume of water into the aerosol phase.

Our methodology suggests that nitrates generally account for about 10-40% of extinction at locations in the northern half of California. The nitrate contributions are especially large, 20-40%, in the Central Valley. As noted previously, the visibility/nitrate relationships are very uncertain because of statistical colinearity problems and because of severe measurement difficulties for nitrates. A thorough study of the role of nitrates in California visibility must await the development of a reliable sampling procedure for nitrate aerosols.

The extinction contribution from "other aerosols" ranges widely among the locations, from 10 to 70%. Based on other studies using more detailed aerosol data, we know that the important components of this "other" category are light absorption by elemental carbon (soot) and light scattering by various fine aerosols (organics, fine particles at the lower end of the soil dust and sea salt size distributions, elemental carbon particles, non-carbonaceous primary aerosols from combustion processes, etc.). In urban areas, elemental carbon (soot) is likely to be the most important contributor to the aerosol category; soot likely accounts for 20 to 40% of extinction in major urban areas of California.

Future Visibility Monitoring

There is a potential need for two distinct types of visibility-related monitoring in California. The first type concerns a statewide network to collect precise instrumental data on visibility for quantifying existing conditions, spatial/temporal patterns, and future trends. The second type involves collection of detailed particulate data for determining exact extinction budgets at selected sites in California.

There are five basic ways of measuring visibility: human observers, telephotometers, photographic photometers, transmissometers, and nephelometers. After reviewing the advantages and disadvantages of these monitoring methods, we conclude that, if the ARB were to create a statewide visibility monitoring network, such a network should consist of either telephotometers or nephelometers. At present, choosing between telephotometers and nephelometers is difficult; before establishing a statewide visibility network, the ARB might want to conduct a seminar with users and proponents of each instrument.

The major advantages of telephotometers are commercial availability, permanent records, and good correlations with human perceptions. Also, the National Park Service is currently operating a telephotometer program throughout the West. The most important disadvantages of telephotometers are the need for a good quality control program, the need for adequate dark targets, the restriction to only daytime measurements, and the problems created by clouds behind targets and by variations in illumination conditions on targets. Nephelometers also are commercially available, yield permanent records, and correlate well with human perceptions. A nephelometry network, however, would measure only particle scattering and would require separate instruments for measuring particle absorption. Other disadvantages of nephelometry are loss of relative humidity and large particles in the sampling train and, possibly, the expense associated with maintaining high quality performance.

At selected locations in California, it would be worthwhile for the ARB to conduct field projects that can provide accurate extinction budgets. Extremely useful studies can be conducted with a heated nephelometer, an ambient nephelometer, a teflon filter dichotomous sampler, and a quartz filter dichotomous sampler. The appropriate statistical analysis of the data from these instruments as well as other readily available data would yield a detailed extinction budget including the following terms: Rayleigh scatter, NO_2 absorption, particle absorption (broken down into fine elemental carbon, coarse elemental carbon, and other aerosols), and particle scattering (broken down into coarse particles and fine particles, with the latter further divided according to sulfates plus water, nitrates plus water, organics, elemental carbon, fine crustal aerosols, and other fines).

The extinction budget monitoring stations should be operated for one year at each location in order to provide robust data sets and in order to avoid seasonal biases. The monitoring stations might be relocated every year to provide data for extinction budgets throughout California.

Once extinction budgets have been calculated, source allocations can be performed by apportioning each component of extinction according to regional emissions. Source allocations would require emission inventories for sulfur oxides, nitrogen oxides, hydrocarbons, elemental carbon, organic aerosols, and other primary fine particles.

1.3 REFERENCES FOR CHAPTER 1

Federal Register, "Identification of Mandatory Class I Federal Areas Where Visibility is an Important Value; Final Rule," Part IV Environmental Protection Agency, November 30, 1979.

Federal Register, "Visibility Protection for Federal Class I Areas," Part IV Environmental Protection Agency, December 2, 1980.

Trijonis, J., "Visibility in California," prepared for the California Air Resources Board, under Contract No. A7-181-30, April 1980.

Trijonis, J., "Visibility in California," Journal of the Air Pollution Control Association, February 1982.

Trijonis, J. and D. Shapland, "Existing Visibility Levels in the U.S., Iso-pleth Maps of Visibility in Suburban/Nonurban Areas During 1974-1976," EPA-450/5-79-010, 1979.

2. REVIEW OF VISIBILITY AIR QUALITY MODELS

The task of predicting the impact of pollutant emissions on visibility is complicated by the presence of a large number of airborne pollutants, the occurrence of various chemical interactions, and major differences in the optical properties of specific gases and aerosols. One major source of complexity is that many of the pollutants that scatter and absorb light are of secondary origin. These materials are not emitted directly in their final form by emissions sources, but rather, are formed as products of chemical reactions in the atmosphere. When coupled with the fact that visibility degradation in any given area has a complex dependence on geography, time of day, and meteorological conditions, the design of an effective visibility improvement program is definitely a difficult undertaking. One issue is clear. A key element of any rational approach for improving visual air quality is a reliable means for evaluating the impact of alternative emission control measures. This chapter reviews a number of different modeling methodologies that can be used to relate precursor emissions and the resulting concentrations of gases and aerosols to ambient visibility.

2.1 ELEMENTS OF THE VISIBILITY MODELING PROBLEM

The ability to define, monitor, model, and control visibility impairment involves an understanding of many different physical processes. Some of the elements that must be considered are illustrated in Figure 2.1. From an examination of this diagram, it can be seen that the visibility modeling problem involves characterizing four basic components: the light source, the object being viewed, the properties of the intervening atmosphere, and the response of the observer. The detailed formulation of a modeling system that links the various parts of the visibility problem is an intricate undertaking. It is necessary to maintain a balance between computational economy, data availability, and the desire for an accurate representation of the underlying physics and chemistry. As will be shown later in this Chapter,

the key factor limiting the usefulness of particular visibility modeling approaches, in many cases, is not a lack of understanding of the basic physical processes governing visual range but rather the availability of field measurements suitable to support accurate calculations.

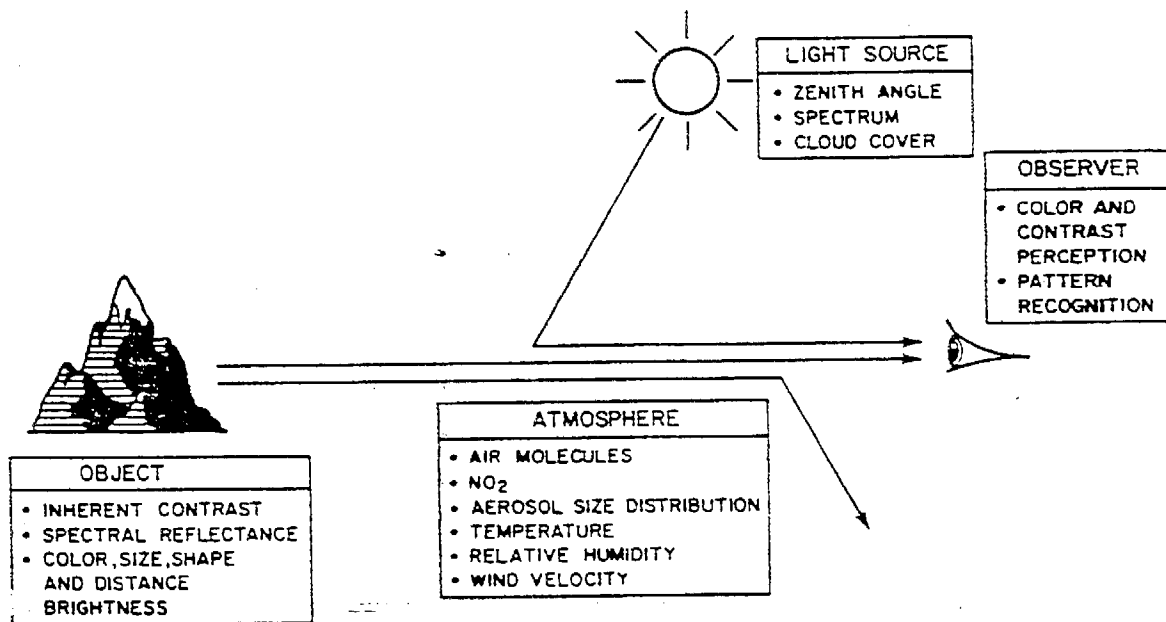


Figure 2.1 Basic elements of the visibility modeling problem.

As part of this project, an extensive literature review was undertaken in order to document the current scientific understanding of visibility impairment resulting from air pollution. A secondary goal was to identify those modeling approaches that might be compatible with air monitoring measurements available in California. Given the importance of being able to predict visibility impairment, there is, as might be expected, a considerable volume of published literature on the subject. Important recent reference works include: White (1981), U.S. EPA (1979), Fox et al. (1979), Latimer et al. (1978), and Charlson et al. (1978). The special issue of Atmospheric Environment (White, 1981) alone includes 55 papers on such topics as: radiative transfer and visual perception, haze and aerosols, source characterization, plume optics, dispersion and transport, and finally, a discussion of atmospheric chemistry. A detailed literature review is presented in the following sections of this chapter.

Despite the diversity of modeling methodologies identified in the review, two basic visibility modeling approaches emerged: empirical methods, and deterministic models based on a fundamental description of the physics and chemistry occurring in the atmosphere. Deterministic, or a priori, models normally incorporate a spatially resolved description of pollutant emission source strength, a mathematical treatment of the chemical and meteorological transport processes that map emissions into observed air quality, and theoretically based calculations that predict visual range. An example of how the various physical and chemical processes might be linked in this class of model is shown in Figure 2.2. The other class of techniques involves the use of a posteriori models in which empirical relationships, between pollutant concentrations and visual range, are deduced from atmospheric measurements. These models are usually very simple and typically bear a close relationship to the actual data upon which they are based. Unfortunately, this latter feature is a basic weakness. Because the empirical models do not explicitly quantify all underlying causal phenomena, they cannot be reliably extrapolated beyond the bounds of the data from which they were derived.

Both a priori and a posteriori methods are useful tools; however, as a rule, if data are available to test and verify a model based on scientific fundamentals, then that approach is preferable. In either case, whether the prediction scheme is a simple formula or a complex numerical procedure, it must have at least two fundamental components. One is a scheme to determine the impact of pollutants on the optical characteristics of the atmosphere, and the other is a means for characterizing human perception of visibility impairment. Subsequent sections of this work are devoted to a discussion of these two basic elements.

2.2 QUANTIFYING VISIBILITY IMPAIRMENT AND THE KOSCHMIEDER FORMULA

Given the concentration and characteristics of pollutants, it is possible to define visibility impairment in terms of the intensity or coloration of distant objects. Three of the common means for quantitatively characterizing the clarity of the atmosphere are: contrast (the relative brightness of various features in a scene), visual range (the farthest distance that one would be able to distinguish a large black object against

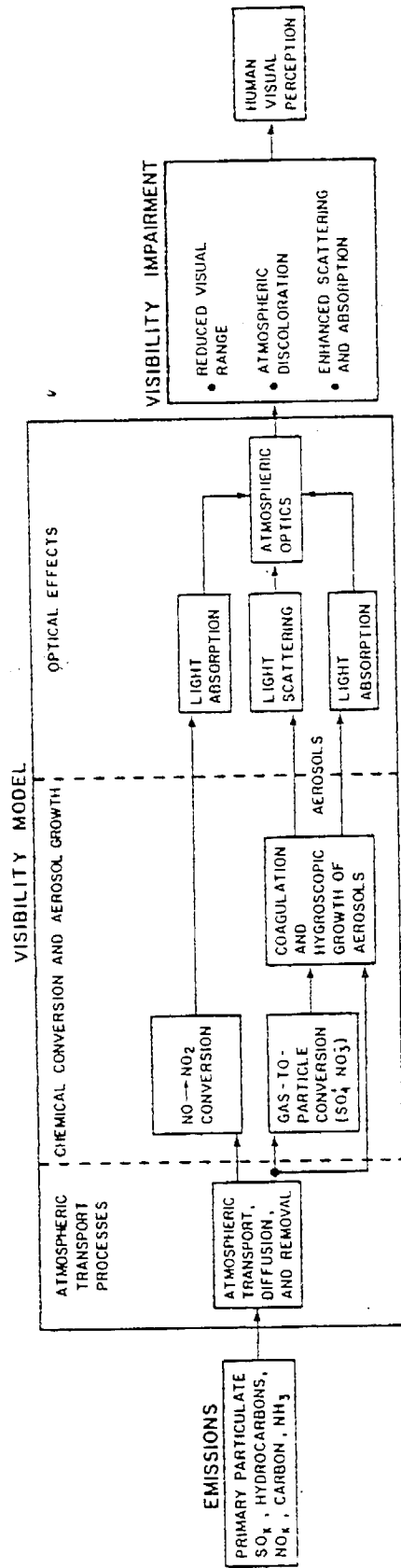


Figure 2.2 A typical example of how the various physical and chemical processes might be linked as part of a complete visibility modeling system.

the horizon sky), and/or discoloration of the intervening atmosphere. While it is straightforward to define these criteria, relating them to human visual perception (particularly of coloration) is an extremely complex undertaking (Malm et al. 1981). Because current understanding of color perception is inadequate, theoretical calculations of atmospheric discolorations are useful only as a guide for experimental measurements (U.S. Environmental Protection Agency 1979). Many visibility models do calculate parameters that are an indication of coloration effects. These indices include: blue-red ratio (relative discoloration defined by the blue/red ratio of light originating from the horizon with and without the pollution), and chromaticity coordinates (Judd and Wyszecki 1963). However, because most routine visibility data are reported in terms of perceived visual range, primary emphasis will be given to modeling this criterion.

Visual range L_V is defined as the farthest distance at which a black object can be perceived against the horizon sky. The contrast between two objects is given by

$$C(\lambda) = \frac{I_1(\lambda) - I_2(\lambda)}{I_2(\lambda)} \quad (2-1)$$

where $I(\lambda)$ is the light intensity or spectral irradiance. If the two objects are the same color (i.e. $I_1(\lambda) = k I_2(\lambda)$ for all visible wavelengths), then the contrast will be constant. When the objects are of different color, then the contrast, C , is a function of the wavelength. Normally in the calculation of visual range, the contrast is evaluated at a wavelength of 0.55 micrometers. This point corresponds to the middle of the visible spectrum and is the wavelength at which the human eye is most sensitive. The intrinsic contrast of a black object ($I_1 = 0$) against the horizon sky ($I_2 = I_h$) is -1. The visual range L_V is defined (Latimer et al. 1978) as the distance at which a black object is barely perceptible against the horizon sky. This occurs when the perceived light intensity of the black object is $(1 + C_{min})I_h$, where C_{min} is the liminal contrast (minimum contrast distinguishable by a human observer). The value of C_{min} is commonly taken to be -0.02, as first suggested by Koschmieder in 1924 (Middleton 1952). It is important to note that the limiting contrast threshold of -0.02 is a physiological property of

the observer. Ninety percent of persons tested show contrast thresholds between -0.01 and -0.07 (Charlson et al. 1978).

A simple model of the change in light intensity, in a homogeneous column of air, over a distance x is given the Beer-Lambert law:

$$\frac{1}{I(\lambda)} \frac{dI(\lambda)}{dx} = -b_{\text{ext}}(\lambda) \quad (2-2)$$

where $b_{\text{ext}}(\lambda)$ is the extinction coefficient, a measurable property of the atmosphere that describes the extent of light scattering and absorption by pollutant particles and gases. If the atmosphere can be assumed to be uniform, then (2-2) can be solved analytically to give the visual range apparent to an average observer as a function of the extinction due to ambient concentrations of gases and particles.

$$L_v = \frac{-\ln(|C_{\text{min}}|)}{b_{\text{ext}}(\lambda)} = \frac{3.912}{b_{\text{ext}}(\lambda)} \quad (2-3)$$

Considering the widespread use of (2-3), (sometimes called the Koschmieder formula) it is important to be aware of its assumptions and limitations. The critical assumptions and limits are: a homogeneous distribution of pollutants, horizontal viewing distance, same sky brightness at both the target object and observer, and finally a contrast threshold of -0.02. Horvath (1971a) discusses the possible errors in using Koschmieder's formula to estimate visibility apparent to a human observer. He suggests that by proper selection of visibility markers, it should be possible to calculate the extinction coefficient from observed visibilities to within an error of about 10%.

2.3 ATMOSPHERIC OPTICS

In the previous section, a simple model was presented for the change in spectral light intensity as a function of distance along the sight path. The effect of the intervening atmosphere on the visibility and coloration of a viewed object (e.g. the horizon sky, a mountain, a cloud) can be determined if the concentration and optical characteristics of air molecules, aerosols, and pollutant gases are known along the line of sight. A rigorous treatment of the effects of air pollution on visibility requires an understanding of atmospheric radiative transfer processes. Since this particular

aspect of the modeling problem is adequately discussed in the text by McCartney (1976) and the classic works of Middelton (1952) and Chandrashekar (1960), only a brief discussion will be presented here. The particular treatment used below is based on the work of Latimer et al. (1978) and has been included because of its direct relationship to the procedures described in the U.S. Environmental Protection Agency workbook for estimating visibility impairment (U.S. EPA 1980). For a more detailed discussion, the reader is referred to Bergstrom et al. (1981a), Dave (1981), Isaacs (1981), or the review article by Hansen and Travis (1974).

The change in spectral light intensity or spectral irradiance $I(\lambda)$ as a function of distance along the sight path at any point in the atmosphere can be defined as follows

$$\frac{dI(\lambda)}{dx} = -b_{\text{ext}}(\lambda)I(\lambda) + \frac{p(\theta, \lambda)}{4\pi} b_{\text{scat}}(\lambda)F_s(\lambda) \quad (2-4)$$

where

- is the distance along the sight path from the object to the observer.
- $p(\theta, \lambda)$ - is the scattering distribution or phase function for the scattering angle θ .
- F_s - the solar flux ($\text{watts m}^{-2} \text{micron}^{-1}$) incident on the atmosphere.
- b_{scat} - is the scattering coefficient composed of the sum of the contributions from gas molecules $b_{\text{Rayleigh}}(\lambda)$ and aerosol particles $b_{\text{scat}_a}(\lambda)$ i.e.

$$b_{\text{scat}}(\lambda) = b_{\text{Rayleigh}}(\lambda) + b_{\text{scat}_a}(\lambda) \quad (2-5)$$

- b_{ext} - is the sum of the scattering, $b_{\text{scat}}(\lambda)$, and absorption coefficients, $b_{\text{abs}}(\lambda)$ i.e.

$$b_{\text{ext}}(\lambda) = b_{\text{scat}}(\lambda) + b_{\text{abs}}(\lambda) \quad (2-6)$$

On the right-hand side of (2-4), the first term represents light absorbed or scattered out of the line of sight; the second term represents light scattered into the line of sight. These processes are illustrated in Figure 2.3. The values of b_{scat} and b_{abs} can be evaluated if the aerosol and gas concentrations and such characteristics as the refractive index and

the air is sometimes nearly particle-free, and visual range approaches the limit of about 320 km imposed by Rayleigh scattering due to air molecules (Trijonis and Yuan 1978a; Charlson et al. 1978). The extinction coefficient contribution due to Rayleigh scattering, b_{Rayleigh} has a value of about $0.12 \times 10^{-4} \text{ m}^{-1}$ at sea level at a wavelength of 550 nm. Extinction due to Rayleigh scattering declines with altitude as shown in Table 2.1.

TABLE 2.1 EXTINCTION COEFFICIENT DUE TO RAYLEIGH SCATTERING AS A FUNCTION OF WAVELENGTH AND ALTITUDE

Wavelength(a) (μm)	$b_{\text{Rayleigh}} (10^{-4} \text{ m}^{-1})$				
	Altitude (m) (b)				
	Sea Level	1000	2000	3000	4000
0.2	9.54				
0.25	3.38				
0.3	1.52				
0.35	0.79				
0.4	0.45				
0.45	0.28				
0.5	0.18				
0.52	0.15				
0.55	0.12	0.11	0.10	0.09	0.08
0.6	0.09				
0.65	0.06				
0.7	0.05				
0.75	0.03				
0.8	0.03				

(a) b_{Rayleigh} as a function of wavelength from Penndorf (1957)

(b) b_{Rayleigh} as a function of altitude from Charlson et al. (1978)

Charlson et al. (1972) observed that while light scattering by particles usually dominates light extinction in the Los Angeles area, light absorption by NO_2 also is significant about 20% of the time. Nitrogen dioxide is the only light absorbing gas that is thought to be present in quantities sufficient to make a significant difference to perceived visual range or quality. As shown in Table 2.2, light absorption by NO_2 is strongly wavelength dependent. As a result, high NO_2 concentrations will cause white objects to appear brown or yellow colored (Horvath 1971b; Horvath 1972; Waggoner et al. 1972).

Light extinction by NO_2 depends on its concentration in the atmosphere

$$b_{\text{abs}_g}(\lambda) = \gamma_{\text{NO}_2}(\lambda) \cdot C_{\text{NO}_2} \quad (2-7)$$

where $\gamma(\lambda)$ is the extinction efficiency per ppm NO_2 at a particular wavelength (λ) and C_{NO_2} is the ambient NO_2 concentration in ppm. The extinction efficiency for NO_2 has been measured in the laboratory. Values of $\gamma_{\text{NO}_2}(\lambda)$ are given in Table 2.2.

Atmospheric coloration is determined by the wavelength-dependent scattering and absorption in the atmosphere. The spectral distribution of $I(\lambda)$ for λ over the visible spectrum determines the perceived color and light intensity of the viewed object. For example, if the atmosphere is uniform (i.e. b_{scat} and b_{abs} do not vary with distance x along the line of sight) (2-4) can be solved to find the horizon brightness $I_h(\lambda)$ as

$$I_h(\lambda) = \frac{\rho(\theta, \lambda) b_{\text{scat}}(\lambda)}{4\pi b_{\text{ext}}(\lambda)} F_s(\lambda) \quad (2-8)$$

Neglecting the effects of multiple scattering, the perceived intensity of progressively more distant bright and dark objects will asymptotically approach the horizon brightness I_h . The relative contributions of scattering (aerosols plus air) and absorption (NO_2 plus elemental carbon) to coloration can be illustrated by rearranging (2-4) to give

$$\frac{1}{I(\lambda)} \frac{dI(\lambda)}{dx} = b_{\text{scat}}(\lambda) \left[\frac{\frac{\rho(\theta, \lambda)}{4\pi} F_s(\lambda)}{I(\lambda)} - 1 \right] - b_{\text{abs}}(\lambda) \quad (2-9)$$

TABLE 2.2 LIGHT ABSORPTION BY NO₂ AS A FUNCTION OF WAVELENGTH

Wavelength (μm)	Extinction Coefficient due to Absorption by NO ₂ $b_{\text{abs}} (10^{-4} \text{ m}^{-1} \text{ ppm}^{-1})$
0.400	16.60
0.425	15.90
0.450	13.55
0.475	10.00
0.500	7.10
0.525	5.30
0.550	3.32
0.575	2.00
0.600	1.23
0.650	0.44
0.700	0.15

From: Hodkinson (1966) and Nixon (1940)

Note that from (2-9) that when light absorption is negligible compared with scattering, the clear horizon intensity is simply

$$I_{ho}(\lambda) = \frac{\rho(\theta, \lambda) F_s(\lambda)}{4 \pi} \quad (2-10)$$

so that (2-9) can be written as

$$\frac{1}{I(\lambda)} \frac{dI(\lambda)}{dx} = b_{scat}(\lambda) \left[\frac{I_{ho}(\lambda)}{I(\lambda)} - 1 \right] - b_{abs}(\lambda) \quad (2-11)$$

This latter equation is thus an expression that relates the effects of light scattering and absorption to the change in spectral light intensity with distance along a sight path. On the right-hand side of (2-11), the first term is the effect of light scattering, and the second term is the effect of light absorption. Given the absorption characteristics of NO₂, it is clear that it tends to cause a decrease in light intensity and a yellow-brown coloration by absorbing blue light. Particles may cause either a blue-white or a yellow-brown coloration depending on the quantity in brackets. If, at a given point along the sight path, I(λ) is greater than the clean horizon sky intensity I_{ho}(λ), then the quantity in the brackets will be negative which in turn means that the net effect of scattering will be to remove predominantly blue light from the line of sight. When the quantity in brackets is positive, the net effect of scattering is to add predominantly blue light into the line of sight. An important point to note is that only absorption can cause I(λ) to be less than I_{ho}(λ). More detailed discussions of the effects of particles and gases on atmospheric coloration can be found in Waggoner et al. (1972), Vanderpool and Humbert (1981), and White and Patterson (1981).

2.4 MODELING THE PROCESSES RESPONSIBLE FOR VISIBILITY IMPAIRMENT

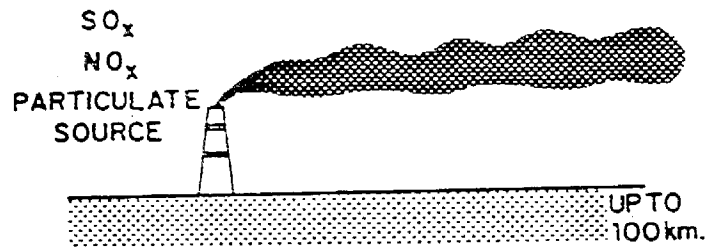
From the discussion in the previous section, it is clear that, given a complete description of pollutant properties and atmospheric conditions, light extinction can be computed from theory. If an accurate physiological description of the observer, his location, and the surrounding terrain is

available, then the apparent visual range can be calculated. Three research groups have developed visibility impairment models in the form of computer codes that represent pollutant emission sources, atmospheric transport, and light extinction in a deterministic manner:

- (a) Systems Application Incorporated (SAI) developed a visibility model for the U.S. Environmental Protection Agency that combines a Gaussian plume model with light extinction calculations. This work, described in Latimer et al. (1978) and Bergstrom et al. (1981ab), forms the basis for the calculation procedure presented in the workbook for estimating visibility impairment distributed by the U.S. Environmental Protection Agency (1980). Some of the components of the SAI plume model also have been used to calculate visual range estimates on a regional scale (Latimer et al. 1978).
- (b) The Los Alamos Scientific Laboratory (LASL) visibility model is capable of producing simulated "before" and "after" pictures that illustrate the visual effects of smoke plumes. The model is described in Williams et al. (1981) and has been under development for several years. Until recently, there has been very little testing of the model against field data.
- (c) Environmental Research and Technology Incorporated (ERT) has developed a visibility model designed to estimate the plume blight resulting from point sources. A detailed discussion of this model is presented in Drivas et al. (1980, 1981).

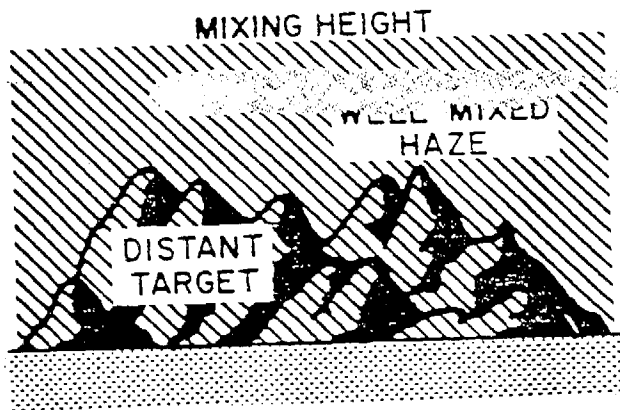
Basically, each of these models is composed of three elements. The first component is a procedure for calculating the concentration fields using the source emissions and atmospheric conditions as input data. Given these concentration fields and the optical characteristics of the gases and aerosols, the second element of a visibility model is the radiative transfer calculation algorithm. The final component of each model is the procedure for translating the changes in light intensity due to the presence of pollutants into measures of human visual perception. The interaction between the various physical and chemical processes that must be incorporated into the model is shown in Figure 2.2.

In practical applications, visibility models must be able to deal with essentially two distance and time scales: transport of plumes from a single source over short to moderate distances (10 to 100 km) and regional scale transport of the emissions from multiple sources over long distances (100 to 500 km). Figure 2.4 is a schematic representation of the two scales of visibility impairment: local plume blight and regional haze. While most of



(a)

LOCAL PLUME BLIGHT



(b)

REGIONAL HAZE

Figure 2.4 Schematic representation of the two basic classes of visibility impairment (a) local plume blight and (b) regional haze.

the development and testing work to date has focused on the use of these models in predicting plume blight, they can also be used to estimate regional impacts. For example, if the concentration field along the line of sight is externally supplied by the user, then the radiative transfer module can be used to predict the resulting visibility impairment. While each of the models are similar in overall structure, there are considerable differences in the detailed implementation of individual subroutines within the computer codes.

The SAI plume visibility model is described in detail by Latimer et al. (1978). The brief summary below has been excerpted from Bergstrom et al. (1981b). The emissions module treats plume rise and initial dilution in the atmosphere as well as the effects of near source chemistry. The transport, diffusion, and removal of pollutants is described by means of a Gaussian plume formulation. The kinetic mechanism, that represents the plume chemistry, applies to clean background atmospheres and involves nine reactions among NO, NO₂, O₃, SO₂ and the hydroxyl radical (OH). In addition, gas-to-particle conversion processes are accounted for, and the oxidation products of NO₂ and SO₂ are allowed to condense in the aerosol phase. Since visibility impairment caused by power plant plumes is primarily a result of light absorption by NO₂ and light scattering by aerosols, rates of NO-to-NO₂ conversion and gas-to-particle conversion are important components of the SAI visibility model.

The optics module in the SAI model includes a definition of the light scattering and absorption properties of aerosols and gases present within the plume. The radiative transfer through aerosols and gases along different lines of sight is calculated using a procedure called the diffuse field approximation. This technique is a simple and economical method for incorporating the effects of multiple scattering. Bergstrom et al. (1981a), Isaacs (1981), and Dave (1981) discuss the validity of this approach and other means for the radiative transfer calculations. The spectral light intensity at the point of observation is determined by integrating the scattering and absorption over the path associated with the line of sight. Once the light intensity has been determined for specific lines of sight, the various quantities that characterize visibility impairment can be calculated. The SAI model determines the visual range, plume contrast, and a series of color indices.

Evaluation studies of the SAI model have been carried out using data collected by the U.S. Environmental Protection Agency's VISTTA field program. Detailed comparisons between theoretical calculations and field observations are presented in Bergstrom et al. (1981b). In that study the various components of the model were independently evaluated and it was found that the greatest uncertainties in the model predictions lie in the pollutant transport and diffusion module. This is not too surprising since pollutant transport in this model is described by a very simple Gaussian plume formulation, the limitations of which are well known. The optics module was evaluated using plume concentration data to calculate the plume/sky intensity ratios. It was found that the optics module tends to slightly overpredict the plume's visual impact. For contrasts below -0.06, the predicted and observed values differed by a factor of two. While the model predictions were in general quite good, there is a critical need for further work to be carried out to test its performance over a wider range of atmospheric conditions.

Williams et al. (1981) presents a discussion of the Los Alamos Scientific Laboratory (LASL) visibility model. There are several components to this model that can be used in different ways to predict different types of visibility impairment. First, if the contaminant concentrations are provided along with relevant parameters such as aerosol size distributions, it can model the radiative transfer and provide numerical or visual representations of a scene being subjected to contamination. Second, it may be used with source emissions and meteorological data to predict the chemistry, dispersion, and radiative transfer associated with pollutants emitted by the source. The output of the model is in the form of a simulated photograph supplemented with various indices such as the blue/red ratio of the plume, plume-to-horizon-brightness ratio, and changes in chromaticity. One of the most interesting features of this model is its ability to produce "before" and "after" pictures of the effects of the pollutant plume. The technique starts by digitizing the color and brightness of different elements of the "clean" background vista. Then the effects of the plume, as predicted by the visibility model, are introduced into the clean picture.

The LASL model uses a lumped parameter approach to particle dynamics and a modified carbon-bond system for the chemistry. Key parameters are

the size distribution of the secondary aerosols and the conversion half lives for NO to NO₂, nitrogen oxides to nitrates, and sulfur oxides to sulfates. The chemistry is based on first order kinetics with the rate coefficients derived from the photochemical mechanism. The radiative transfer calculations are performed with a modified version of the multiple scattering program described in Dave (1981). While the LASL visibility model has perhaps one of the most sophisticated treatments of atmospheric optics, its use of the Gaussian plume formulation for describing the atmospheric dispersion of the pollutants is a major weakness. In passing, it is important to point out that all of the models described in this section used this approximation.

The LASL visibility model has been tested against actual plumes under a number of different conditions. Details of these tests are presented in Williams et al. (1981) where it is noted that qualitatively the model seems to provide reasonable representations of the actual plumes. However, in many cases, the plumes are more diffuse than those observed in the field and as a result are not as visually apparent. As in the case of the SAI model, there is a great need for additional sensitivity studies and comparisons against a wider range of atmospheric conditions.

The ERT visibility model (Drivas et al. 1981a,b) has been developed over the last two years for predicting the plume blight resulting from point sources. Like the previous models, the ERT computer code can be used to describe a single point source, or it can combine concentration fields derived from external single- or multiple-source dispersion models with radiative transfer calculations. In either option, the model accounts for extinction by NO₂, nitrates, and sulfates, with the remainder of the aerosol grouped into two different classes: carbonaceous and non-carbonaceous. The model produces information about visual range reduction, plume contrast, object contrast degradation, and plume/sky coloration. At present, however, relatively little has been published about the model's performance in reproducing the observed visibility impairments caused by actual plumes. In addition, there are many simplifications in the ERT model formulation that have not been invoked in either the SAI or LASL models. For example, the ERT radiative transfer model does not incorporate the effects of multiple scattering and so it must be confined to clear sky or near observer conditions. Given the lack of field verification results, considerable care needs to be exercised if this model is to be used in regulatory applications.

Visibility models of the type discussed in this section are usually implemented in the form of quite large computer programs. This imposes additional constraints on the choice of a modeling procedure. A potential user of any of these techniques, in addition to asking how well they treat the various physical processes, must also assess the resource requirements needed to collect the necessary data and whether the computer codes and their documentation are readily available. Of the three models discussed above, only the SAI Plume View Model (Latimer et al. 1978) is in the public domain with sufficient documentation to be readily usable. The LASL Visibility Model is undergoing further validation and, at present, there is no documentation manual that describes its use in practical applications. Williams et al. (1981), U.S. Environmental Protection Agency (1979), Bergstrom et al. (1981b) and Drivas et al. (1981) all state that more validation studies and field measurements are required to test model predictions over a wider range of atmospheric conditions.

In summary, while there are a number of candidate modeling techniques and theoretical formulations of the various physical and optical processes that lead to visibility deterioration, additional development work is needed before the modeling tools can be considered for routine application by regulatory agencies. Despite the inherent uncertainties, however, models of the type described in this section can and should be used in preliminary evaluations of source impacts. Single-source models can estimate the expected visual effects of primary particulate emissions at distances of up to 50 to 100 km from the source (U.S. Environmental Protection Agency 1979). These models can be used to provide rough estimates of the likely impact from single sources located in clean or isolated environments. At this time, there is no validated air quality model that is capable of assessing the impact of multiple sources on regional visibility impairment.

2.5 EMPIRICAL VISIBILITY MODELS

The quantity of experimental data needed if visibility calculations are to proceed directly from theory alone usually exceeds that available routinely from pollutant monitoring and meteorological monitoring networks. As a result, a large family of empirical visibility modeling methods have come into use that employ less than the data required for Mie theory calcu-

lations. In almost all of these models, pollutant concentrations are related to visual range through the Koschmieder formula after first computing the extinction coefficient, b . Following Charlson (1969), the extinction coefficient can be broken down into its components due to scattering and absorption by particles and gases:

$$b = b_{\text{scat}_a} + b_{\text{abs}_a} + b_{\text{scat}_g} + b_{\text{abs}_g} \quad (2-12)$$

where b_{scat_a} is extinction due to light scattering by aerosols, b_{abs_a} is extinction due to light absorption by aerosols, b_{scat_g} is extinction due to light scattering by gas molecules, and b_{abs_g} is extinction due to light absorption by gases. A separate approach for estimating each of these terms contributing to the extinction coefficient often is employed.

Light scattering and absorption by aerosols almost always dominates light extinction in polluted urban areas. Let the total light extinction coefficient due to aerosols, b_{ext_a} , be given by

$$b_{\text{ext}_a} = b_{\text{scat}_a} + b_{\text{abs}_a} \quad (2-13)$$

This aerosol extinction coefficient can be subdivided into contributions due to each of the many aerosol species present in the atmosphere (soil dust, sulfates, etc.)

$$b_{\text{ext}_a} = \sum_{i=1}^N b_{\text{ext}_{a_i}} \quad (2-14)$$

where the subscript i refers to the i -th chemical constituent. Information on the extinction contribution from each of several chemical components of the aerosol often is sought because chemical composition serves to identify the emission source types contributing to the aerosol (and hence visibility) problem (see Cooper and Watson 1980; Gordon 1980).

In order to compute the contribution of a particular aerosol species to the extinction coefficient from first principles, extensive information would be needed on the size distribution of the aerosol, its refractive index, particle shape, and humidification of the atmosphere. Such detailed data usually are lacking, however. Instead, routine air monitoring data available to most pollution control agencies are based on atmospheric filter samples.

In many cases, only total aerosol mass concentration is known; the chemical composition of the aerosol also may be known in whole or in part. On occasion, some aerosol size resolution may be available in the form of separate measurements of fine particle and coarse particle concentrations.

In order to make use of such routine air monitoring data based on filter samples, a family of empirical visibility models has been constructed. In these models, it is assumed that the extinction coefficient due to aerosols can be described as a linear combination of contributions due to each identifiable aerosol chemical species:

$$b_{\text{ext}_a} = \sum_{i=1}^N B_i M_i \quad (2-15)$$

where M_i is the mass concentration of species i , [in micrograms/m⁻³], and B_i is the extinction efficiency of aerosol species i , [in m² g⁻¹ or in (10⁻⁴ m⁻¹)/ (μg/m³)].

Ouimette (1981) has ~~investigated the conditions~~ that underlie visibility models based on expression (2-15). He finds that if the aerosol is an external mixture, in which each particle is composed of only a single chemical species, then (2-15) will hold as long as the normalized size (hence mass) distribution of each aerosol species does not vary from day to day. This is the assumption invoked by Cass (1979). Equation (2-15) also will hold in some more realistic cases where each aerosol particle is composed of many chemical constituents. In particular, if all particles of the same size have the same chemical composition, then (2-15) holds if (Ouimette 1981):

1. The normalized size (mass) distribution of each aerosol species does not vary from day-to-day.
2. The normalized total aerosol volume distribution is preserved.
3. The refractive indices of all chemical species are equal.
4. The partial molar volume of each species remains constant with the addition or removal of other species (aqueous solutions would violate this requirement).

Substituting (2-7) (2-13) and (2-15) into (2-12), and noting that light scattering by air molecules is available in tabulated form, one obtains

$$b_{\text{ext}} = \sum_{i=1}^N B_i M_i + Y_{\text{NO}_2} C_{\text{NO}_2} + b_{\text{Rayleigh}} \quad (2-16)$$

This is a typical structure against which most empirical visibility models can be compared. Specific visibility models based on (2-16) are usually formulated from long time series of simultaneous observations on extinction coefficient and pollutant species concentrations. Light extinction due to scattering and absorption by gases would be computed from tabulated values. The B_i then are fit to these observations by least squares regression techniques. Depending on the extent of the air quality data base available, the aerosol species considered may range from a single measure of total suspended particulate matter concentrations to a very detailed size-resolved and chemically-resolved apportionment of the extinction coefficient with allowance for nonlinear effects due to aerosol humidification.

2.6 EMPIRICAL EXTINCTION MODEL APPLICATIONS

A wide variety of empirical models for the extinction coefficient have been reported in the scientific literature. Most can be related to (2-16) by deleting terms or by elaborating on the form of the aerosol light extinction efficiency coefficients, B_i , in that equation.

2.6.1 Models Based on Total Suspended Particulate (TSP) Data

In the late 1960's, measurements made by Charlson and co-workers showed that total suspended particulate matter concentrations were correlated with light scattering measurements and were inversely correlated with prevailing visibility. From a variety of simultaneous nephelometer measurements of light scattering and aerosol mass, Charlson et al. (1968) reported that

$$L_V \cdot TSP = \frac{3.9 \text{ TSP}}{b_{\text{scat}}} \cong 1.2 \text{ g m}^{-2} \quad (2-17)$$

or restated in units that we will use in this review:

$$b_{\text{scat}} = 0.0325 \cdot TSP \quad (2-18)$$

where b_{scat} is expressed in $[10^4 \text{ m}]^{-1}$ and TSP is total suspended particulate mass in micrograms/m³. Equation (2-18) has the form

$$b_{\text{scat}} = B_{\text{TSP}} \cdot TSP \quad (2-19)$$

which can be obtained from (2-16) by neglecting all effects other than aerosol light scattering and by considering only a single aerosol species.

Later studies in California show that a similar proportionality can be determined by conversion of prevailing visibility observations to extinction coefficient estimates through the Koschmieder formula followed by regression of the extinction coefficient estimates on simultaneous measurements of TSP (Noll et al. 1968; Cass 1976). In studies like that of Cass (1976), the following model is used:

$$b_j = B_{TSP} \cdot TSP_j + B_0 + e_j \quad (2-20)$$

where b_j is the total atmospheric extinction coefficient during sampling period j , B_{TSP} is the extinction per unit total suspended particulate matter concentration, B_0 is a regression constant, and e_j is the residual difference term for sampling period j that results from an inexact fit between observed extinction coefficient and TSP values. Equation (2-20) also can be related to (2-16), but in a slightly different manner than (2-19). In (2-20), the total atmospheric extinction coefficient is used, which includes effects due to light absorption by gases and particles. However, lacking data on NO_2 concentrations, light absorption due to NO_2 has been neglected on the right-hand side of that equation. Only a single aerosol species is considered, and the effect of Rayleigh scattering has been absorbed into the regression equation as an undetermined constant. When fit as an undetermined constant, if the estimate for B_0 does not match the Rayleigh scattering value to within reasonable error bounds, then there is an indication that the calculation is not capturing some important aspects of the system being modeled.

A variety of studies in which TSP concentration fluctuations have been used in an attempt to explain changes in light scattering or prevailing visibility are summarized in Table 2.3. Estimates obtained for the extinction efficiency of total suspended particulate matter are reasonably similar, regardless of whether equations like 2-19 or 2-20 are used. This would be expected if light scattering by aerosols dominates visibility reduction (which it often does) and if the underlying aerosol properties (e.g. normalized size distributions) are not greatly different from place to place.

The disadvantages of visibility models based on TSP data alone are many. First, the correlation between observed and predicted extinction co-

TABLE 2.3 ESTIMATES OF EXTINCTION COEFFICIENTS PER
UNIT TOTAL SUSPENDED MASS CONCENTRATION(a)

Reference	Measurement Method	Location	Extinction Efficiency(b) ($10^{-4} \text{ m}^{-1}/\mu\text{g m}^{-3}$)	Correlation Coefficient
Charlson et al. (1968)	Nephelometer, low volume filter mass concentration	New York City, NY	0.0302	0.92
		San Jose, CA	0.0166	0.56
		Seattle, WA	0.0353	0.83
		Seattle, WA	0.0359	0.73
Noll et al. (1968)	Prevailing visibility, low volume filter mass concentration	Oakland, CA	0.011	0.92
Ettinger and Royer (1972)	Nephelometer, Hi-vol	Los Alamos, NM	0.01	-
Kretzschmar (1975)	Nephelometer, 24-hr Hi-vol samples	Belgium	0.034	0.91
White and Roberts (1977)	Nephelometer, 2-hr average filter samples	Los Angeles, CA	0.032	-
Cass (1976, 1979)	Prevailing visibility, 24-hr Hi-vol samples, 1965-1974.	Los Angeles, CA (Downtown)	0.037	0.40
Patterson and Wagman (1977)	Nephelometer, Hi-vol samples		0.016	-

TABLE 2.3 (Continued) ESTIMATES OF EXTINCTION COEFFICIENTS
PER UNIT TOTAL SUSPENDED MASS CONCENTRATION(a)

Reference	Measurement Method	Location	Extinction Efficiency(b) ($10^{-4} \text{ m}^{-1}/\mu\text{g m}^{-3}$)	Correlation Coefficient
Clarke et al. (1977)	Nephelometer, total filter mass	Leeds, United Kingdom	0.022	0.92
Trijonis and Yuan (1978a)	Prevailing Visibility, 24-hr Hi-vol samples	Phoenix area, Arizona	0.0025	0.31

(a) References identified by Charlson et al. (1978)

(b) Extinction coefficient per unit total suspended particulate
mass concentration

efficient estimates often is low, particularly for long time series data in heavily polluted areas like Los Angeles where aerosol properties are complex and are not preserved from day to day. Secondly, even if the model fits well, it yields very little information about efficient control strategies for visibility improvement. No hint is given of the sources contributing to the TSP problem. More importantly, if some particulate sources were controlled but not others (i.e. if large soil dust particles alone were somehow removed from the atmosphere) the model would not correctly predict the change in visual range. Because the TSP mass reduction would be accompanied by a shift in the particle size distribution, the assumptions of this single species model would be upset.

2.6.2 Models That Incorporate the Chemical Composition of Total Filter Samples

If total suspended particulate matter samples are subdivided chemically, a significant improvement in visibility model performance can be obtained. Chemical species data serve as a guide to particle size, solubility, and refractive index.

Much of the total suspended particulate matter in the atmosphere resides in a large particle mode ($d_p \geq 2$ microns) whose contribution to light scattering per unit mass concentration is well below that for the aerosol as a whole. Most of that large particle mass consists of soil dust-like materials that can be identified by a chemical fingerprint that is rich in aluminum, silicon, iron, and manganese. In a similar fashion, smaller particles of diameter nearly equal to that of visible solar radiation ($d_p \approx 0.5$ micron) have a disproportionately high light scattering efficiency per unit mass concentration. Size-resolved samples taken in many locations show that the fine particle mode in the atmosphere consists mostly of sulfates, nitrates, lead salts, and carbon containing aerosols. Thus, if data on chemical composition alone were available from total filter samples, some inferences can be drawn about the likely size distribution (and hence extinction efficiency) of the aerosol mixture collected on the filters.

A regression model for the extinction coefficient at time j , drawn directly from (2-16) might be specified in this case as:

$$b_j = \sum_{i=1}^N B_i M_{ij} + \gamma_{NO_2} \cdot C_{NO_2_j} + b_{Rayleigh} + e_j \quad (2-21)$$

where each term is as previously defined except that the B_i are undetermined constants representing the average extinction efficiency of each chemical species i (i = sulfates, soil dust, nitrates, etc.), and the M_{ij} are measurements of the mass concentration of each species i at time j .

The selection of species to be used with equations like (2-21) in practice depends on the availability of air monitoring data. When using routine high volume sampler data from the National Air Surveillance Network (NASN) or state and local government Hi-Vol networks, the actual equations estimated typically look like

$$\begin{aligned}
 b_j = & B_{SO_4} \cdot \text{SULFATES}_j + B_{NO_3} \cdot \text{NITRATES}_j + \\
 & B_{\text{TSP-SO}_4\text{-NO}_3} (\text{TSP-SULFATES-NITRATES})_j + \\
 & \gamma_{NO_2} \cdot C_{NO_2} + B_o + e_j
 \end{aligned}
 \tag{2-22}$$

where B_{SO_4} , B_{NO_3} , and $B_{\text{TSP-SO}_4\text{-NO}_3}$ are constants. SULFATES_j and NITRATES_j are daily SO_4^{2-} and NO_3^- ion mass concentrations scaled up by a factor of about 1.3 in order to represent the mass of the likely sulfate and nitrate compounds present in the atmosphere (usually ammonium salts). The term (TSP-SULFATES-NITRATES) represents the non-sulfate, non-nitrate portions of the aerosol mass, and is obtained from TSP data by subtraction. When equations like (2-22) are fit to routine Hi-Vol data, one typically finds that B_{SO_4} is much greater than $B_{\text{TSP-SO}_4\text{-NO}_3}$. This is expected since the sulfate aerosol is usually submicron in size and thus scatters light effectively, while the remainder of the particulate mass (TSP-SULFATES-NITRATES) is often large particle soil-dust-like material that is very ineffective at scattering light. Values obtained for B_{NO_3} in such regression models often are inconsistent with that expected for submicron aerosols. Poor results for light scattering by nitrates may be due to the difficulties inherent in obtaining accurate atmospheric nitrate concentration measurements (Appel et al. 1981; Witz and Wendt 1981). Table 2.4 lists values for the light extinction efficiency of particular chemical species obtained from regression analysis based on models similar to (2-22). Actual references cited should be examined, as model structure varies from study to study (some studies do not allow for NO_2 effects; some examine a differing list of aerosol species).

TABLE 2.4 LIGHT EXTINCTION EFFICIENCIES OF AEROSOL CHEMICAL SPECIES AS INFERRED FROM EMPIRICAL VISIBILITY MODELING STUDIES

(From: White and Roberts, 1980)

	White, Roberts, 1977 Equation 9	White, 1976 Double Regression	Cass, 1976 Table III, Entry 3	Grosjean et al., 1976 Page 5	Trijonis, Yuan, 1978 Phoenix - Regression	Trijonis, Yuan, 1978 Phoenix - Strike	Trijonis, Yuan, 1978 Salt Lake City	Leaderer et al., 1979 Santa Monica - LAX
<u>Efficiencies,</u> $10^{-4} \text{ m}^2/\mu\text{g}$								
Sulfates								
30% RH ^a			.101		.033	.039	.031	
50% RH			.126				.043	
70% RH ^a	.062	.085	.177	.165			.071	.14
Nitrates								
30% RH ^a	.027	.030	.045				.072	
50% RH	.035	.040					.101	
70% RH ^a	.047	.042	.080	.028			.169	.03
Other ^c								
All RH	.022	.022	<.01				.003	
<u>Fraction of variance</u> <u>accounted for (r^2)</u>	.93	--	.64	.59	.76	--	.66	.83

* Efficiencies represent statistical increment in total scattering or extinction coefficient (10^{-4} m^{-1}) per increment in individual compound concentration ($\mu\text{g}/\text{m}^3$). The data of Lundgren (excessive colinearity), and of Grosjean and Friedlander (insufficient observations), do not support distinct component efficiencies.

^a Efficiencies not differentiated by RH are entered nearest the average RH for the data set.

^b Extinction efficiencies (cf. note to Table A1) are based on Middleton's experimental value $\epsilon_{\text{m}} = .031$ for the contrast threshold (Middleton, 1952, p. 220), rather than the traditional but arbitrary value $\epsilon_{\text{m}} = .020$ used by Cass, Trijonis, and Yuan, and Leaderer et al.

2.6.3 Separation of Aerosol Light Absorption from Aerosol Light Scattering

Extinction efficiencies per unit aerosol mass concentration, B_i , in equations like (2-21) include effects due to both light scattering and absorption. It is possible to separate these two effects. Total light scattering can be measured using integrating nephelometers (Charison et al. 1978), while aerosol light absorption can be determined from filter samples by the integrating plate method (Lin et al. 1973). Separate linear models for species contributions to b_{scat} and b_{abs_a} can be formulated and the coefficients estimated by regression analysis:

$$b_{scat_j} = \sum_{i=1}^N B_{s_i} M_{ij} + b_{Rayleigh} + e_j \quad (2-23)$$

$$b_{abs_{a_j}} = \sum_{i=1} B_{a_i} M_{ij} + e_j \quad (2-24)$$

where b_{scat_j} is the total light scattering (gases + aerosols) at time j , $b_{abs_{a_j}}$ is aerosol light absorption at time j , the B_{s_i} refer to aerosol light scattering efficiency by species i , the B_{a_i} indicate aerosol light absorption efficiency, and other terms are as previously defined. Adding (2-23) to (2-24) and inserting a term for light absorption by NO_2 , one obtains a model for the total light extinction coefficient.

$$b_{ext_j} = \sum_{i=1} B_{s_i} M_{ij} + \sum_{i=1} B_{a_i} M_{ij} + \gamma_{NO_2} \cdot C_{NO_2} + b_{Rayleigh} + e_j \quad (2-25)$$

A variety of studies show that graphite-like "elemental" carbon particles are the most abundant light absorbing aerosol species in the atmosphere. Field measurements in Los Angeles (Conklin et al. 1981) and in Denver (Groblicki et al. 1980) indicate that the light absorption efficiency, B_{a_i} , of ambient agglomerates of elemental carbon is about $0.12 \cdot 10^{-4} \text{ m}^{-1}$ per microgram m^{-3} if measured by the integrating plate method.

2.6.4 Incorporation of Relative Humidity Effects

Hygroscopic and deliquescent particles in the atmosphere take up water at high humidity and grow in size. The water attached to the aerosol increases

the volume (mass) of scattering material. Also, light scattering efficiency by aerosols is a strong function of particle size. Thus, humidity-induced aerosol growth is often accompanied by increases in the extinction coefficient and a reduction in visual range for the same quantity of pollutant material in the atmosphere.

The diameter of a solution droplet in equilibrium with a surrounding humid atmosphere is determined by a competition between the vapor pressure lowering effects of dissolved substances in the particle and the vapor pressure raising effects of particle surface curvature. For a particle with a fixed mass of solute (e.g. a fixed mass of a sulfate salt), the change in particle radius with humidity would be predicted to vary in proportion to the quantity $(1-RH)^{-1/3}$ (Neiburger and Wurtele 1949; Hanel 1972, 1976, 1981).

Light scattering by large particles with diameter greater than several microns is expected to increase in proportion to particle cross-sectional area. Hence, light scattering by large solution droplets should change in proportion to $(1-RH)^{-2/3}$. Smaller particles with a diameter closer to 0.5 microns fall in a size range where Mie theory would not predict such a simple dependence on particle cross-sectional area. But empirical studies in Los Angeles (Hidy et al. 1974) show that light scattering by submicron aerosols is highly correlated with submicron aerosol volume. Thus changes in light scattering by submicron aerosol droplets might be proportional to the function $(1-RH)^{-1}$ (i.e. in proportion to changes in particle radius cubed). Since the atmosphere contains a mixture of both large and small particles, only some of which are hygroscopic, regression effects are often specified with terms containing $(1-RH)^{-\alpha}$. In these expressions, α is an undetermined coefficient to be fit during the analysis with α expected to fall between 1 and 0.667 for hygroscopic aerosol particles, and with $\alpha = 0$ for non-hygroscopic species. In a manner analogous to (2-25)

$$b_j = \sum_{i=1}^N \frac{B_{s_i} M_{ij}}{(1-RH_j)^{\alpha_i}} + \sum_{i=1}^N B_{a_i} M_{ij} + Y_{NO_2} \cdot C_{NO_2_j} + b_{Rayleigh} + e_j \quad (2-26)$$

where the regression constants, B_{s_i} , in (2-25) are replaced by a hyperbolic function of relative humidity. An expression similar to this was tested by Cass (1979) in Los Angeles. Light scattering by substances like sulfates

and nitrates was best fit by values of α between 1.09 and 0.53, while light scattering by the largely non-hygroscopic substances present in the remainder of the aerosol mass showed a much smaller dependence on relative humidity ($\alpha = 0.28$, with α not significantly different from zero in a statistical sense).

Non-linear regression equations like (2-26) offer some hope of at least approximately incorporating the important effects of humidification on visual range. But regression models based on such a structure must be viewed with caution. The ability to separate light scattering by aerosol species having different humidity dependencies into additive terms depends in the strict sense on having an aerosol that is an external mixture (e.g. each particle must be a pure example of species i). Secondly, it must be noted that many salts [e.g. $(\text{NH}_4)_2\text{SO}_4$, NH_4NO_3] exhibit pronounced deliquescence. A dry particle of a deliquescent salt when subjected to increasing humidification does not grow initially. Then as its humidity of deliquescence is reached, the particle goes suddenly into solution and grows rapidly upon further humidification. Such behavior is illustrated in Figure 3.2. However, since a variety of deliquescence points exist for different sulfate species, and since the actual chemical compounds present are seldom distinguished in routine filter analysis for the $\text{SO}_4^{=}$ ion alone, often there is no practical way to include deliquescence effects in an empirical visibility model. Equations of the form (2-26) represent the growth of externally mixed aerosols after they are in the liquid phase, but do not track the changes that occur at the deliquescence point of the aerosol.

The non-linear form of (2-26) can cause computational problems when trying to estimate the coefficients α_j and B_{S_j} . First, if both α_j and B_{S_j} are to be estimated, a non-linear method for minimizing the sum of the squares of the residual error terms is needed. Secondly, the questions of using time averaged data must be addressed. The extinction coefficient, b_j , in that equation prevails for an instantaneous time and should be used with short term pollutant concentration and humidity data. If equations like (2-26) are averaged over time in order to report daily average values of pollutant mass concentration and relative humidity, cross product terms involving short term fluctuations in aerosol mass and humidity would be created. Methods for

addressing both the time averaging problem and the non-linear fitting problem are given by Cass (1979). Since the data analysis procedures needed to fix these problems are cumbersome, most investigators that evaluate large data sets have chosen to use more approximate approaches. Typically, the values of α_i in (2-26) have been set equal to 1.0, 0.67, or zero based on a priori expectations that a particular aerosol species is submicron in size and hygroscopic, large in size and hygroscopic, or non-hygroscopic, respectively. With the α_i fixed, then linear regression techniques would be used to estimate the B_i . Secondly, the time averaging question often is treated by using short term data or by assuming (often implicitly) that the value of the cross product terms is zero.

An empirical visibility model for use with routine high volume sampler data that has been tested widely by Trijonis is of the form:

$$b_j = \sum_{i=1} \frac{B_i}{(1 - RH_j)} \cdot \bar{M}_{ij} + B_0 + e_j \quad (2-27)$$

where the overbars indicate time averaged data, the α 's are fixed to 1.0 in addition to sulfates and nitrates, and light absorption by NO_2 is neglected (as NO_2 data are often lacking). Estimates for light extinction per unit mass concentration by sulfates, nitrates, and the remainder of the atmospheric aerosol are summarized in Table 2.4.

2.6.5 Incorporation of Partial Information on Aerosol Size Distribution

A variety of relatively inexpensive sampling devices exist that can separate ambient aerosols into coarse particle ($d_p \geq 2$ micron) and fine particle ($d_p \leq 2$ micron) modes. Size segregated sampling of this sort is possible with virtual impactors like the dichotomous sampler. Alternatively, fine particle samples might be collected using an AIHL-design cyclone (John and Reischl 1980), with coarse aerosol determined by subtracting the fine aerosol mass from simultaneous filter samples that give total aerosol mass.

Light extinction usually is dominated by scattering and absorption of fine aerosols. Therefore, even a single coarse/fine particle size cut provides valuable data on the concentration of those particles that actually cause most visibility reduction. The simplest empirical visibility model using size segregated data could be based on (2-16) as follows:

$$b_{\text{ext}} = \sum_{i=1}^N B_{fi} M_{fi} + \sum_{i=1}^N B_{ci} M_{ci} + \gamma_{\text{NO}_2} \cdot C_{\text{NO}_2} + b_{\text{Rayleigh}} \quad (2-28)$$

where the subscripts f and c refer to fine and coarse aerosol, respectively. Often, one sees such a model abbreviated to the form of regression equations like:

$$b_{\text{ext}_j} = B_f \cdot M_{fj} + e_j \quad (2-29)$$

or

$$b_{\text{scat}_j} = B_{sf} \cdot M_{fj} + e_j \quad (2-30)$$

where the M_{fj} 's are total fine aerosol mass concentration data at time j, and the implicit assumption is made that the extinction coefficient is largely due to light scattering (and absorption) by fine aerosols. By comparison with (2-25) and (2-26), it is clear that many other factors are being ignored. The correlation between aerosol light scattering and both fine and coarse particle mass is shown in Figure 2.5. Extinction efficiencies per unit fine aerosol mass estimated from regression of extinction coefficient estimates on fine aerosol mass measurements alone are given in Table 2.5. In spite of their simplicity, empirical visibility models based on equations (2-29 - 2-30) work quite well, because they do capture the most important determinant of aerosol extinction efficiency: particle size. Such models do not however, yield any useful information about which sources contribute to the fine aerosol, and hence to the visibility problem. Thus little will be learned about how to improve visual range if fine aerosol mass alone is used to model the extinction coefficient.

2.6.6 Special Studies Based on High Quality Data Sets

If a special air monitoring study can be designed for the purpose, then empirical visibility models can be constructed and tested that include all of the features enumerated previously. Such studies have recently been completed by General Motors Research Laboratories in order to assess the origin of visibility reduction in Denver (Groblicki et al. 1980) and the rural Northeast (Ferman et al. 1981).

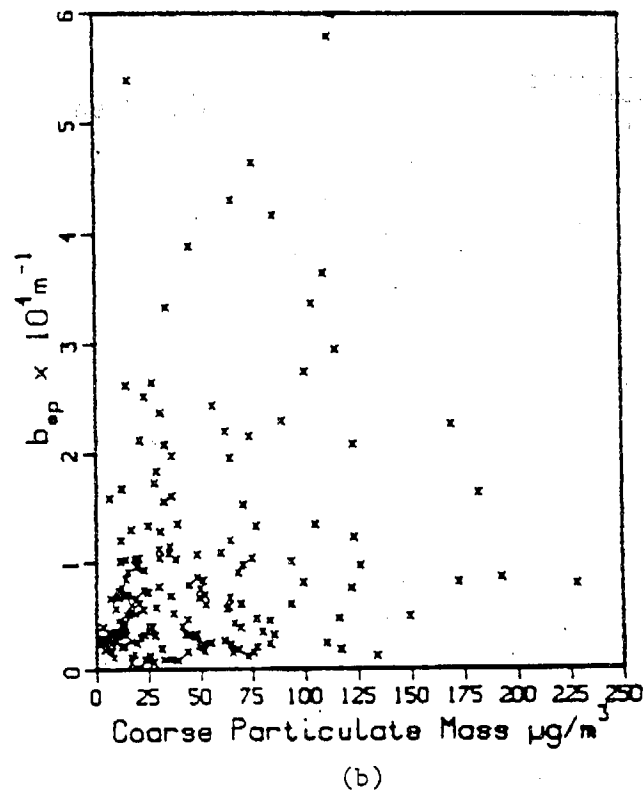
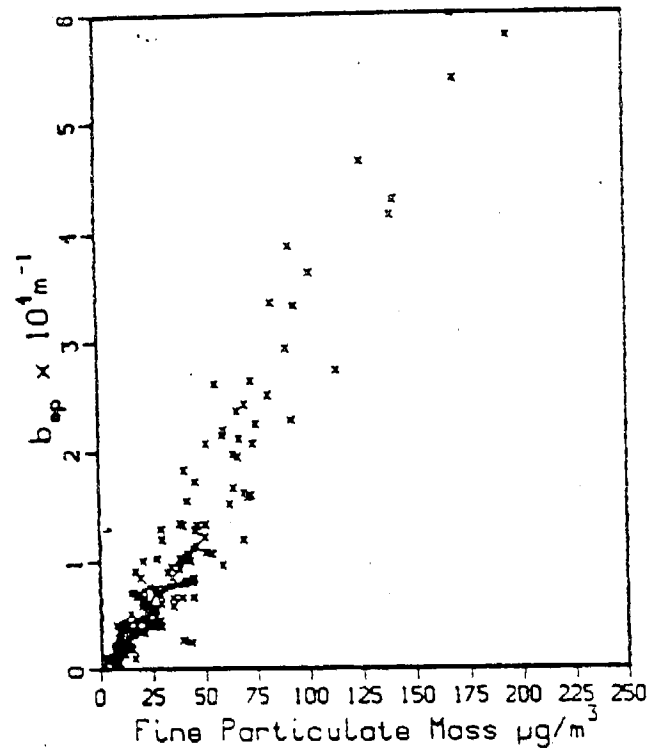


Figure 2.5 Correlation between aerosol light scattering and (a) fine particle and (b) coarse particle mass (From: Groblicki et al. 1980)

TABLE 2.5 ESTIMATES OF EXTINCTION COEFFICIENT PER
UNIT FINE PARTICULATE MASS CONCENTRATION

Reference	Measurement Method	Location	Extinction Efficiency(a) ($10^{-4} \text{ m}^{-1} / \mu\text{g m}^{-3}$)	Correlation Coefficient
Waggoner and Weiss (1980)	Nephelometers,	Mesa Verde, CO	0.0294	-
	Dichotomous	Seattle, WA	0.0313	0.95
	samplers, fine	Seattle, WA	0.0323	0.97
	$d_p \leq 3$ micron	Puget Island, WA	0.0303	0.97
		Portland, OR	0.0323	0.95
Groblicki et al. (1980)	Heated nephelometers, filter preceeded by a cyclone separator, fine $d_p \leq 2.5$ micron	Denver, CO	0.033	0.98
Ferman et al. (1981)	Heated nephelometer, dichotomous sampler, $d_p \leq 2.5$ micron	Shenandoah Valley, VA	0.073	0.91

(a) Extinction coefficient per unit fine aerosol mass

In their approach, the extinction coefficient was first partitioned as follows:

$$b_{\text{ext}} = b_{\text{scat}_a} + b_{\text{scat}_w} + b_{\text{abs}_a} + b_{\text{abs}_g} + b_{\text{Rayleigh}} \quad (2-31)$$

where the b's are extinction coefficient contributions as defined previously, but with aerosol scattering divided into contributions from dehumidified aerosol (b_{scat_a}) plus associated water (b_{scat_w}). Each of these contributions to the extinction coefficient was measured separately. Scattering by dehumidified aerosols, b_{scat_a} , was measured using a heated nephelometer. Then b_{scat_a} was attributed to chemical constituents of the fine aerosol mass by regression analysis

$$b_{\text{scat}_a j} = \sum_{i=1}^N B_{sf_i} M_{sf_{ij}} + e_j \quad (2-32)$$

In Denver, 157 4-hour average fine particle filter samples were used in a regression analysis to estimate the coefficients in (2-32). The final regression equation took the form

$$b_{\text{scat}_a} = 0.066 \left[(\text{NH}_4)_2\text{SO}_4 \right] + 0.023 \left[\text{NH}_4\text{NO}_3 \right] + 0.044 \left[1.2C_{\text{ao}} \right] + 0.032 \left[C_{\text{ae}} \right] + 0.017 \left[\text{Remainder} \right] - 0.17 ; (r^2 = 0.94) \quad (2-33)$$

where the constants are extinction efficiencies at low humidity for the aerosol species shown (10^{-4}m^{-1} per microgram/ m^3), $1.2 C_{\text{ao}}$ is an estimate of organic material mass concentration based on scale up of organic carbon (C_{ao}) concentrations present, C_{ae} is elemental carbon concentration, and "Remainder" is the non-sulfate, non-nitrate, non-carbonaceous fine aerosol mass concentration.

Scattering by water present in the aerosol was identified from the differences in data from heated and unheated nephelometers. An expression was used to account for water present on the basis of atmospheric hygroscopic salt concentrations:

$$b_{\text{scat}_w} = \frac{0.0173 \left[(\text{NH}_4)_2\text{SO}_4 \right]}{(1 - \text{RH})} + \frac{0.0147 \left[\text{NH}_4\text{NO}_3 \right]}{(1 - \text{RH})}; r^2 = 0.87 \quad (2-34)$$

were the constants were fitted by regression analysis.

Aerosol light absorption was attributed to elemental carbon aerosols with an absorption efficiency of $0.125 \cdot 10^{-4} \text{ m}^{-1} / \text{microgram m}^{-3}$ for fine particle elemental carbon (C_{aef}) plus $0.038 \cdot 10^{-4} \text{ m}^{-1} / \text{microgram m}^{-3}$ for coarse particle elemental carbon (C_{aec}). NO_2 concentrations were measured and used to estimate b_{abs_g} , with γ_{NO_2} at $3.3 \cdot 10^{-4} \text{ m}^{-1} / \text{ppm}$.

The final empirical visibility model constructed was

$$b_{\text{ext}} = 0.066 S + 0.028 N + 0.44(1.2C_{\text{aof}}) + 0.032C_{\text{aef}} + 0.017 R - 0.17 + \frac{0.0173 S}{(1 - \text{RH})} + \frac{0.0147 N}{(1 - \text{RH})} + 0.125C_{\text{aef}} + 0.038C_{\text{aec}} + 3.3C_{\text{NO}_2} \quad (2-35)$$

where

S - 4-hour average $(\text{NH}_4)_2\text{SO}_4$ concentration in fine particles ($\mu\text{g}/\text{m}^3$)

N - 4-hour average NH_4NO_3 concentration in fine particles

R - 4-hour average for remainder of fine aerosol mass concentration

b_{ext} - the extinction coefficient in 10^{-4} m^{-1}

and other terms are as previously defined. This expression fits the Denver extinction coefficient data extremely well with a correlation coefficient of 0.975. Key reasons for the good fit include the completeness and high quality of the pollutant chemistry measurements, the short sample averaging times, and the size segregated nature of the aerosol data. Given high quality measurements designed for the purpose of a visibility study, empirical visibility models can be structured that make physical sense, that track changes in total extinction extremely well, and that yield insight into the portion of the visibility problem attributable to different pollutants and sources.

2.6.7 Hybrid Models that Closely Approach a Complete Mie Scattering and Absorption Calculation

A basis for comparing empirical extinction coefficient models to Mie theory calculations is provided by Ouimette (1981). Let the total light extinction coefficient due to aerosols, b_{ext_a} , be given by

$$b_{\text{ext}_a} = b_{\text{scat}_a} + b_{\text{abs}_a} \quad (2-36)$$

This aerosol extinction coefficient can be broken down into contributions due to each of the many aerosol species present in the atmosphere (soil dust, sulfates, etc.),

$$b_{\text{ext}_a} = \sum_{i=1}^N b_{\text{ext}_{a_i}} \quad (2-37)$$

where the subscript i refers to the i -th chemical constituent. Assume that the aerosol is either an external mixture (each particle is a pure example of some species i) or a specific mixture (all particles of the same size and chemical composition). Then, the extinction coefficient to each aerosol species i can be written as

$$b_{\text{ext}_{a_i}} = \int_0^{\infty} E(m_a(x), x, \lambda) f_i(x) dx \quad (2-38)$$

where the mass distribution by particle diameter, d , of species i is $f_i(x) = dM_i/dx$, where $x = \log(d/d_0)$, and E is the mass extinction efficiency for species i as a function of its volume average refractive index $m_a(x)$, particle size x , and wavelength λ . Equation (2-38) can be used as a basis for a semi-empirical visibility model that is very close to a full Mie scattering and absorption calculation. The integral in (2-38) is replaced by a summation over each of the size ranges defined by the stages of a cascade impactor. A description of an appropriate cascade impactor is given by Hering et al. (1978). The chemical composition of the mass distribution collected on each impactor stage is measured. From the chemical composition data, approximate refractive index data are selected from the literature for each chemical species i . Then Mie theory calculations for $E(m_a(x), x, \lambda)$ are executed using a computer code developed for single scattering by spherical particles (see Wickramasinghe 1973).

Ouimette and Flagan (1981) have compared extinction efficiencies estimated from chemically resolved impactor data using Mie theory approximations (like equation 2-38) to the results obtained using linear statistical models (like equation 2-15). Results are given in Table 2.6 for aerosol collected under low humidity conditions at China Lake, California. Values in parenthesis below the mass scattering efficiency estimates represent one standard deviation on their results. 95% confidence intervals on the theoretically and statistically estimated mass scattering efficiencies overlap for each chemical species studied indicating that the two methods in this case yield indistinguishable results.

Visibility models based on the approach of Ouimette (1981) are probably the best presently available for use by regulatory agencies. Unfortunately, the chemically resolved cascade impactor data required for use in such calculations are not collected routinely.

2.7 CONCLUSIONS

Over a number of different approaches have been examined for relating atmospheric concentrations of gases and aerosols to perceived visibility. As a practical matter, the choice facing a person who must select a visibility model is frequently dictated by data availability. For example, vast amounts of information are needed by regional radiative transfer models if they are to accurately characterize the simultaneous effects of: emissions, transport, dispersion, chemical transformations, and optical interactions. For this practical reason, the most appropriate choice of a modeling methodology for immediate practical application is the class of methods based on regression analysis, or the receptor oriented theoretical calculation scheme of Ouimette (1981). Given high quality measurements, these two types of empirical visibility models can be structured to make physical sense, track changes in total extinction extremely well, and yield insight into the portion of the visibility problem attributable to different pollutants.

TABLE 2.6 AEROSOL SPECIES CONTRIBUTIONS TO THE PARTICLE SCATTERING COEFFICIENT: COMPARISON OF STATISTICAL AND THEORETICAL RESULTS FOR CHINA LAKE
(From: Ouimette and Flagan, 1981)

Aerosol Species, f	1979 Average Mass Concentration, M_f $\mu\text{g}/\text{m}^3$	Mass Scattering Efficiency, α_f m^2/g		Contribution to b_{sp} , 10^{-4}m^{-1}		% Contribution to Total Measured b_{sp}	
		Stat. (S.E.)	Theor. (S.E.)	Stat.	Theor.	Stat.	Theor.
Sulfates	2.55	5.03 (0.64)	3.20 (0.96)	12.8	8.2	50.4	32.3
Organics	1.97	1.54 (0.62)	2.46 (0.75)	3.0	4.8	11.8	18.9
Crustal	1.94	2.36 (0.67)	1.42 (0.42)	4.5	2.8	18.1	11.0
Unaccounted	4.24	1.00 (0.31)	2.35 (0.71)	4.2	9.9	16.5	39.0
Computed Total				24.6	25.7	97	101
Measured Total				25.4	25.4	100	100

Stat. - Statistical
Theor. - Theoretical
(S.E.) - Standard error

2.8 REFERENCES FOR CHAPTER 2

- Appel, B.R., Y. Tokiwa, and M. Haik, "Sampling of Nitrates in Ambient Air," Atmospheric Environment, 15, pp. 283-289, 1981.
- Bergstrom, R.W., B.L. Babson, and T.P. Ackerman, "Calculation of Multiply-Scattered Radiation in Clean Atmospheres," Atmospheric Environment, 15, pp. 1821-1826, 1981a.
- Bergstrom, R.W., C. Seigneur, B.L. Babson, H-Y Holman, and M.A. Wojcik, "Comparison of the Observed and Predicted Visual Effects Caused by Power Plant Plumes," Atmospheric Environment, 15, pp. 2135-2150, 1981b.
- Cass, G.R., "The Relationship Between Sulfate Air Quality and Visibility at Los Angeles," Environmental Quality Laboratory Memorandum 18, California Institute of Technology, Pasadena, California, 1976.
- Cass, G.R., "On the Relationship Between Sulfate Air Quality and Visibility with Examples in Los Angeles," Atmospheric Environment, 13, pp. 1069-1084, 1979.
- Chandrasekhar, S., Radiative Transfer, Dover Publications, New York, 1960.
- Charlson, R.J., "Atmospheric Visibility Related to Aerosol Mass Concentration -- a Review," Environmental Science and Technology, 3, pp. 913-918, 1969.
- Charlson, R.J., N.C. Ahlquist, and H. Horvath, "On the Generality of Correlation of Atmospheric Aerosol Mass Concentration and Light Scatter," Atmospheric Environment, 2, pp. 455-464, 1968.
- Charlson, R.J., D.S. Covert, Y. Tokiwa, and P.K. Mueller, "Multiwavelength Nephelometer Measurements in Los Angeles Smog Aerosol - III Comparison to Light Extinction by NO_2 ," J. Colloid and Interface Science, 39, pp. 260-265, 1972.
- Charlson, R.J., A.P. Waggoner, and J.F. Thielke, Visibility Protection for Class I Areas: The Technical Basis, Council on Environmental Quality, Washington, D.C., 1978.
- Clarke, A.G., M.A. Moghadassi, and A. Williams, "A Comparison of Techniques for Automatic Aerosol Mass Concentration Measurement," J. Aerosol Science, 8, pp. 73-81, 1977.
- Conklin, M.C., G.R. Cass, L-C Chu, and E.S. Macias, "Wintertime Carbonaceous Aerosols in Los Angeles, An Exploration of the Role of Elemental Carbon," in Atmospheric Aerosol: Source/Air Quality Relationships, eds. E.S. Macias and P.K. Hopke, ACS Symposium Series, 167, American Chemical Society, Washington, D.C., 1981.
- Cooper, J.A., J.G. Watson, Jr., "Receptor Oriented Methods of Air Particulate Source Apportionment," Journal of the Air Pollution Control Association, 30, pp. 1116-1125, 1980.

Dabberdt, W.F. and S.L. Eigsti, "Regional Visibility Modeling for the Eastern United States," Atmospheric Environment, 15, pp. 2055-2061, 1981.

Dave, J.V., "Transfer of Visible Radiation in the Atmosphere," Atmospheric Environment, 15, pp. 1805-1820, 1981.

Drivas, P.J., A. Bass, and D.W. Heinhold, "A Plume Blight Visibility Model for Regulatory Use," Atmospheric Environment, 15, pp. 2179-2184, 1981.

Drivas, P.J., S. Machiraju, and D.W. Heinhold, ERT Visibility Model: Version 3 - Technical Description and User Guide, Environmental Research and Technology Technical Document No. M-2020-001, Concord, Massachusetts, 1980.

Ettinger, H.J. and G.W. Royer, "Visibility and Mass Concentration in a Non-urban Environment," Journal of the Air Pollution Control Association, 22, pp. 108-111, 1972.

Ferman, M.A., G.Y. Wolff, and N.A. Kelly, "The Nature and Sources of Haze in the Shenandoah Valley/Blue Ridge Mountains Area," Journal of the Air Pollution Control Association, 31, pp. 1074-1082, 1981.

Fox, D., R.J. Loomis, and T.C. Greene, eds., Proceedings of the Workshop in Visibility Values, Fort Collins, Colorado, January 28-February 1, 1979, U.S. Department of Agriculture, Forest Service, Washington, D.C., 1979.

Gordon, G.E., "Receptor Models," Environmental Science and Technology, 14, pp. 792-800, 1980.

Groblicki, P., G.T. Wolff, and R.J. Countess, "Visibility Reducing Species in the Denver 'Brown Cloud'. Part I Relationships Between Extinction and Chemical Composition," in Plumes and Visibility: Measurements and Model Components, Proceedings of the Symposium held at Grand Canyon National Park, Arizona, Sponsored by USEPA, USNPS, EPRI, and Salt River Project, 10-14 November, 1980.

Grosjean, D., G.J. Doyle, T.M. Mischke, M.P. Poe, D.R. Fitz, J.P. Smith, and J.N. Pitts, Jr., Annual Meeting Paper No. 76-20.3, Air Pollution Control Association, 1976.

Hanel, G., "Computation of the Extinction of Visible Radiation by Atmospheric Aerosol Particles as a Function of the Relative Humidity, Based on Measured Properties," Aerosol Science, 3, pp. 377-386, 1972.

Hanel, G., "The Properties of Atmospheric Aerosol Particles as Functions of Relative Humidity at Thermodynamic Equilibrium With Surrounding Moist Air," Advances in Geophysics, 19, pp. 73-188, 1976.

Hanel, G., "An Attempt to Interpret the Humidity Dependencies of the Aerosol Extinction and Scattering Coefficients," Atmospheric Environment, 15, pp. 403-406, 1981.

Hansen, J.E. and L.D. Travis, "Light Scattering in Planetary Atmospheres," Space Science Reviews, 16, pp. 527-610, 1974.

Hering, S.V., R.C. Flagan, and S.K. Friedlander, "Design and Evaluation of a New Low-Pressure Impactor I," Environmental Science and Technology, 12, pp. 667-673, 1978.

Hodkinson, J.R., "Calculations of Color and Visibility in Urban Atmospheres Polluted by Gaseous NO₂," Int. J. of Air and Water Pollution, 10, pp. 137-144, 1966.

Horvath, H., "On the Applicability of the Koschmieder Visibility Formula," Atmospheric Environment, 5, pp. 177-184, 1971a.

Horvath, H., "On the Brown Colour of Atmospheric Haze," Atmospheric Environment, 5, pp. 333-344, 1971b.

Horvath, H., "Author's Reply - On the Brown Colour of Atmospheric Haze," Atmospheric Environment, 6, pp. 144-148, 1972.

Hidy, G.M., et al., "Characterization of Aerosols in California (ACHEX)," Prepared for the California Air Resources Board Under Contract No. 358 by Rockwell International Science Center, 1974.

Isaacs, R.G., "The Role of Radiative Transfer in Visibility Modeling: Efficient Approximate Techniques," Atmospheric Environment, 15, (10,11), pp. 1827-1834, 1981.

John, W. and G. Reischl, "A Cyclone for Size-Selective Sampling of Ambient Air," J. of the Air Pollution Control Association, 30, pp. 872-876, 1980.

Judd, D.B. and G. Wyszecski, Color in Business, Science and Industry, John Wiley and Sons, New York, 1963.

Kretzschmar, J.G., "Comparison Between Three Different Methods for the Estimation of the Total Suspended Matter in Urban Air," Atmospheric Environment, 9, pp. 931-934, 1975.

Latimer, D.A., R.W. Bergstrom, S.R. Hayes, M.K. Liu, J.H. Seinfeld, G.Z. Whitten, M.A. Wojcik, and M.J. Hillyer, The Development of Mathematical Models for the Prediction of Anthropogenic Visibility Impairment, U.S. Environmental Protection Agency Report No. EPA-450/3/78-110abc, 1978.

Leaderer, B.P., T.R. Holford, and J.A.J. Stolwijk, "J. of the Air Pollution Control Association, 29, p. 154, 1979.

Lin, C., M. Baker, and R.J. Charlson, "Absorption Coefficient of Atmospheric Aerosol: A Method for Measurement," Applied Optics, 12, pp. 1356-1363, 1973.

- Malm, W., K. Kelley, J. Molenaar, and T. Daniel, "Human Perception of Visual Air Quality (Uniform Haze)," Atmospheric Environment, 15, (10/11), pp. 1875-1890, 1981.
- McCartney, E.J., Optics of the Atmosphere - Scattering by Molecules and Particles, John Wiley and Sons, New York, 1976.
- Middleton, W.E.K., Vision Through the Atmosphere, Toronto University Press, 1952.
- Neiburger, M. and M.G. Wurtele, "On the Nature and Size of Particles in Haze, Fog and Stratus of the Los Angeles Region," Chemistry Reviews, 44, pp. 321-335, 1949.
- Nixon, J.K., "The Absorption Coefficient of Nitrogen Dioxide in the Visible Spectrum," J. Chemical Physics, 8, pp. 157-160, 1940.
- Noll, K.E., P.K. Mueller, and M. Imada, "Visibility and Aerosol Concentrations in Urban Air," Atmospheric Environment, 2, pp. 465-475, 1968.
- Ouimette, J.R., Chemical Species Contributions to the Extinction Coefficient, Ph. D. Thesis, California Institute of Technology, Pasadena, California, 1981.
- Ouimette, J.R. and R.C. Flagan, "Chemical Species Contributions to Light Scattering by Aerosols at a Remote Arid Site," in Atmospheric Aerosol: Source/Air Quality Relationships, eds. E.S. Macias, and P.K. Hopke, ACS Symposium Series, 107, American Chemical Society, Washington, D.C., 1981.
- Patterson, R.K. and J. Wagman, "Mass and Composition of an Urban Aerosol as a Function of Particle Size for Several Visibility Levels," J. Aerosol Science, 8, pp. 269-279, 1977.
- Penndorf, R.B., J. Optical Society of America, 47, p. 176.
- Trijonis, J. and K. Yuan, "Visibility in the Southwest: An Exploration of the Historical Data Base," U.S. Environmental Protection Agency Report EPA-600/3-78-039, Research Triangle Park, North Carolina, 1978a.
- Trijonis, J. and K. Yuan, "Visibility in the Northeast: Long-Term Visibility Trends and Visibility/Pollutant Relationships," U.S. Environmental Protection Agency Report EPA-600/3-78-075, Research Triangle Park, North Carolina, 1978b.
- U.S. Environmental Protection Agency, Protecting Visibility - An EPA Report to Congress, U.S. Environmental Protection Agency Report No. EPA-450/5-79-008, 1979.
- U.S. Environmental Protection Agency, Workbook for Estimating Visibility Impairment, U.S. Environmental Protection Agency Report No. EPA-450/3-80-009a, 1980.
- Vanderpol, A.H. and M.E. Humbert, "Coloration of Power Plant Plumes--NO₂ or Aerosols?" Atmospheric Environment, 15, (10/11), pp. 2105-2110, 1981.

Waggoner, A.P. and R.E. Weiss, "Comparison of Fine Particle Mass Concentration and Light Scattering Extinction in Ambient Aerosol," Atmospheric Environment, 14, pp. 623-626, 1980.

White, W.H., Nature, 264, 1976.

White, W.H., ed. "Plumes and Visibility: Measurements and Model Components," Atmospheric Environment (Special Issue), 15-10/11, pp. 1785-2406, 1981.

White, W.H. and D.E. Patterson, "On the Relative Contributions of NO₂ and Particles to the Color of Smoke Plumes," Atmospheric Environment, 15, (10/11), pp. 2097-2104, 1981.

White, W.H. and P.T. Roberts, "On the Nature and Origins of Visibility Reducing Aerosols in the Los Angeles Air Basin," Atmospheric Environment, 11, pp. 803-812, 1977.

White, W.H. and P.T. Roberts, "On the Nature and Origins of Visibility Reducing Aerosols in the Los Angeles Air Basin," in The Character and Origins of Smog Aerosols, eds. G.M. Hidy et al., Advances in Environmental Science and Technology, 9, John Wiley and Sons, New York, 1980.

Micheneringho, H.C., Light Scattering Functions for Small Particles With Applications in Astronomy, John Wiley, New York, 1973.

Williams, M., L.Y. Chan, and R. Lewis, "Validation and Sensitivity of a Simulated-Photograph Technique for Visibility Modeling," Atmospheric Environment, 15, (10/11), pp. 2151-2170, 1981.

Witz, S. and J.G. Wendt, "Artifact Sulfate and Nitrate Formation at Two Sites in the South Coast Air Basin: A Collaborative Study Between the South Coast Air Quality Management District and the California Air Resources Board," Environmental Science and Technology, 15, pp. 79-83, 1981.

3. VISIBILITY/AEROSOL RELATIONSHIPS BASED ON HI-VOL DATA

As discussed in the previous chapter, one worthwhile approach for quantifying visibility/aerosol relationships is regression analysis. The most plentiful data base for regression studies consists of routine airport visibility data and routine Hi-Vol particulate data. This chapter describes regression studies based on these routine data sets at 34 locations in California.

3.1 DESCRIPTION OF THE DATA BASE

The data used in this chapter are airport visibility observations, airport relative humidity readings, and Hi-Vol particulate measurements. This section discusses data sources, site selection, and data quality considerations.

3.1.1 Airport Visibility Data

The visibility data used in this report consist of "prevailing visibility" readings made at weather stations (airports). According to National Weather Service procedures, prevailing visibility is defined as the greatest visual range that is attained or surpassed around at least half of the horizon circle, but not necessarily in continuous sectors (Williamson 1973). Daytime visibility is measured by observing markers (e.g. buildings, mountains, towers, etc.) against the horizon sky; nighttime visibility measurements are based on unfocused, moderately intense light sources. Because our experience indicates that daytime and nighttime observations are often incompatible, and that daytime data are usually of higher quality (Trijonis and Yuan 1978; Trijonis 1979), only daytime observations are employed in this study.

Weather observers usually perform visibility measurements each hour, but only the readings from every third hour are entered into the National Climatic Center computerized data base. The visibility reading times that we used for each day at each site are 7:00 AM, 10:00 AM, 1:00 PM, and 4:00 PM PST. At many of our airport study locations, computerized records are

unavailable, so we had to compile the data for these sites from hard-copy NCC records.

3.1.2 Study Locations

The selection of sites for this study is based on several criteria. First, the study is restricted to airports that have an adequate set of markers for estimating visual range. In particular, we have chosen airports that have farthest markers at distances greater than the typical visibility levels for the surrounding areas. Second, we have selected locations where Hi-Vol monitors are situated fairly close to airports. The average distance between our Hi-Vol sites and visibility sites is 4 miles. Third, we have given preference to Hi-Vol sites that report details regarding the chemical composition of TSP; at a minimum each site is required to report SO_4^{2-} and NO_3^- in addition to TSP. Finally, we have attempted to achieve broad geographical coverage of California.

The 34 locations selected for the study are illustrated in Figure 3.1 and listed on the left-hand side of Table 3.1 also indicates the Hi-Vol monitoring agency (NASN - National Air Surveillance Network, ARB - Air Resources Board, or AQMD - Air Quality Management District), the airport data source, and the years of data. It should be remarked that in compiling the data, we have eliminated days with daytime precipitation (because of the possibility that precipitation rather than aerosol concentrations could be dominating visibility). Also, the reader should note that we have selected three duplicate sites to check the equivalency of different Hi-Vol monitoring programs -- NASN versus ARB in San Diego and Sacramento, and AQMD versus ARB in San Jose.

3.1.3 Types of Data

Three types of data are used in this chapter -- visibility data, relative humidity data, and Hi-Vol particulate data. With a few exceptions*,

* Because relative humidity is not taken at certain weather stations, we have made the following substitutions for relative humidity data: Miramar for Gillespie, Tustin MCAS for Orange Co., Tustin MCAS for Fullerton, Thermal for Palm Springs, Castle AFB for Merced, and San Francisco Int. for San Carlos.



Figure 3.1 Locations for visibility/aerosol regression studies based on Hi-Vol data.

TABLE 3.1 SUMMARY OF HI-VOL DATA USED IN VISIBILITY/AEROSOL REGRESSION STUDIES.

HI-VOL SITE	DATA SOURCE	WEATHER STATION (AIRPORT)	HI-VOL TO AIRPORT (MILES)	YEARS OF DATA	TYPES OF HI-VOL DATA					
					TSP	SO ₄	NO ₃	Pb	ORG	OTHER
SAN DIEGO AREA										
San Diego	NASH	San Diego Int.	6	66-76	x	x	x			
San Diego	ARB	San Diego Int.	6	76-79	x	x	x	x		
El Cajon	ARB	Gillespie	3	76-79	x	x	x	x	x	
LOS ANGELES AREA (Coastal)										
Long Beach	NASH	Long Beach	4	67-77	x	x	x			
Costa Mesa	ARB	Orange Co.	4	76-79	x	x	x	x		
Lennox	AQMD	Los Angeles Int.	3	73-77	x	x	x	x		Mn Ni
Downtown L.A.	AQMD	SOLA - AQMD	0	73-77	x	x	x	x		Mn Ni
Santa Barbara	ARB	Santa Barbara	8	76-79	x	x	x	x	x	
LOS ANGELES AREA (Inland)										
Burbank	NASH	Burbank	1	66-74	x	x	x			
La Habra	ARB	Fullerton	2	76-79	x	x	x	x		
Ontario	NASH	Ontario Int.	5	68-73	x	x	x			
San Bernardino	NASH	Norton AFB	4	68-76	x	x	x			
SOUTHEAST DESERT AREA										
Palm Springs	ARB	Palm Springs	3	76-79	x	x	x			
Lancaster	AQMD	Lancaster	6	74-77	x	x	x	x		Mn Ni
Victorville	ARB	George AFB	6	75-79	x	x	x	x		
El Centro	ARB	Imperial Co.	4	76-79	x	x	x	x	x	
CENTRAL COAST AREA										
Salinas	ARB	Salinas	2	6-77	x	x	x	x	x	
Paso Robles	ARB	Paso Robles	6	76-79	x	x	x	x	x	
CENTRAL VALLEY AREA										
Bakersfield	ARB	Bakersfield	4	76-79	x	x	x	x	x	
Fresno	NASH	Fresno	5	70-76	x	x	x			
Merced	ARB	Merced	3	76-79	x	x	x	x		
Sacramento	NASH	Sacramento Exec.	5	68-76	x	x	x			
Sacramento	ARB	Sacramento Exec.	5	76-79	x	x	x	x		
SAN FRANCISCO BAY AREA (Urban)										
Redwood City*	AQMD	San Carlos	3	70-75	x	x	x	x	x	Si
Oakland	NASH	Oakland	7	66-76	x	x	x			
San Jose*	AQMD	San Jose	4	70-75	x	x	x	x	x	Si
San Jose	ARB	San Jose	3	76-79	x	x	x	x		
SAN FRANCISCO BAY AREA (Suburban)										
Livermore*	AQMD	Livermore	3	73-75	x	x	x	x	x	Si
Concord*	AQMD	Concord	3	73-75	x	x	x	x	x	Si
Napa*	AQMD	Napa	6	72-75	x	x	x	x	x	Si
Santa Rosa*	AQMD	Santa Rosa	4	72-75	x	x	x	x	x	Si
NORTHERN COAST AREA										
Humboldt	NASH	Arcata	5	66-70	x	x	x			
NORTHERN INLAND AREA										
Red Bluff	ARB	Red Bluff	1	76-79	x	x	x	x	x	
Yreka	ARB	Montague	9	76-77	x	x	x	x	x	

* Cellulose filter data

the relative humidity data are obtained from the same airport as the visibility observations. The visibility and relative humidity data represent averages of four daytime recordings, while the particulate data represent complete 24-hour averages.

The specific types of Hi-Vol particulate data at each location are summarized in the right hand side of Table 3.1. As noted previously, TSP, SO_4^- , and NO_3^- data are available at all 34 locations. We also have Pb (a tracer for primary particles from highway vehicles) at 24 locations and ORG (organic aerosols) at 14 locations. At a few sites there are data for Si (soil dust tracer), Mn (soil dust tracer), and/or Ni (fuel oil particulate tracer).

At all locations except the six AQMD sites in the San Francisco Bay Area, the Hi-Vol data represent measurements on glass fiber filters. The San Francisco AQMD data are collected on cellulose filters.* Also, ORG represents benzene soluble organic aerosols, except at San Francisco AQMD sites where organics are determined through a filter charring technique.

3.1.4 Data Quality Considerations

Several previous studies (Cass 1979; Trijonis and Yuan 1978; Trijonis 1979, 1980; Leaderer and Stolwijk 1979) have shown that airport visibility data are of good quality for use in characterizing visibility/aerosol relationships. The quality of the data are indicated by the high correlations (typically .7 to .9) obtained in relating the airport visibility data to particulate measurements and/or meteorological measurements.

The most significant quality problem associated with the Hi-Vol data concerns the artifacts and interferences in nitrate measurements (Harker et al. 1977; Spicer and Schumacher 1979; Appel et al. 1979). The implications of the nitrate measurement problems and of certain spatial/temporal mismatches between the airport and Hi-Vol data are discussed later in Section 3.2.5 (Limitations of the Analysis).

*The San Francisco Bay Area AQMD switched to glass fiber filters in 1976.

3.2 STATISTICAL MODELING APPROACH

Our analysis of routine airport and Hi-Vol data follows the statistical procedures established by Cass (1979), White and Roberts (1977), and Trijonis (1979, 1980). Regression equations are developed which relate daytime average visibility to daytime average relative humidity and to 24-hour averages of total suspended particles (TSP), sulfates (SO_4^{2-}), nitrates (NO_3^-), and other Hi-Vol parameters (e.g. benzene soluble organics, lead, nickel, etc.). The coefficients in the regression equations can be interpreted as estimates of "extinction efficiencies" or "extinction coefficients per unit mass" for each aerosol species. These extinction efficiencies can be used to estimate the fraction of haze (or fraction of visibility loss) attributable to each aerosol component. The following subsections summarize the statistical techniques and discuss some of the limitations of the methodology.

3.2.1 Definition of Variables

The parameters for the regression studies consist of visual range [miles], relative humidity [fraction, no units], and particulate concentrations [$\mu\text{g}/\text{m}^3$]. Before conducting the regressions, however, we must perform some simple transformations in the forms of the variables. For example, instead of using visual range (V) as the dependent variable, it is much more appropriate to use the extinction coefficient (B), which is inversely proportional to visual range. As explained in Section 1.1, the extinction coefficient is a linear sum of four components: light scattering by gases, light scattering by aerosols, light absorption by gases, and light absorption by aerosols. Extinction coefficient is most appropriate for use in linear regression models because each of the components of extinction should be directly proportional to aerosol or gas concentrations (assuming other factors, such as light wavelength, aerosol size distribution, particle shape, and refractive index remain constant).

We compute extinction coefficient from visual range data using a modified Koschmeider formula:

$$B = \frac{3.0}{V} \quad (3-1)$$

* For consistency with established convention, we change the units of extinction to [10^{-4}m^{-1}] after applying Equation (3-1).

Equation (3-1) differs from the usual Koschmeider formula, $B = 3.9/V$, in the sense that Equation (3-1) assumes a 5% contrast detection threshold for the visibility observer rather than a 2% detection threshold. We have chosen the modified Koschmeider formula because recent studies (Allard and Tombach 1980; Malm et al. 1979; Trijonis 1979) suggest that airport visibility observations underestimate true instrumental visual range (defined as the distance at which the contrast for a perfectly black target is reduced to 2%). Several investigators specifically recommend using a contrast threshold of 5% (Koschmeider constant of 2.9) in order to obtain an unbiased estimate of extinction coefficient from human observations of visual range (Allard and Tombach 1980; Malm 1979; Middleton 1952; Douglas and Young 1945).

The choice of a Koschmeider constant has a proportional effect on the aerosol extinction efficiencies that we calculate from the regression analysis. The choice has no effect, however, on extinction budgets because total extinction and the extinction contributions from individual aerosol species are both changed in proportion.

Slight transformations must also be applied to the independent variables. Following Went and Roberts (1977), we define

$$\text{SULFATE} = 1.3 \text{SO}_4^- \quad (3-2a)$$

and

$$\text{NITRATE} = 1.3 \text{NO}_3^- \quad (3-2b)$$

in order to account for the mass of cations (mostly ammonium) associated with the measured values of SO_4^- and NO_3^- . The variable,

$$\text{OTHERTSP} = \text{TSP} - \text{SULFATE} - \text{NITRATE} \quad (3-3)$$

is used to represent the non-sulfate, non-nitrate fraction of TSP.

At some of our study sites, we have chemical data for organics and various trace elements (e.g. Pb). The stoichiometric coefficients for converting these chemical data into estimates of suspended particle mass from various source types are as follows (Cass and McRae 1980):

$$\text{Organics} = 1.0 \times \text{ORG}, \quad (3-4a)$$

$$\text{Motor Vehicle Particles} \equiv \text{VEHICLE} = k \times \text{Pb}, \quad (3-4b)$$

where "k" is 7.3 for 1974 and prior years and increases linearly to 14.6 in 1979. Note that vehicular particles include auto exhaust, diesel exhaust, tire wear, and brake wear.

$$\begin{aligned} \text{Soil Dust Particles} = \text{SOILDUST} &= 4 \times \text{Si}^* & (3-4c) \\ &\text{or} = 900 \times \text{Mn} \end{aligned}$$

$$\text{Fuel Oil Particles} = \text{FUELOIL} = 50 \times \text{Ni}. \quad (3-4d)$$

It is important to note that the organic and Pb data are partly redundant in the sense that a substantial portion of primary motor vehicle particulate emissions are organic aerosols. Because of this redundancy, we never include both ORG and Pb in the same regression. At those sites which have data for both ORG and Pb, we run two sets of regressions -- one with the ORG variable and one with the Pb variable.

When the parameters defined in Equation (3-4) are included in the analysis, an appropriate modification is made in Equation (3-3), the definition for "remainder of TSP". For example, if the Pb and Si variables are included, then equation (3-3) becomes

$$\begin{aligned} \text{OTHER TSP} &= \text{TSP} - \text{SULFATE} - \text{NITRATE} - k \text{ Pb} - 4 \text{ Si} \\ &= \text{TSP} - \text{SULFATE} - \text{NITRATE} - \text{VEHICLE} - \text{SOILDUST} \end{aligned}$$

3.2.2 Multi-Variate Regression

When several independent variables (RH, SULFATE, NITRATE, VEHICLE, ..., OTHER TSP) are affecting a dependent variable (B), it is important to perform a multi-variate analysis that can separate out the individual impact of each independent variable, discounting for the simultaneous effects of other independent variables. Uni-variate analyses, based on simple one-on-one relationships, can lead to spurious results because of intercorrelations among the independent variables. For example, in some cases, NITRATE might be correlated with B only because it is correlated with SULFATE which, in turn, is significantly related to B.

* Note that the San Francisco Bay Area data for silicon are actually reported as silicate concentrations, which are approximately twice as great as silicon concentrations.

An appropriate tool for multi-variate analysis is multiple regression. Following the procedure of Cass (1979), White and Roberts (1977), and Trijonis (1979, 1980), we perform multiple linear regressions of the form,

$$B = a + b_1 \text{SULFATE} + b_2 \text{NITRATE} + b_3 \text{VEHICLE} + \dots + b_n \text{OTHERTSP} + b_{n+1} \text{RH}, \quad (3-5)$$

We also perform multiple regressions that include relative humidity effects in a nonlinear manner. Cass (1979) indicates that light scattering by a submicron, hygroscopic aerosol might be proportional to $(1-\text{RH})^{-\alpha}$, where the exponent α is expected to occur in the range 0.67 to 1.0. To account for this type of effect, we perform two sets of regressions of the form,

$$B = a + b_1 \frac{\text{SULFATE}}{(1-\text{RH})^\alpha} + b_2 \frac{\text{NITRATE}}{(1-\text{RH})^\alpha} + b_3 \text{VEHICLE} + \dots + b_n \frac{\text{OTHERTSP}}{(1-\text{RH})^\alpha}, \quad (3-6)$$

one set with $\alpha = 0.67$ and one set with $\alpha = 1.0$. Because we do not expect the organic, primary automotive, fuel oil, or soil dust particles to be hygroscopic, the relative humidity factor is not added to the variables ORG, VEHICLE, FUELOIL, or SOILDUST.

The regressions are performed stepwise but are allowed to run to the final step (with all the variables entered). This permits us to examine the resulting equation under the restriction that all coefficients are statistically significant (at a 95% confidence level) as well as for the case where all variables are included.

Regression analysis is a purely statistical technique, and there is no guarantee that the observed relationships represent cause-and-effect. However, if -- as in the above analysis -- the regression is structured to reflect fundamental principles, the results will strongly suggest certain physical interpretations. In our analysis, the regression coefficients, b_i in Equation (3-5) and $b_i/(1-\text{RH})^\alpha$ in Equation (3-6), are readily interpreted as extinction coefficients per unit mass (extinction efficiencies) for sulfates, nitrates, primary automotive particles, other TSP, etc.

3.2.3 Role of Aerosol Water

The role of aerosol water is so important to visibility that it deserves a special discussion. Thermodynamic calculations (Tang 1981) as

well as measurements made with microwave watermeters, nephelometers, and multi-stage cascade impactors (Covert et al. 1972; Hidy et al. 1974; Ho et al. 1974; Stelson and Seinfeld 1981; Ferman et al. 1981; Countess et al. 1981) suggest that, at relative humidities of 65-75%, the mass of water associated with fine ambient aerosols is approximately equal to or slightly greater than the mass of aerosol electrolytes (e.g. sulfates and nitrates). As relative humidity increases toward 100%, the mass of aerosol water rises hyperbolically.

Figure 3.2 demonstrates that the dependence of aerosol water content on relative humidity varies significantly with the specific chemical form of the aerosol electrolyte (in this case, sulfates). For example, pure sulfuric acid aerosol retains water even at very low relative humidities. Pure ammonium sulfate aerosol, on the other hand, does not hydrate until the deliquescent point at 80% relative humidity. Under real atmospheric conditions, several chemical forms of sulfate are probably present, so that the aerosol water/relative humidity dependence would be intermediate to the various curves shown in Figure 3.2. Under real atmospheric conditions, the deliquescent points might be smoothed out by irreversible (hysteresis) effects.

The role of water becomes all the more critical when one realizes that, because of density differences, water should scatter more light per unit mass than the aerosol electrolytes. For example, White (1981) has suggested that, because water is 1.7 times less dense than sulfate, it should scatter approximately 1.7 times as much light per unit mass than does sulfate. Thus, if there is typically slightly more water mass than electrolyte mass in the aerosol, the total amount of light scattering from the water should be about twice that from the electrolyte. This hypothesis is supported by recent field studies comparing scattering levels from "wet" versus "dry" aerosols (Groblicki et al. 1980; Ferman et al. 1981).

The above observations help to explain why several statistical studies have found that sulfate aerosol is a major, if not the dominant, contributor to atmospheric light extinction (White and Roberts 1977; Cass 1979; Trijonis 1979, 1980; Trijonis and Yuan 1978; Leaderer and Stolwijk 1979; Barone et al. 1978). Not only do sulfates constitute a significant fraction of the fine

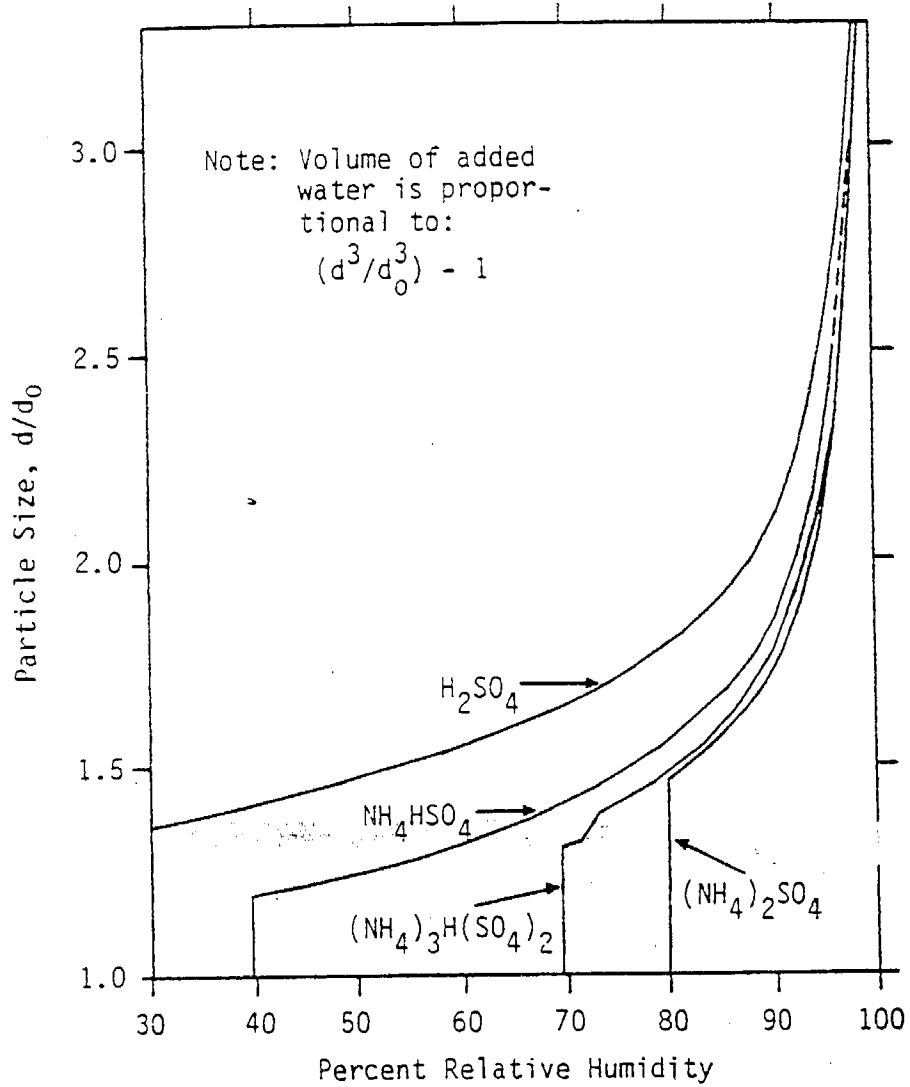


Figure 3.2 Growth curves for sulfate aerosols as a function of relative humidity (Tang 1981).

(optically active) aerosol, but also they often carry with them a substantial volume of water.

Figure 3.3 illustrates the geographical pattern of average relative humidity in California. This figure shows that average relative humidity exceeds 50% over most of California and approaches 70 or 80% in the coastal areas. Of course, on an individual daily basis, relative humidity can reach very high levels at nearly all locations in California. Because of the fairly high relative humidity levels, water should be a very important component of the fine aerosol in much of California.

As a final remark of this subsection, we note that water should be regarded as an integral part of the aerosol to which it is attached. That is -- if the sulfate aerosol were eliminated, the water associated with the sulfate would also be eliminated from the aerosol phase. (Note that transferring water from the aerosol to the gas phase produces essentially no change in relative humidity, because the total water in the gas phase is typically orders of magnitude greater than the total water in the particulate phase. Thus, there would be no reason for the water associated with the sulfate to tend to become attached to the remainder of the aerosol). Because water is an integral part of the aerosol to which it is attached, regression Equation (3-6), which includes relative humidity as an inherent part of the aerosol variables, is physically more meaningful than Equation (3-5), which arbitrarily segregates relative humidity. Also, the $(1-RH)^{-\alpha}$ term in Equation (3-6) approximates the hyperbolic relationship between aerosol water and relative humidity much better than does the linear RH term in Equation (3-5).

3.2.4 Average Extinction Budgets

The regression coefficients (extinction efficiencies) for the various aerosol species allow calculation of average extinction budgets -- the fraction of visibility loss, on the average, attributable to each aerosol species. In Chapter 5, we will compute these extinction budgets for several areas of California.

Many previous authors have calculated extinction budgets for individual locations by directly using the regression equations (White and Roberts 1977;

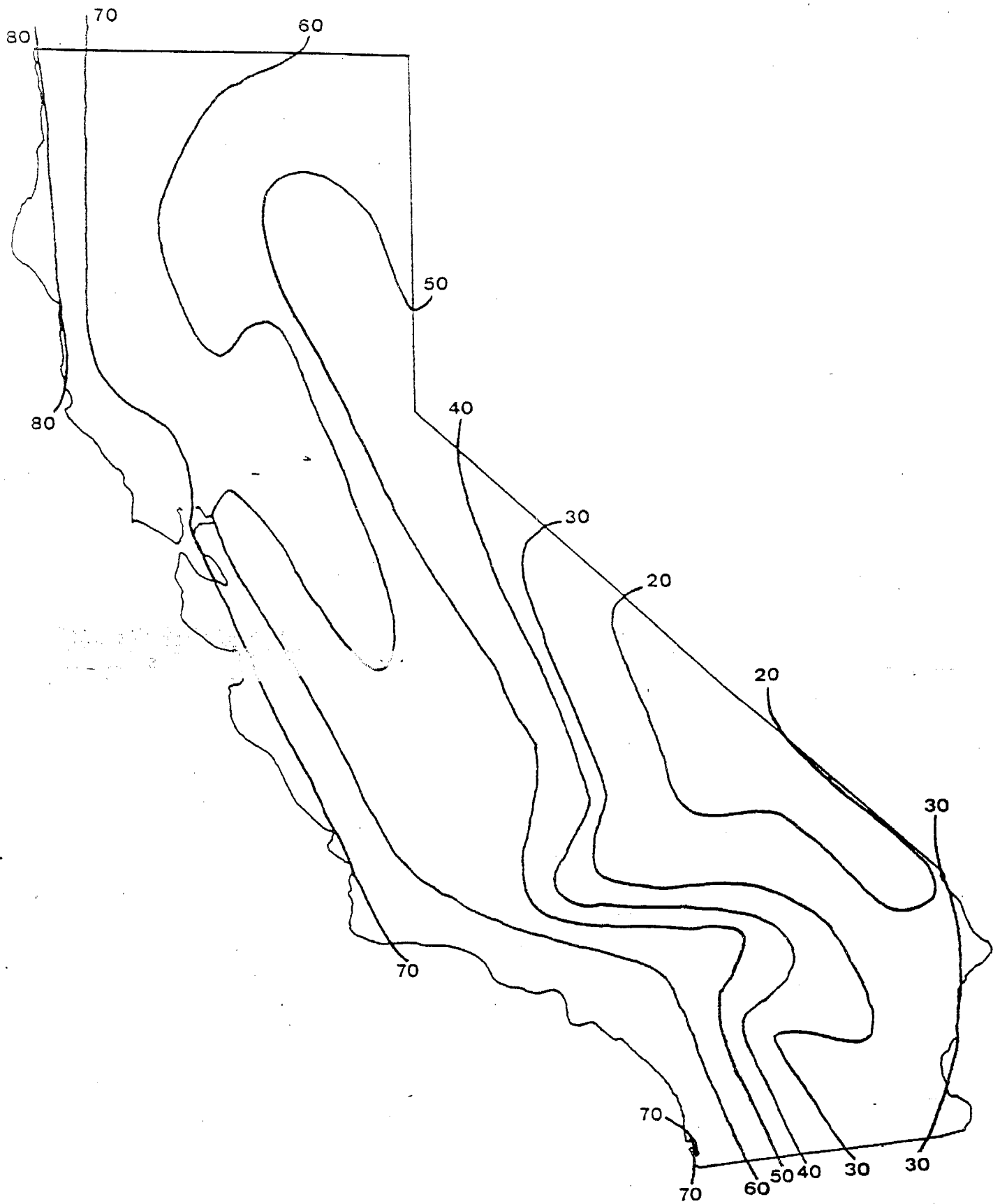


Figure 3.3 Geographical distribution of annual average relative humidity (percent) in California (NOAA 1977).

Cass 1979; Trijonis and Yuan 1978; Trijonis 1979, 1980; Leaderer and Stolwijk 1979). For example, in Equation (3-6), the average extinction from sulfates is simply assumed to be " b_1 " multiplied by the average value of $\text{SULFATE}/(1-\text{RH})^\alpha$. Similarly, the average extinction from "other TSP" is assumed to be " b_3 " times the average value of $\text{OTHERTSP}/(1-\text{RH})^\alpha$. Part of the constant term "a" is identified as Rayleigh scatter by air molecules, while the remainder of the constant "a" is called "unaccounted for" extinction.

Because of certain statistical problems inherent in our regression methodology (see next subsection), we do not think it is appropriate to calculate extinction budgets by directly plugging into the regression equations. Rather, in Chapter 5, we will use a modified approach in arriving at the extinction budgets. First, we will calculate the average extinction contributions from air molecule light scattering and from NO_2 absorption by using known values for Rayleigh scattering and NO_2 absorption efficiency and existing data on NO_2 concentrations. Next, for certain individual aerosol species, such as sulfates, we will identify region specific extinction efficiencies based mostly on our regression coefficients but also based on other theoretical and empirical results. These extinction efficiencies can be multiplied by average values of certain aerosol terms, e.g. $\text{SULFATE}/(1-\text{RH})^\alpha$, to yield average extinction contributions from the individual aerosol species. Whatever fraction of total extinction that is not accounted for by Rayleigh scattering, NO_2 absorption, or the individual aerosol species will be contributions from "remainder of the aerosol".*

3.2.5 Limitations of the Analysis

There are several limitations to the use of regression models for quantifying visibility/aerosol relationships. One limitation involves random errors in the data base produced by imprecision in the measurement techniques (for airport visibility or aerosol concentrations) and by the fact that the airport and Hi-Vol site are often located several miles apart.

* In using this approach, we do not consider "OTHERTSP" as an individual aerosol species. Contributions from "OTHERTSP", as well as what we previously called "unaccounted for", now both naturally fit into the single category "remainder of the aerosol".

Random errors in the data tend to weaken the statistical relationships, leading to lower correlation coefficients and lower regression coefficients. This causes an underestimate of the extinction coefficients per unit mass (extinction efficiencies) for individual aerosol species and, therefore, an underestimate of the contributions of individual aerosol species to the total extinction budget. The overall effect of random errors in the data base should not be excessive, however, because good correlations (typically 0.7 to 0.9) are usually obtained in the analysis.

Incompatibilities between the airport visibility data base and the aerosol data base can lead to at least two types of systematic bias. The aerosol concentrations measured at the downtown Hi-Vol locations may be systematically higher than the aerosol concentrations averaged over the visual range surrounding the airport. The bias caused by relatively high aerosol measurements would result in an underestimate of extinction coefficients per unit mass for the aerosol species. A reverse type of bias, e.g. an overestimate of extinction coefficients per unit mass, would result if daytime aerosol levels (corresponding to the time period of the visibility measurements) were higher than the 24-hour average aerosol levels measured by the Hi-Vol. Although these systematic errors could bias the extinction coefficients per unit mass, they should not bias the extinction budgets which are based on a multiplication of extinction coefficients per unit mass times the measured mass of the aerosol.

Another limitation is that the regression analysis may overstate the importance of the aerosol variables if these variables are correlated with other visibility-related pollutants omitted from the analysis. In particular, nitrates may act, in part, as surrogates for other related photochemical pollutants, such as secondary organic aerosols and nitrogen dioxide. For this reason, the nitrate contributions to the extinction budget might best be viewed as representing nitrate aerosols plus related photochemical pollutants.

Potential errors in Hi-Vol measurements of sulfate and nitrate are another important caveat. Artifact sulfate (formed by SO_2 conversion on the measurement filter) may cause a slight underestimation of the extinction coefficient per unit mass for sulfates. The greatest measurement concern,

however, involves nitrates (Spicer and Schumacher 1979; Appel et al. 1979). Nitrate data may represent gaseous compounds (NO_2 and especially nitric acid) as well as nitrate aerosols. Also, high sulfate concentrations may negatively interfere with nitrate measurements (Harker et al. 1977). Because of potentially severe measurement errors, the visibility/nitrate relationships are especially uncertain.

A final difficulty in the regression analysis is the problem of colinearity, i.e. the intercorrelations that exist among the "independent" variables (SULFATE, NITRATE, OTHER TSP, etc.). Although these intercorrelations (see Table 3.2) are not extremely high, they usually are significant (typically on the order of 0.1 to 0.7). Multiple regression is designed to estimate the individual effect of each variable, discounting for the simultaneous effects of other variables, but the colinearity problem can still lead to distortions in the results. It is likely that certain pollutant variables at certain sites are assigned little statistical significance and near-zero regression coefficients in the multiple regressions because these variables are colinear with another pollutant which bears a stronger relation to extinction. In such cases, the regression coefficient (extinction efficiency) for the latter pollutant is likely to be artificially raised because it also is representing the effect of the colinear pollutants.

As noted in the previous subsection, because of the statistical problems in the regressions, we have decided not to calculate extinction budgets by simply plugging average aerosol concentrations into the regression formulae. Rather, in Chapter 5, the extinction budgets will be based not only on the regression results but also on other empirical and theoretical considerations.

3.3 DATA OVERVIEW

As indicated in Section 3.1, the visibility/aerosol regression analysis based on routine Hi-Vol data is conducted at 34 locations. At each location, the regression models are applied to two data sets: (1) eliminating days with precipitation or severe fog (defined as at least one daytime fog observation and average relative humidity exceeding 96%) and (2) eliminating days with precipitation or any fog (defined as at least one daytime fog observation).

TABLE 3.2 INTERCORRELATIONS AMONG THE INDEPENDENT VARIABLES.

DATA: EXCLUDING DAYS WITH PRECIPITATION OR FOG.

	SULFATE versus NITRATE	SULFATE versus OTHERTSP	SULFATE versus RH	NITRATE versus OTHERTSP	NITRATE versus RH	OTHERTSP versus RH	SULFATE/(1-RH) versus NITRATE/(1-RH)	SULFATE/(1-RH) versus OTHERTSP/(1-RH)	OTHER
SAN DIEGO AREA									
Tan Diego (NASH)	.21	.15	.39	.26	-.11*	-.49	.30	.44	.30
Tan Diego (ARB)	.40	.27	.36	.39	-.01*	-.43	.60	.52	.36
El Cajon	.33	.04*	.23	.18	-.04*	-.51	.51	.30	.35
LOS ANGELES AREA (Coastal)									
Long Beach	-.16	.05*	.25	.32	-.12*	-.52	.03*	.31	.32
Costa Mesa	.36	.02*	.21	.54	.31	-.60	.47	.25	.75
Lennox	.04*	-.28	.49	.13	-.03*	-.45	.15	.23	.10*
Downtown L.A.	.08*	.10*	.43	.20	-.09*	-.27	.30	.42	.50
Santa Barbara	.60	.11*	.39	.35	.22	-.33	.76	.55	.65
LOS ANGELES AREA (Inland)									
Urbank	.17	.20	.19	.46	-.09*	-.20	.25	.33	.50
La Habra	.52	.11*	.33	.43	.04*	-.47	.78	.63	.73
Ontario	.31	.64	-.10*	.49	-.24	-.39	.34	.51	.42
San Bernardino	.61	.71	.20	.59	.13*	-.12*	.66	.79	.66
SOUTHEAST DESERT AREA									
Alm Springs	.61	.33	.03*	.20	-.12*	-.04*	.74	.50	.66
Yucca	.49	.15	-.02*	-.04*	-.12*	-.15*	.54	.21	-.02*
Victorville	.69	.15	.05*	.08*	-.12*	-.24	.69	.19	.09*
El Centro	.43	.53	-.14*	.19	.06*	.03*	.63	.61	.37
CENTRAL COAST AREA									
Salinas	.60	.46	-.03*	.35	-.09*	-.67	.61	.61	.43
San Luis Obispo	.36	.26	-.23	.60	-.08*	-.31	.41	.41	.63
CENTRAL VALLEY AREA									
Yakersfield	.36	.42	.27	.47	.22	-.24	.32	.65	.67
Fresno	.39	.16*	-.01*	.30	.22	-.15*	.60	.36	.53
Merced	.73	.40	-.13*	.26	.03*	-.23	.78	.42	.34
Sacramento (NASH)	.30	.17	-.03*	.35	.01*	-.27	.34	.22	.51
Sacramento (ARB)	.46	.11*	.05*	.24	-.03*	-.42	.43	.10*	.38
SAN FRANCISCO BAY AREA (Urban)									
Redwood City*	.65	.43	.03*	.46	-.00*	.00*	.66	.55	.44
Oakland	.33	.63	.11*	.45	-.08*	-.22	.37	.68	.14
San Jose* (AQMD)	.52	.18	-.11*	.34	-.19	-.36	.56	.28	.45
San Jose (ARB)	.34	.02*	-.02*	.41	-.42	-.04	.44	.26	.51
SAN FRANCISCO BAY AREA (Suburban)									
Livermore*	.76	.60	-.45	.48	-.25*	-.33	.67	.47*	.59
Concord*	.66	.65	-.16*	.58	-.12*	-.28	.63	.67	.62
Hayward*	.63	.51	-.35	.44	-.21	-.29	.65	.51	.43
Santa Rosa*	.54	.48	-.21*	.48	.27	-.12*	.51	.49	.78
NORTHERN COAST AREA									
Eureka	.42	.19*	.15*	.31	-.13*	-.01*	.56	.35	.30
NORTHERN INLAND AREA									
Red Bluff	.42	.53	.01*	.46	.30	-.17*	.53	.58	.53
Yreka	.66	.56	.50	.51	.23*	.24	.72	.76	.69
Average:	.44	.29	.02	.36	-.02	-.23	.53	.46	.47

Cellulose filter data

* Not statistically significant at a 95% confidence level.

Note that, in this table, OTHERTSP is defined as TSP - SULFATE - NITRATE

Note that the intercorrelations between VEHICLE or ORG and the other independent variables are also on the order of 0.1 to 0.7.

The multiple correlation coefficients for the first data set, typically about .70 to .90 for the nonlinear RH model [Equation (3-6)], tend to be higher than those for the second data set, typically about .65 to .85 for the nonlinear RH model. The regression coefficients (extinction efficiencies), however, are more consistent and physically reasonable for the second data set.* Only the results for the second data set will be presented in this chapter; Appendix B contains tabulations (similar to Tables 3.2 to 3.7) of corresponding results for the first data set.

Table 3.3 lists the number of data points and the average value for various parameters at each study location. The sampling agencies, years of data, and filter types were described earlier in Section 3.1.

Table 3.4 presents the correlation coefficients between extinction (B) and the independent variables. The left hand side of Table 3.4 pertains to the linear RH regression, Equation (3-5), while the right hand side of Table 3.4 pertains to the nonlinear RH regression, Equation (3-6). Averaged over all sites, extinction correlates best with the linear RH regression variables in the order: SULFATE, NITRATE, RH, ORG, OTHERTSP, and VEHICLE. Averaged over all sites, extinction correlates best with the nonlinear RH variables in the order: SULFATE/(1-RH), NITRATE/(1-RH), and OTHERTSP/(1-RH). It is notable that B typically correlates with SULFATE/(1-RH) alone at levels of 0.50 to 0.80.

Certain interesting geographical features are evident in the correlations of Table 3.4. For example, the correlations between extinction and SULFATE or SULFATE/(1-RH) tend to be highest in the southern half of California. On the other hand, the correlations between extinction and NITRATE or NITRATE/(1-RH) tend to be highest in the northern half of California.

3.4 REGRESSION RESULTS

This section presents the results of multiple correlations/regressions

*The days with fog included in the first data set generally represent days with very high extinction coefficients which contribute greatly to the total variance in the extinction data. These outliers evidently can be explained fairly well by the nonlinear RH regression models, leading to high correlation coefficients. A few outliers, however, can severely distort the regression coefficients, explaining why the regression coefficients tend to be less reasonable and consistent for the first data set.

TABLE 3.3 AVERAGE VALUES FOR STUDY VARIABLES.
 DATA: EXCLUDING DAYS WITH PRECIPITATION OR FOG.

DATA POINTS	AVERAGE VALUE OF VARIABLES						
	B 10-4m-1	RH	SULFATE ($\mu\text{g}/\text{m}^3$)	NITRATE ($\mu\text{g}/\text{m}^3$)	OTHER TSP ($\mu\text{g}/\text{m}^3$)	VEHICLE ($\mu\text{g}/\text{m}^3$)	ORG ($\mu\text{g}/\text{m}^3$)
SAN DIEGO AREA							
San Diego (NASN)	204	1.85	.60	9.9	7.1	56.7	
San Diego (ARB)	169	1.73	.52	9.8	9.5	55.7	14.8
El Cajon	134	1.23	.53	8.1	9.4	67.9	20.4 7.7
LOS ANGELES AREA (Coastal)							
Long Beach	199	2.07	.55	13.8	9.5	78.7	
Costa Mesa	125	2.02	.61	10.2	13.4	52.6	17.5
Lennox	257	2.39	.64	16.0	9.6	90.4	29.5
Downtown L.A.	191	3.05	.55	15.9	14.0	91.5	26.6
Santa Barbara	104	1.29	.63	7.1	7.1	59.4	16.8 6.4
LOS ANGELES AREA (Inland)							
Burbank	150	2.10	.48	12.5	10.3	107.2	
La Habra	143	1.82	.63	9.7	17.0	81.4	18.7
Ontario	89	2.98	.43	12.6	13.1	106.2	
San Bernardino	151	2.38	.42	13.6	17.1	95.3	
SOUTHEAST DESERT AREA							
Palm Springs	229	0.86	.35	6.0	10.4	48.2	
Lancaster	137	0.77	.36	5.3	5.7	94.6	6.3
Victorville	253	0.74	.32	6.6	9.5	74.2	5.4
El Centro	147	0.74	.38	5.9	5.2	112.8	5.7 4.2
CENTRAL COAST AREA							
San Luis Obispo	113	1.10	.64	4.9	6.0	47.0	5.3 2.7
Paso Robles	140	0.86	.43	6.9	5.5	70.2	6.5 4.5
CENTRAL VALLEY AREA							
Bakersfield	156	1.81	.45	12.6	18.1	121.3	20.1 8.9
Fresno	121	1.49	.47	6.3	10.7	113.9	
Merced	122	1.30	.43	5.6	10.3	82.2	6.5
Sacramento (NASN)	173	1.37	.49	5.7	5.5	51.5	
Sacramento (ARB)	154	1.31	.49	4.9	6.4	67.4	7.5
SAN FRANCISCO BAY AREA (Urban)							
Redwood City*	218	1.49	.65	2.9	4.1	45.4	6.0 28.9
Oakland	211	1.63	.70	3.5	5.1	63.0	
San Jose* (AQMD)	193	1.27	.57	2.9	5.7	52.9	9.9 39.0
San Jose (ARB)	156	1.35	.56	4.6	7.4	58.5	11.9
SAN FRANCISCO BAY AREA (Suburban)							
Livermore*	54	0.88	.53	2.5	4.8	71.3	4.7 35.9
Concord*	62	0.91	.54	3.2	4.7	38.0	3.7 26.2
Napa*	117	0.87	.55	2.9	4.3	54.9	5.0 33.3
Santa Rosa*	57	0.88	.57	2.3	2.9	38.3	3.9 25.1
NORTHERN COAST AREA							
Humboldt	65	1.55	.74	4.0	0.8	42.8	
NORTHERN INLAND AREA							
Red Bluff	115	0.53	.41	3.4	4.7	51.3	3.8 4.7
Yreka	73	0.55	.48	3.9	1.6	42.1	2.6 3.8

* Cellulose filter data

Note that, in this table, OTHER TSP is defined as TSP - SULFATE - NITRATE.

TABLE 3.4 CORRELATION BETWEEN EXTINCTION AND THE INDEPENDENT VARIABLES.

DATA: EXCLUDING DAYS WITH PRECIPITATION OR FOG.

	B versus RH	B versus SULFATE	B versus NITRATE	B versus OTHER TSP	B versus VEHICLE	B versus ORG	B versus SULFATE/(1-RH)	B versus NITRATE/(1-RH)	B versus OTHER TSP
SAN DIEGO AREA									
San Diego (NASN)	.42	.77	.23	.10*			.80	.39	.45
San Diego (ARB)	.43	.75	.39	.09*	-.05*		.78	.57	.39
El Cajon	.54	.65	.08*	-.37	-.38	-.35	.77	.37	.1*
LOS ANGELES AREA (Coastal)									
Long Beach	.36	.78	.00*	.11*			.79	.14*	
Costa Mesa	.43	.77	.38	-.03*	-.18		.83	.54	
Lennox	.51	.80	.03*	-.06*	-.19		.83	.17	.40
Downtown L.A.	.39	.73	.00*	.24	.06*		.65	.12*	.45
Santa Barbara	.54	.77	.44	-.09*	-.13	-.10*	.86	.61	
LOS ANGELES AREA (Inland)									
Burbank	.53	.67	-.01*	.07*			.79	.25	
La Habra	.40	.72	.59	.11*	.00*		.52	.61	
Ontario	.26	.53	.13*	.38			.59	.26	.55
San Bernardino	.44	.73	.51	.51			.83	.65	.73
SOUTHEAST DESERT AREA									
Palm Springs	.29	.52	.27	.54			.57	.31	.53
Lancaster	.29	.37	.16	.52	-.17		.52	.30	
Victorville	.30	.36	.30	.18	-.06*		.47	.44	
El Centro	.10*	.58	.51	.39	-.07*	.12*	.55	.47	.34
CENTRAL COAST									
Salinas	.30	.45	.35	.07*	.19	.35	.53		.71
Paso Robles	.27	.40	.59	.53	.42	.52	.53	.65	.67
CENTRAL VALLEY AREA									
Bakersfield	.34	.79	.89	.35	.47	.53	.73	.90	.56
Fresno	.22	.36	.83	.25			.52	.81	
Merced	.19	.62	.77	.50	.75		.69	.77	
Sacramento (NASN)	.27	.37	.46	.25			.54	.52	.40
Sacramento (ARB)	.12*	.44	.75	.42	.60		.39	.77	.61
SAN FRANCISCO BAY AREA (Urban)									
Redwood City*	.17	.54	.53	.48	.48	.50	.50	.49	.43
Oakland	.24	.67	.51	.54			.57	.56	
San Jose* (AQMD)	.16	.55	.56	.31	.24	.41	.51	.62	
San Jose (ARB)	.22	.31	.56	.36	.43		.38	.64	
SAN FRANCISCO BAY AREA (Suburban)									
Livermore*	.15*	.45	.33	.03*	.15*	.04*	.51	.29	.65
Concord*	.22*	.50	.45	.20*	-.13*	.31	.64	.51	.32
Napa*	.21	.51	.41	.24	.07*	.30	.57	.52	.22
Santa Rosa*	.34	.38	.32	-.01*	-.13*	.26*	.57	.43	
NORTHERN COAST AREA									
Humboldt	.35	.20*	.23*	.15*			.25	.37	
NORTHERN INLAND AREA									
Red Bluff	.42	.27	.67	.43	.28	.54	.51	.71	
Yreka	.45	.29	.26	.14*	.20*	.24	.36	.28	
AVERAGE	.32	.55	.40	.23	.12	.26	.51	.48	

* Cellulose filter data

* Not statistically significant at a 95% confidence level.

Note that, in this table, OTHER TSP is defined as TSP - SULFATE - NITRATE.

relating extinction to Hi-Vol parameters. The most significant aspect of the analysis concerns the regression coefficients -- estimates of extinction efficiencies for various aerosol components. As part of this section, we also interpret our results in light of other theoretical and empirical studies.

3.4.1 Insignificant Aerosol Variables

To simplify the discussion later in this section, it is worthwhile to first dispose of those aerosol variables that proved to be insignificantly related to extinction (visibility). Generally, we found that all of the "tracer" variables defined previously in Equation (3-4) -- VEHICLE, ORG, SOILDUST, and FUELOIL -- lacked consistent, significant relationships with extinction. Figure 3.4 summarizes the regression coefficients (extinction efficiencies) for VEHICLE (24 sites), ORG (14 sites), SOILDUST (6 silicon sites, 2 manganese sites), and FUELOIL (3 sites). Figure 3.4 shows that most of the coefficients are statistically insignificant (open dots) and that the distributions of the coefficients center around zero. In fact, those coefficients that are statistically significant are as likely as not to be negative (a physically unacceptable result).

It should be stressed that the lack of statistically significant relationships does not imply that these aerosol components have zero or negligible effect on visibility. On the contrary, from fundamental physical principles, we know that these aerosols must affect visibility. Rather, our results indicate that the effect is not overwhelming enough so that one can determine the extinction efficiencies from the (admittedly limited) airport and Hi-Vol data. For the parameters fuel oil and soil dust, the lack of a statistically significant relationship most likely reflects the fact that fuel oil and soildust particles constitute only very small components of the fine (0.1 to 1.0 micron), optically active aerosol. For the parameters VEHICLE and ORG, the lack of a significant relationship may reflect data quality or statistical problems (i.e. the failure of benzene soluble organics to adequately represent total fine organic aerosols, the failure of Hi-Vol Pb data to be a perfect tracer for fine vehicular aerosols and intercorrelations between VEHICLE or ORG and SULFATE, NITRATE, etc.).

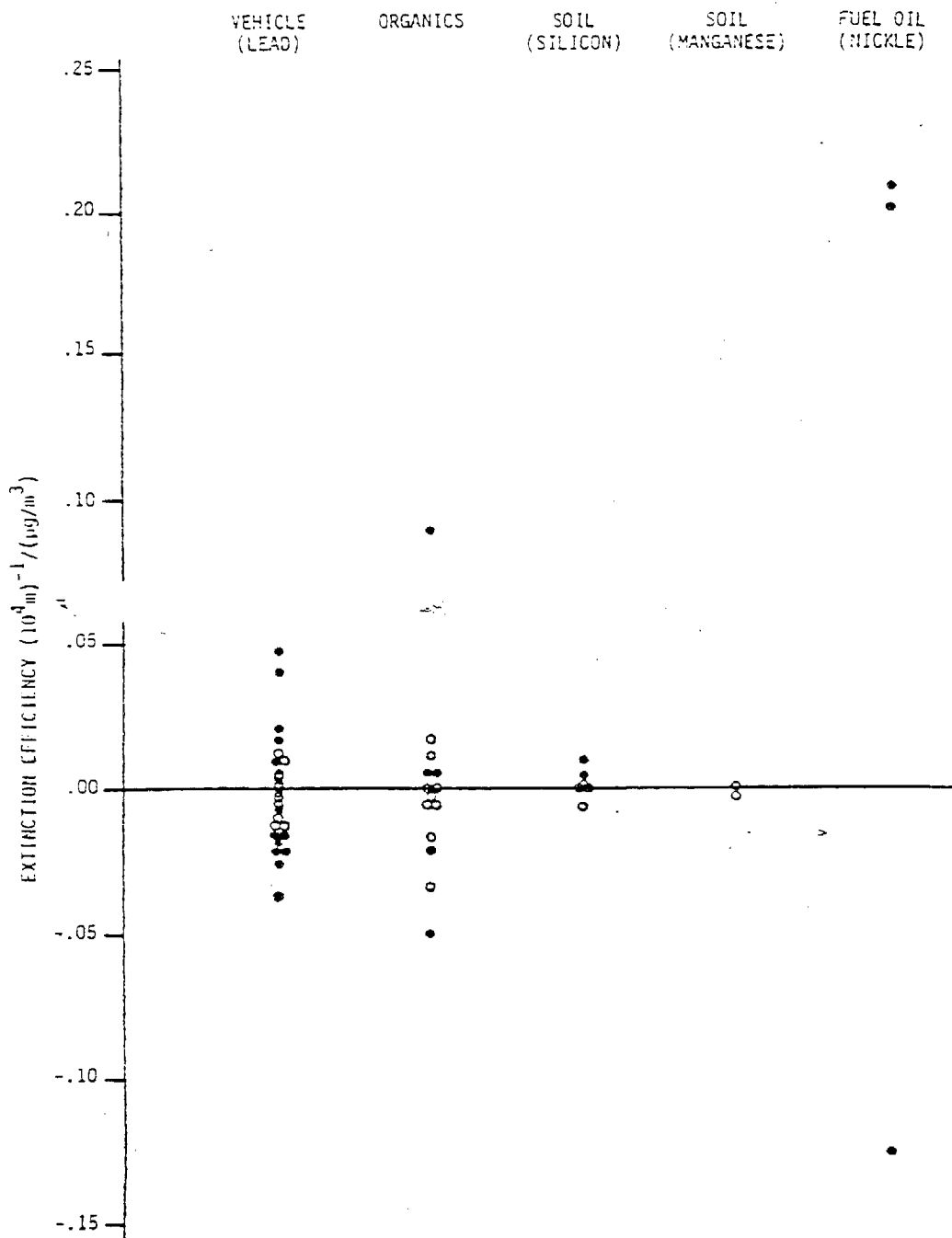


Figure 3.4 Regression coefficients for variables found to be generally insignificant.

Actually, from the results of other studies performed with more detailed aerosol data (Hidy et al. 1974; Groblicki et al. 1980; Wolff et al. 1980; Cass et al. 1981; Conklin et al. 1981), we know that vehicular particles (elemental carbon, organics, lead, etc.) and organic particles do constitute a significant fraction of the fine aerosol and do contribute significantly to visibility reduction. Unfortunately, we are unable to isolate and quantify this contribution with the routine airport and Hi-Vol data.

For the remainder of this chapter, we will not consider the variables VEHICLE, ORG, SOILDUST, and FUELOIL. The regression results will be limited to the variables SULFATE, NITRATE, OTHERTSP, and RH. Also, OTHERTSP will hereafter be defined specifically as TSP - SULFATE - NITRATE at all the study sites.

3.4.2 Different Monitoring Programs

Another preliminary issue that must be resolved is the equivalency of the results based on different Hi-Vol monitoring programs. In this study, we are using data from four Hi-Vol monitoring networks: EPA/NASN, California ARB, South Coast AQMD, and San Francisco Bay Area AQMD. All of the Hi-Vol data are on glass fiber filters except the San Francisco AQMD data, which are on cellulose filters. We purposely selected pre-1976 San Francisco AQMD data so that we could determine if different results are obtained with cellulose Hi-Vol filter data (the San Francisco AQMD switched to glass fiber filters in 1976).

We have addressed the equivalency question for our regression coefficients by examining the three duplicate sites -- San Diego NASN versus ARB, Sacramento NASN versus ARB, and San Jose AQMD versus ARB -- and by conducting statistical tests comparing statewide and regional results from the various monitoring programs. We have found that the results from the various monitoring programs are equivalent with one, not surprising exception -- the San Francisco AQMD cellulose filter data. In general, we find that the San Francisco AQMD data give higher regression coefficients for nitrates and especially sulfates. The reason for this finding can be understood by referring back to Table 3.3. Table 3.3 reveals that the San Francisco AQMD cellulose filter data are lower than glass fiber filter data for

nitrate and especially for sulfates. In the sense that the nitrate and sulfate concentrations are biased low for the cellulose data, it is somewhat expected that the regression coefficients would be biased high.

The reasons why cellulose filter data give lower estimates for nitrate and especially sulfate are not fully understood. The most likely reasons are that the cellulose filters may have less artifact sulfate and nitrate than the glass filters and that the cellulose filters may not collect fine particles as effectively as glass filters (Sandberg 1981). One could adjust the cellulose filter data to be equivalent to the glass filter data if one could derive a consistent relationship between the two. Both we and the San Francisco AQMD have made brief but unsuccessful attempts at finding a consistent relationship. Because we cannot adjust the cellulose filter data to be equivalent to the glass filter data, we will treat the cellulose filter data separately throughout this report, denoting it by asterisks in the tables and figures.

3.4.3 Linear Regression Equation

Table 3.5 summarizes the regression coefficients for the linear RH model, Equation (3-5). The multiple correlation coefficients for the linear regression equation are fairly good, typically 0.60 to 0.80. Also, the regression coefficients for the aerosol variables agree with our qualitative expectation that extinction efficiencies for sulfates and nitrates should be an order of magnitude greater than extinction efficiencies for the remainder of TSP (see later discussion of theoretical results concerning extinction efficiencies).

Some of the values in Table 3.5, however, violate fundamental physical principles. Specifically, the regression coefficients for sulfates are on the order of 0.07 to 0.13 (10^{-4}m^{-1})/($\mu\text{g}/\text{m}^3$) at many locations; these values are much greater than the extinction efficiencies for sulfates expected from theoretical principles -- on the order of 0.02 to 0.04 (10^{-4}m^{-1})/($\mu\text{g}/\text{m}^3$) (see later discussion). The most obvious reason for severely inflated sulfate coefficients is that the SULFATE variable is representing not only sulfate compounds but also the water attached to those compounds.* As discussed

*The sulfate coefficients may also be inflated because sulfates are colinear with other visibility reducing pollutants and because there are mismatches in the daily timing of the Hi-Vol data and visibility data (see Section 3.2.5).

TABLE 3.5 REGRESSION COEFFICIENTS FOR THE LINEAR RH MODEL: EQUATION (3-5).
DATA: EXCLUDING DAYS WITH PRECIPITATION OR FOG.

	MULTIPLE CORRELATION COEFFICIENTS	b1 SULFATE	b2 NITRATE	b3 OTHER TSP	b4 RH
SAN DIEGO AREA					
San Diego (NASN)	.80	.134	.021	.0028*	1.67
San Diego (ARB)	.78	.111	.025	-.0024*	1.20
El Cajon	.78	.090	-.008*	-.0066	1.13
LOS ANGELES AREA (Coastal)					
Long Beach	.83	.120	.021	.0080	2.98
Costa Mesa	.83	.178	.009*	.0073*	3.92
Lennox	.84	.117	.003*	.0103	2.86
Downtown L.A.	.77	.103	-.010*	.0090	1.72
Santa Barbara	.82	.196	.000*	-.0029*	1.64
LOS ANGELES AREA (Inland)					
Burbank	.80	.133	-.042	.0050	5.76
La Habra	.79	.122	.038	.0000*	1.57
Ontario	.67	.103	-.014*	.0140	5.45
San Bernardino	.80	.117	.017*	.0053*	4.95
SOUTHEAST DESERT AREA					
Palm Springs	.71	.040	-.003*	.0062	0.73
Lancaster	.70	.038	.010	.0028	1.07
Victorville	.53	.019	.014	.0022	1.00
El Centro	.67	.081	.037	.0008*	0.59
CENTRAL COAST AREA					
Salinas	.59	.085	-.001*	.0036*	2.10
Paso Robles	.79	.061	.041	.0074	1.89
CENTRAL VALLEY AREA					
Bakersfield	.90	.026*	.066	-.0007*	1.37
Fresno	.83	.010*	.105	.0002*	0.44*
Merced	.86	.027*	.074	.0077	2.73
Sacramento (NASN)	.61	.070	.091	.0044	2.39
Sacramento (ARB)	.85	.037	.105	.0085	2.19
SAN FRANCISCO BAY AREA (Urban)					
Redwood City*	.65	.071	.043	.0063	1.01
Oakland	.80	.077	.067	.0085	2.77
San Jose* (AQMD)	.73	.106	.061	.0065	2.16
San Jose (ARB)	.69	.056	.054	.0117	2.93
SAN FRANCISCO BAY AREA (Suburban)					
Livermore*	.66	.133	-.007*	-.0023	0.73
Concord*	.62	.081	.023	-.0034*	0.64
Napa*	.66	.117	.015*	.0006*	1.34
Santa Rosa*	.61	.117	.000*	-.0063	1.25
NORTHERN COAST AREA					
Humboldt	.46	.006*	.225	.0023*	2.74
NORTHERN INLAND AREA					
Red Bluff	.75	-.030*	.046	.0051	1.07
Yreka	.48	.002*	.025*	-.0002*	0.66

* Cellulose filter data

* Not statistically significant at a 95% confidence level.

Note that, in this table, OTHER TSP is defined as TSP - SULFATE - NITRATE.

previously in Section 3.2.4, the linear RH term in Equation (3-5) does not adequately reflect the role of aerosol water; it is not surprising that the effects of aerosol water will also be partly represented in the sulfate term. Because the linear regression equation ambiguously includes the role of aerosol water in both the RH and sulfate terms, we do not think that the linear equation provides results that are appropriate for our later calculations of extinction budgets.

3.4.4 Nonlinear RH Regression Equation

As discussed previously in Section 3.2.2, we have conducted two types of nonlinear RH regressions of the form:

$$B = a + b_1 \frac{\text{SULFATE}}{(1-\text{RH})^\alpha} + b_2 \frac{\text{NITRATE}}{(1-\text{RH})^\alpha} + b_3 \frac{\text{OTHER TSP}}{(1-\text{RH})^\alpha}. \quad (3-6)$$

One type uses a value of $\alpha = 0.67$; the other type uses a value of $\alpha = 1.0$. After completing the regressions and studying the results, we find that the values for α perform about equally as well. The total regression coefficients at each study site are about the same for the two values of α , typically 0.65 to 0.85 (slightly greater than the degree of correlation achieved by the linear RH model). The site-to-site variations in the regression coefficients also are quite parallel for the two values of α . Of course, for $\alpha = 0.67$, the regression coefficients "b_i" are consistently larger, compensating for the denominator $(1-\text{RH})^{.67}$ being consistently larger.

In order to simplify the following discussion, we will present results only for one value of α , $\alpha = 1.0$. Although, as mentioned above, we have found little statistical difference between the two values of α , we think that $\alpha = 1.0$ is more appropriate based on the following considerations:

- Latimer et al. (1978) have concluded that the mass of water associated with hygroscopic aerosols should vary specifically as $(1-\text{RH})^{-1}$.
- Groblicki et al. (1980), using very detailed aerosol data for Denver, have concluded that $\alpha = 1.0$ yields a slightly better statistical fit than $\alpha = 0.67$.
- In comparing our results with the published literature, using $\alpha = 1.0$ is more appropriate because $\alpha = 1.0$ is most often assumed in

other studies (Trijonis and Yuan 1978; Trijonis 1979, 1980; Latimer et al. 1978; Groblicki et al. 1980; Ferman et al. 1981).

Table 3.6 and Figure 3.5 summarize the regression coefficients at each site for Equation (3-6). The statistical significance of the coefficients is indicated in both the table and the figure. It is apparent that the sulfate term generally bears the strongest relationship with extinction; the coefficients for SULFATE/(1-RH) are statistically significant at 27 of the 34 study sites. The nitrate and other TSP coefficients are both statistically insignificant at 11 of the study locations; also the coefficients for NITRATE/(1-RH) and OTHERTSP/(1-RH) are negative (physically unreasonable) at several locations.

We have also conducted the regressions combining the data for all sites in each region and for all sites in California.* The regression coefficients for the grouped data are presented in Table 3.7 and indicated by the large dots in Figure 3.5. Because of the greater number of data points, nearly all the coefficients for the combined data sets are statistically significant.

One general theme apparent in Figure 3.5 and Tables 3.6 and 3.7 is that the extinction efficiencies for sulfates are generally an order of magnitude greater than the extinction efficiencies for the remainder of TSP (OTHERTSP). This result has also been demonstrated in many previous statistical studies (Trijonis and Yuan 1978; Trijonis 1979, 1980; White and Roberts 1977; Cass 1979; Grosjean et al. 1976; Leaderer and Stolwijk 1979). Qualitatively, this finding agrees with known principles of aerosol physics. Sulfates are secondary aerosols that tend to form in the particle size range of 0.1 to 1.0 micron, called the accumulation size range (NRC 1979; Whitby and Cantrell 1976; Willeke and Whitby 1975; Hidy et al. 1974). The remainder of TSP mass is usually dominated by the coarse particle mode residing in the size range above 2 microns (Whitby and Sverdrup 1978; Bradway and Record 1976; Willeke and Whitby 1975). As shown in Figure 3.6, light scattering per unit mass of aerosol as a function of particle size exhibits a pronounced peak at a particle size of about 0.5 microns;

* Because of the significant differences between glass and cellulose filters, we have grouped the San Francisco Bay Area sites by filter type rather than by geography. The cellulose data have also been excluded from the "all California" regression.

TABLE 3.0 REGRESSION COEFFICIENTS FOR THE NONLINEAR MODEL EQUATION (3-6).

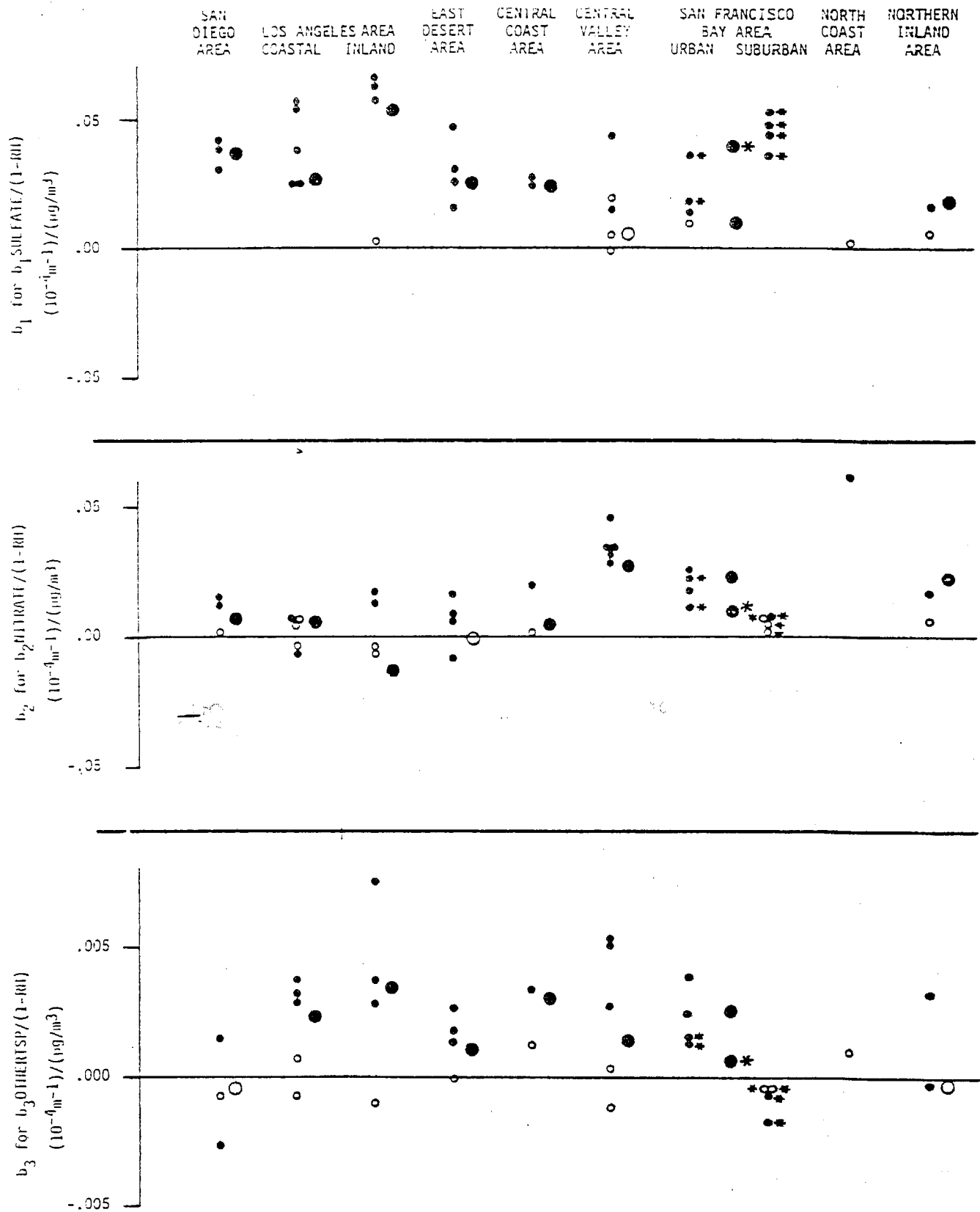
DATA: EXCLUDING DAYS WITH PRECIPITATION OR FOG.

	MULTIPLE CORRELATION COEFFICIENTS	b ₁ SULFATE (1-RH)	b ₂ NITRATE (1-RH)	b ₃ OTHERTSP (1-RH)
SAN DIEGO AREA				
San Diego (NASN)	.82	.041	.013	.0014
San Diego (ARB)	.81	.030	.014	-.0003*
El Cajon	.80	.038	.001*	-.0026
LOS ANGELES AREA (Coastal)				
Long Beach	.82	.038	-.004*	.0038
Costa Mesa	.84	.055	.007	.0008*
Lennox	.85	.024	.003*	.0029
Downtown L.A.	.69	.024	-.006	.0032
Santa Barbara	.87	.056	-.004*	-.0007*
LOS ANGELES AREA (Inland)				
Burbank	.81	.062	-.005*	.0029
La Habra	.62	.002*	.017	-.0010*
Ontario	.66	.058	-.004*	.0077
San Bernardino	.85	.064	.013	.0038
SOUTHEAST DESERT AREA				
Palm Springs	.67	.030	-.009	.0027
Lancaster	.77	.025	.007	.0018
Victorville	.55	.015	.009	.0014
El Centro	.59	.046	.016	.0000*
CENTRAL COAST AREA				
Salinas	.54	.026	.001*	.0012*
Paso Robles	.77	.025	.020	.0033
CENTRAL VALLEY AREA				
Bakersfield	.90	-.001*	.033	-.0011*
Fresno	.81	.005*	.033	.0003*
Merced	.87	.019*	.032	.0051
Sacramento (NASN)	.67	.042	.030	.0028
Sacramento (ARB)	.85	.015	.046	.0052
SAN FRANCISCO BAY AREA (Urban)				
Redwood City*	.57	.018	.011	.0013
Oakland	.78	.014	.018	.0024
San Jose* (AQMD)	.71	.036	.022	.0015
San Jose (ARB)	.69	.010*	.024	.0039
SAN FRANCISCO BAY AREA (Suburban)				
Livermore*	.56	.047	.001*	-.0007
Concord*	.67	.045	.006*	-.0017
Napa*	.68	.052	.007	-.0005*
Santa Rosa*	.58	.035	.004*	-.0004*
NORTHERN COAST AREA				
Humboldt	.42	.001*	.062	.0010*
NORTHERN INLAND AREA				
Red Bluff	.79	.006*	.017	.0032
Yreka	.42	.017	.007*	-.0002

* Cellulose filter data

• Not statistically significant at a 95% confidence level.

Note that, in this table, OTHERTSP is defined as TSP - SULFATE - NITRATE.



Note: Open dots are not statistically significant at a 95% confidence level.
 Note: Large dots represent results for regionally grouped data.
 * Cellulose filter data.

Figure 3.5 Regression coefficients for the nonlinear RH model.

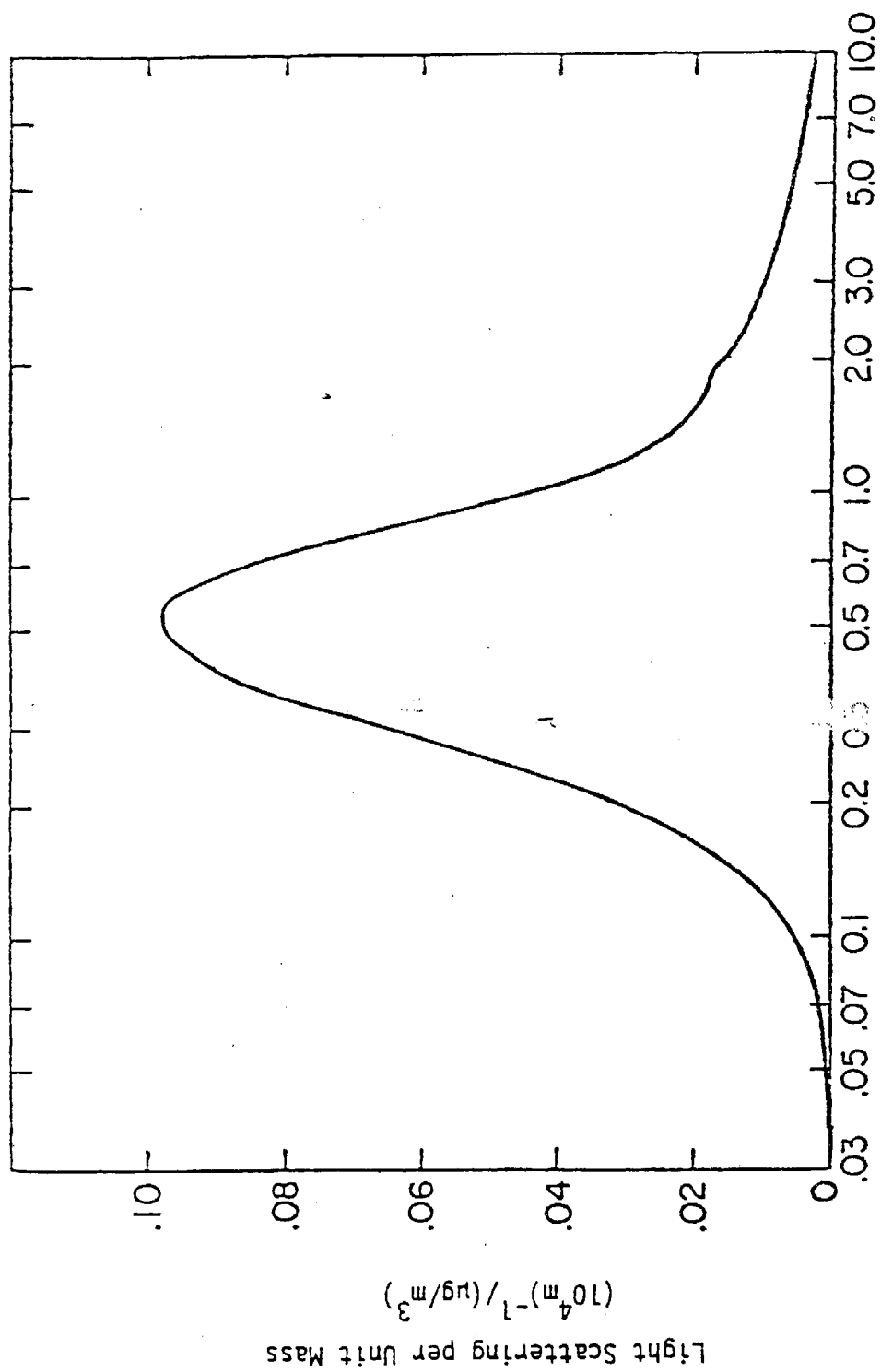
TABLE 3.7 REGIONAL REGRESSION COEFFICIENTS FOR THE NONLINEAR RH MODEL:

$$B = a + b_1 \frac{\text{SULFATE}}{(1-\text{RH})} + b_2 \frac{\text{NITRATE}}{(1-\text{RH})} + b_3 \frac{\text{OTHERTSP}}{(1-\text{RH})}$$

DATA: Excluding days with precipitation or fog.

AREA	NUMBER OF DATA POINTS	MULTIPLE CORRELATION COEFFICIENT	b ₁ <u>SULFATE</u> (1-RH)	b ₂ <u>NITRATE</u> (1-RH)	b ₃ <u>OTHERTSP</u> (1-RH)
SAN DIEGO AREA	507	.79	.037	.007	-.0004●
LOS ANGELES AREA (Coastal)	875	.76	.026	.004	.0022
LOS ANGELES AREA (Inland)	533	.65	.052	-.013	.0034
SOUTHEAST DESERT AREA	816	.56	.024	.001●	.0010
CENTRAL COAST AREA	228	.61	.022	.004	.0029
CENTRAL VALLEY AREA	726	.78	.005●	.028	.0013
SAN FRANCISCO BAY AREA (Glass Filters)	367	.74	.010	.023	.0025
SAN FRANCISCO BAY AREA (Cellulose Filters)	701	.60	.039	.009	.0006
NORTHERN INLAND AREA	189	.66	.019	.021	-.0003●
STATEWIDE	4306	.74	.028	.010	.0019

● Not statistically significant at a 95% confidence level.



Particle Diameter (microns)

Figure 3.6 Light scattering by aerosols as a function of particle diameter. Computed for unit density spherical particles of refractive index 1.5 (White and Roberts 1977).

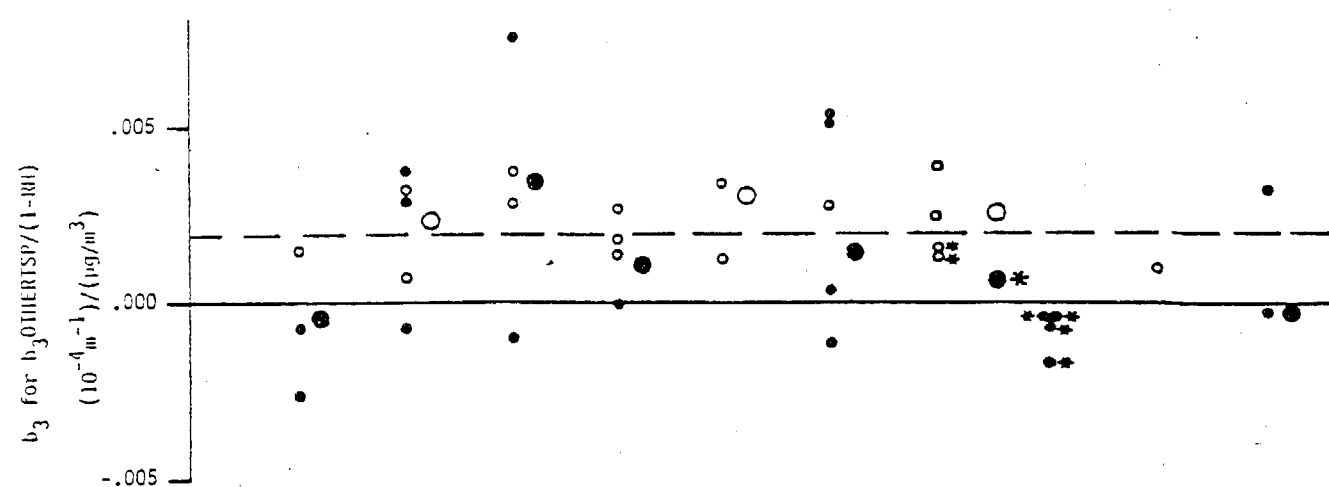
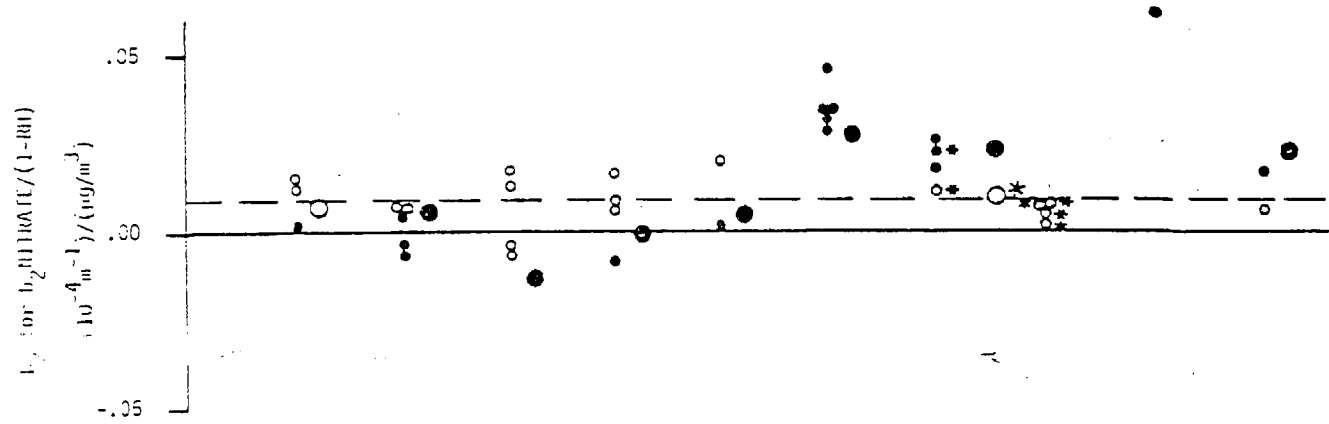
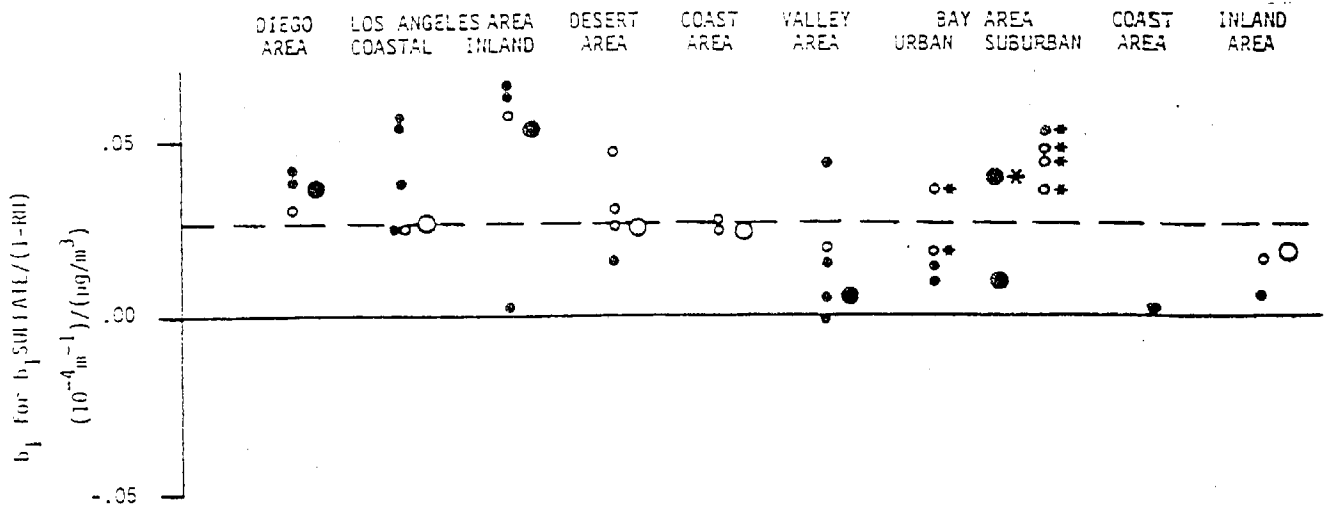
particles in the 0.1 to 1.0 micron size range scatter much more light per unit mass than particles above 2 microns in size.

Not only are the sulfate and other TSP coefficients qualitatively of the correct relative magnitude, but also the sulfate coefficients agree quantitatively with theoretical results. Mie theory calculations by Latimer et al. (1978) and White and Roberts (1977) suggest that "dry", accumulation-mode, sulfate particles should have an average extinction (scattering) efficiency of .02 to .04 ($10^{-4} \text{ m}^{-1} / (\mu\text{g}/\text{m}^3)$), the specific value depending on the details of the sulfate size distribution. The results in Tables 3.6 and 3.7 indicate that sulfates in California do indeed typically exhibit "dry" extinction efficiencies (b_1 's) of .02 to .04 ($10^{-4} \text{ m}^{-1} / (\mu\text{g}/\text{m}^3)$). It is also interesting to note that, in the northern half of California where the nitrate variable becomes very significant, nitrates also typically exhibit "dry" extinction efficiencies (b_2 's) of .02 to .04 ($10^{-4} \text{ m}^{-1} / (\mu\text{g}/\text{m}^3)$), approximately what one would expect for an accumulation-mode secondary aerosol.

Figure 3.5 and Tables 3.6 and 3.7 contain some interesting geographical features. For example, the sulfate extinction efficiencies are greater in the southern half of California than in the northern half of California. The nitrate extinction efficiencies exhibit exactly the opposite geographical pattern. It is natural to pose the question "Are these geographical variations statistically significant?" Figure 3.7 answers that question. Figure 3.7 is exactly the same as Figure 3.5 except that the closed dots represent coefficients that are significantly different from the statewide value (rather than significantly different from zero).^{*} Figure 3.7 indicates that the north-south variations in the sulfate and nitrate coefficients are statistically significant.

What causes the north/south dichotomy in the sulfate and nitrate coefficients? The north/south variation in the coefficients might be partly spurious -- caused by statistical problems introduced by colinearity between

^{*} Note that the cellulose filter data are excluded from Figure 3.7. We already know that the cellulose data are not comparable to the glass filter data.



Note: Open dots are not statistically significant from statewide values at a 95% confidence level.

Note: Large dots represent results for regionally grouped data.

Note: Dashed line represents statewide coefficient, .028 for sulfates, .010 for nitrates, and .0019 for other TSP.

* Cellulose filter data.

Figure 3.7 Regression coefficients for the nonlinear RH model compared to statewide coefficients.

SULFATE/(1-RH) and NITRATE/(1-RH).^{*} As noted before (Table 3.4), extinction correlates much better with sulfate than with nitrate in southern California but slightly better with nitrate than with sulfate in northern California. In each case, the "stronger" correlator may be stealing some of the effect of the colinear "weaker" variable; that is -- the coefficient of the stronger correlator may be inflated, while the coefficient of the weaker variable is correspondingly deflated.

The north/south variations, however, might also represent physical realities. In the case of nitrates, Stelson et al. (1979) have pointed out the extreme temperature sensitivity of the equilibrium between ammonium nitrate aerosol and gaseous NH_3 and HNO_3 . In northern California, with lower temperatures, one would expect relatively more of the nitrate to be in the aerosol phase than in southern California. The higher correlation between extinction and nitrate in northern California, and the more significant and more physical reasonable nitrate regression coefficients in northern California, ~~from the regression that most of the measured Hi-Vol nitrate in northern California is real nitrate aerosol.~~ In southern California, on the other hand, relatively more of the atmospheric nitrate may be in the gaseous state (as HNO_3), and relatively more of the Hi-Vol nitrate may be an artifact (e.g. collection of gaseous HNO_3). The presence of substantial artifact Hi-Vol nitrate in southern California would account for the weaker correlation between extinction and nitrate in the south. Extinction is physically related to the part of the nitrate measurement that represents real aerosol; artifact nitrate would tend to confuse and mask this relationship.

In the case of sulfates, several investigators have emphasized that scattering efficiency may depend strongly on the specific size distribution of the particles within the accumulation mode (Ouimette 1981; White 1981; Latimer et al. 1978). Based on the calculations of Faxvog and Roessler (1978), we would expect sulfates to have higher extinction coefficients per unit mass if the size distribution were centered in the upper part of the accumulation mode, e.g. in the size range 0.5 to 1.0 microns. To see if

^{*}As indicated by Table 3.2, SULFATE/(1-RH) and NITRATE/(1-RH) typically correlate with one another at a level of about 0.5 to 0.7.

sulfate size distribution might explain the observed geographical patterns in sulfate extinction efficiency, we have plotted our regional sulfate coefficients against regional sulfate size distribution data reported by Cahill (1980). Figure 3.8 shows that our regional sulfate extinction efficiencies do correlate in the expected manner with sulfate size distribution. In fact, the correlation would be extremely high were it not for the Central Valley point.* Figure 3.8 strongly suggests that at least some of the geographical variation in sulfate extinction efficiency is related to the phenomenon of sulfate size distribution.

The one remaining issue to be resolved in this chapter is -- What extinction efficiencies should be used in calculating extinction budgets? Because of the statistical problems alluded to several times in this chapter, we do not think it is appropriate to blindly use the regression coefficients obtained for each site (Table 3.6) or each region (Table 3.7). On the other hand, we know that part of the geographical variation in extinction efficiencies is reasonable based on physical principles (e.g. sulfate size distribution). For the extinction budget calculations, we have decided to use the regional extinction efficiencies for sulfates and nitrates listed in Table 3.8.** The values in Table 3.8 are approximately the same as regional regression results (Table 3.7), but they have tempered by the following considerations:

- All extinction efficiencies are reported only to the nearest .005 (10^{-4}m^{-1})/($\mu\text{g}/\text{m}^3$) rather than to the nearest .001 (10^{-4}m^{-1})/($\mu\text{g}/\text{m}^3$) to better reflect the uncertainties.
- The nitrate coefficients for the southern part of California are listed as "not calculated" in Table 3.8. We failed to obtain consistent or physically reasonable nitrate regression coefficients for southern California (Table 3.7) because of severe measurement

* We think that the sulfate extinction efficiency in the Central Valley is severely underestimated due to a strong colinearity between SULFATE/(1-RH) and NITRATE/(1-RH) in the Central Valley. Using the somewhat expanded "no severe fog" data base in Appendix A, we obtain a sulfate extinction efficiency for the Central Valley that is nearly an order of magnitude greater. The instability of the sulfate coefficient is a reflection of the colinearity problem.

** Note that the extinction budgets do not require extinction efficiencies for "OTHER TSP". As explained earlier, the extinction contribution from the remainder of TSP is simply defined as what is left over after we have accounted for Rayleigh scatter, NO₂ absorption, and various individual parts of the aerosol.

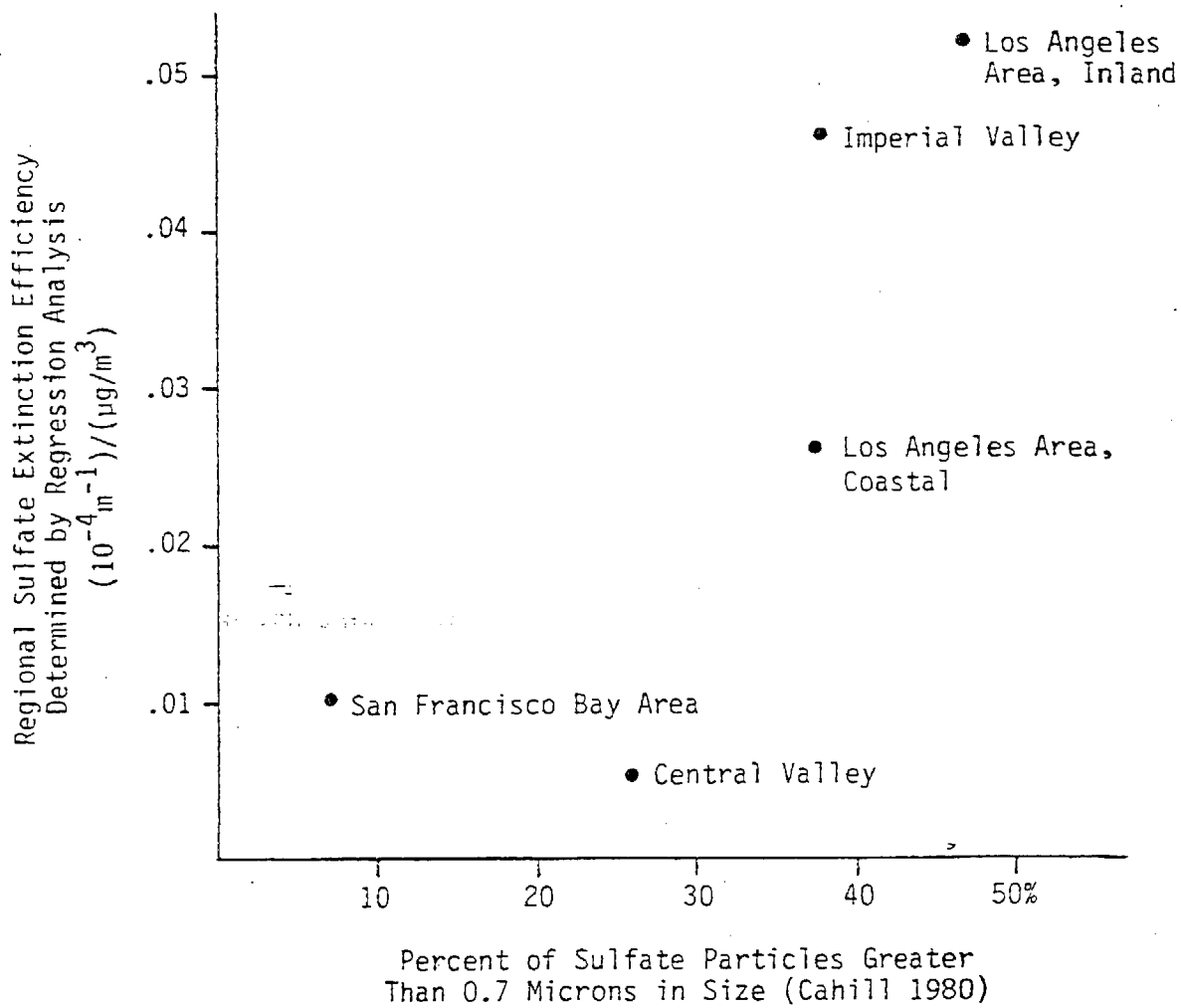


Figure 3.8 Relationship between regional extinction efficiency for sulfates and sulfate size distribution.

TABLE 3.8 EXTINCTION EFFICIENCIES SELECTED FOR EXTINCTION BUDGET CALCULATIONS.

LOCATION	$b_1 \cdot \frac{\text{SULFATE}}{(1-RH)}$	$b_2 \cdot \frac{\text{NITRATE}}{(1-RH)}$
	b_1	b_2
	$(10^{-4} \text{m}^{-1})/(\mu\text{g}/\text{m}^3)$	$(10^{-4} \text{m}^{-1})/(\mu\text{g}/\text{m}^3)$
SAN DIEGO AREA	.035	NC
LOS ANGELES AREA		
Coastal	.03	NC
Inland	.045	NC
SOUTHEAST DESERT AREA	.025	NC
CENTRAL COAST AREA	.02	NC
CENTRAL VALLEY	.02	.02
SAN FRANCISCO BAY AREA	.015	.02
NORTHERN COAST AREA (Humboldt)	.01	.02
NORTHERN INLAND AREA	.02	.02

NC Not calculated

Note: For the cellulose filter data in the San Francisco Bay Area, the statistical coefficients are used without modifications: $b_1 = .04$ and $b_2 = .01$.

problems with the nitrate variable and because of colinearity problems between the nitrate and sulfate variables. The nitrate term will not be specifically included in the extinction budgets for locations in southern California.

- Table 3.8 lists a nitrate coefficient of $.02 (10^{-4} \text{m}^{-1})/(\mu\text{g}/\text{m}^3)$ for all of northern California. This value is slightly less than the regression coefficients for northern California presented in Table 3.7. The regression coefficients for nitrate in northern California may have been slightly inflated because of colinearity with the sulfate variable.
- The sulfate coefficients for southern California in Table 3.8 are slightly deflated compared to those in Table 3.7; they are now more in line with the physically reasonable range of $.02$ to $.04 (10^{-4} \text{m}^{-1})/(\mu\text{g}/\text{m}^3)$. The sulfate regression coefficients in southern California (Table 3.7) may have been slightly overestimated due to colinearity problems.
- The sulfate coefficients for northern California in Table 3.8 are somewhat inflated compared to Table 3.7. The sulfate regression coefficients in northern California (Table 3.7) were probably underestimated due to colinearity with the nitrate variable. This is especially true in the Central Valley where the sulfate regression coefficient was very unstable (see previous footnote on page 78).
- For the cellulose filter data in the San Francisco Bay Area, we have no basis for interregional comparisons of the regression coefficients. We have adopted the statistical regression coefficients with no adjustments for the cellulose data.

3.5 REFERENCES FOR CHAPTER 3

- Allard, D. and I. Tombach, "Evaluation of Visibility Measurement Methods in the Eastern United States", Presented at the 73rd Annual Meeting of the Air Pollution Control Association, Montreal, June 22-27, 1980
- Appel, B.R., et al., "Interference Effects in Sampling Particulate Nitrate in Ambient Air," Atmospheric Environment, 13, pp. 319-325, 1979.
- Barone, J.B., T.A. Cahill, R.A. Eldred, R.G. Flocchini, D.J. Shadoan, and T.M. Dietz, "A Multivariate Statistical Analysis of Visibility Degradation at Four California Cities", Atmospheric Environment, 12, pp. 2213-2221, 1978.
- Bradway, R.M. and F.A. Record, "National Assessment of the Urban Particulate Problem, Volume II Particulate Characterization," EPA-450/3-76-025, 1976.
- Cahill, T., Personal communication of data, Air Quality Group, University of California, Davis, 1980.

Cass, G.R., "On the Relationship Between Sulfate Air Quality and Visibility With Examples in Los Angeles", Atmospheric Environment, 13, pp. 1069-1084, 1979.

Cass, G.R., P.M. Boone, and E.S. Macias, "Emissions and Air Quality Relationships for Atmospheric Carbon Particles in Los Angeles", Particulate Carbon: Atmospheric Life Cycle, G.T. Wolff and R.L. Klimish editors, Plenum Press, New York, 1981.

Cass, G.R. and G. McRae, "Source Contributions to Ambient Aerosol Samples", Report prepared under subcontract to Technology Service Corporation, California Institute of Technology, Pasadena, California, 1980.

Conklin, M.H., G.R. Cass, L.C. Chu, and E.S. Macias, "Wintertime Carbonaceous Aerosols in Los Angeles: An Exploration of the Role of Elemental Carbon", Atmospheric Aerosols: Source/Air Quality Relationships, American Chemical Society, 1981.

Countess, R.J., S.H. Cadle, P.J. Groblicki, and G.T. Wolff, "Chemical Analysis of Size-Segregated Samples of Denver's Ambient Particulate", Journal of the Air Pollution Control Association, 31, pp. 247-252, 1981.

Covert, D.S., R.J. Charlson, and N.C. Ahlquist, "A Study of the Relationship of Chemical Composition and Humidity to Light-Scattering by Aerosols", Journal of Applied Meteorology, 11, pp. 968-976, 1972.

Douglas, C.A. and L.L. Young, "Development of a Transmissometer for Determining Visual Range, U.S. C.A.A. Technical Development Report 78-197, 1948."

Faxvog, Fred R. and David M. Roessler, "Carbon Aerosol Visibility Vs. Particle Size Distribution", Applied Optics, Volume 17, 1978.

Groblicki, P.J., G.T. Wolff, and R.J. Countess, "Visibility Reducing Species in the Denver 'Brown Cloud': 1. Relationships Between Extinction and Chemical Composition", Atmospheric Environment, 1981.

Harker, A.B., L.W. Richards, and W.E. Clark, "The Effect of Atmospheric SO₂ Photochemistry Upon Observed Nitrate Concentrations in Aerosols," Atmospheric Environment, 11, pp. 87-91, 1977.

Hidy, G.M. et al, "Characterization of Aerosols in California", Rockwell International Science Center Report, California Air Resources Board, Contract No. 358, 1974.

Ho, W.W., G.M. Hidy, and R.M. Govan, "Microwave Measurements of the Liquid Water Content of Atmospheric Aerosols", Journal of Applied Meteorology, 13, pp. 871-879, 1974.

Latimer, D.A., R.W. Bergstrom, S.R. Hayes, M.T. Liu, J.H. Seinfeld, G.F. Whitten, M.A. Wojcik, and M.J. Hillyer, "The Development of Mathematical Models for the Prediction of Atmospheric Visibility Impairment", EPA-450/3-78-110a,b,c, EPA Office of Air Quality Planning and Standards, Research Triangle Park, North Carolina, 1978.

Leaderer, B.P. and J.A. Stolwijk, "Optical Properties of Urban Aerosol and Their Relation to Chemical Composition", Proceedings of the Symposium on Aerosols: Anthropogenic and Natural -- Sources and Transport, New York, NY, January 9-12, 1979.

Malm, Wm. C., "Visibility: A Physical Perspective", Proceedings of the Workshop in Visibility Values, Fort Collins, Colorado, Sponsored by U.S. Forest Service, January 28-February 1, 1979.

Malm, Wm. C., M.L. Pitchford, and S.F. Archer, "Comparison of Electro-Optical Measurements Made by Various Visibility Monitoring Instruments", Proceedings of Conference on View on Visibility -- Regulatory and Scientific, Sponsored by APCA, pp. 222-231, 1979.

Middleton, W.E.K., "Vision Through the Atmosphere", Toronto, University Press, 1952.

NRC (National Research Council), Airborne Particles, University Park Press, Baltimore, MD, 1979.

Quimette, J.R., "Chemical Species Contributions to the Extinction Coefficient", Ph.D. thesis, California Institute of Technology, Pasadena, California, 1981.

Sandberg, J.S., Personal communication, Bay Area Air Pollution Control District, San Francisco, California, 1981.

Spicer, C.W. and P.M. Schumacher, "Particulate Nitrate: Laboratory and Field Studies of Major Sampling Interferences," Atmospheric Environment, 13, pp. 543-552, 1979.

Stelson, A.W., S.K. Friedlander, and J.H. Seinfeld, "A Note on the Equilibrium Relationship Between Ammonia and Nitric Acid and Particulate Ammonium Nitrate", Atmospheric Environment, 13, pp. 369-371, 1979.

Stelson, A.W. and J.H. Seinfeld, "Chemical Mass Accounting of Urban Aerosol", Environmental Science Technology, 14, pp. 1491-1498, 1981.

Tang, I.N., "Deliquescence Properties and Particle Size Change of Hygroscopic Aerosols", Generation of Aerosols and Facilities for Exposure Experiments, Ann Arbor Science Publishers Inc., Ann Arbor, Michigan, 1981.

Trijonis, J.C., "Visibility in the Southwest: An Exploration of the Historical Data Base", Atmospheric Environment, 13, pp. 833-843, 1979.

Trijonis, J.C., "Visibility in California," Prepared under contract A7-181-30 and, also accepted for publication in the Journal of the Air Pollution Association, 1980.

Trijonis J. and K. Yuan, "Visibilities in the Northeast: Long-Term Visibility Trends and Visibility/Pollution Relationships," EPA-600/3-78-075, 1978.

Whitby, K.T. and B. Cantrell, "Fine Particles," in International Conference on Environmental Sensing and Assessment, New York: Institute of Electrical and Electronics Engineers, 1976.

Whitby, K.T. and G.M. Sverdrup, "California Aerosols: Their Physical and Chemical Characteristics," to be published in the ACHEX Hutchinson Memorial Volume, Particle Technology Laboratory Publication No. 347, University of Minnesota, Minneapolis, Minnesota, 1978.

White, W.H., "The Role of Particulate Sulfates and Nitrates in Reducing Visibility", Presented at the 74th Annual Meeting of the Air Pollution Control Association, Philadelphia, Pennsylvania, June 21-26, 1981.

White, W.H. and P.T. Roberts, "On the Nature and Origins of Visibility-Reducing Aerosols in the Los Angeles Air Basin," Atmospheric Environment, 11, p. 803, 1977.

Willeke, K., and K.T. Whitby, "Atmospheric Aerosols: Size Distribution Interpretation," Journal of the Air Pollution Control Association, Vol. 25, pp. 529-534, 1975.

Williamson, S.J., Fundamentals of Air Pollution, Addison Wesley, Reading, Massachusetts, 1973.

Wolff, G.T., R.J. Countess, P.J. Groblicki, M.A. Ferman, S.H. Cadle, and J.L. Muhlhaier, "Visibility-Reducing Species in the Denver 'Brown Cloud.' ~~Part II. Sources and Temporal Patterns~~", for the Symposium at the Grand Canyon, Sponsored by USEPA, USNPS, EPRI, and Salt River Project, November 1980.

4. EXTINCTION BUDGETS

This chapter presents extinction budgets for the 34 Hi-Vol sites at which we performed visibility/aerosol regression studies (in Chapter 3). First, we calculate gaseous extinction using known values for light scattering by air molecules and light absorption by NO_2 . Then, we apportion aerosol extinction among sulfates, nitrates, and other particles using the aerosol extinction efficiencies tabulated at the end of Chapter 3.

4.1 EXTINCTION BY GASES

At sea level, the extinction due to Rayleigh (blue-sky) scatter by air molecules is $0.12 \cdot 10^{-4} \text{ m}^{-1}$ (EPA 1979). Rayleigh scattering decreases with altitude, i.e. with the density of air, but none of our study sites is sufficiently elevated to affect Rayleigh scattering significantly. The value of $0.12 \cdot 10^{-4} \text{ m}^{-1}$ applies uniformly to all of our study locations.

The extinction due to light absorption by NO_2 can be calculated by the formula;

$$B_{\text{NO}_2} = 3.3[\text{NO}_2], \quad (4-1)$$

where the units of B_{NO_2} are 10^{-4} m^{-1} and the units of $[\text{NO}_2]$ are ppm (Nixon 1940; Hodkinson 1966; Groblicki et al. 1980; Ferman et al. 1980). The constant, 3.3, in Equation (4-1) corresponds to the absorption efficiency of NO_2 at a light wavelength of 550 nm, the center of the wavelength response range for the human eye. Of course, NO_2 absorbs light much more efficiently for shorter (blue) wavelengths than longer (red) wavelengths, explaining why NO_2 is particularly important with respect to discoloration (producing a brownish effect). We are not concerned here with discoloration, however, but only with the aggregate effect of NO_2 on extinction and visual range.

Table 4.1 presents average NO_2 concentrations for our study locations and study periods.* The right hand column of Table 4.1 lists the average extinction contribution from NO_2 , calculated by Equation (4-1).

* In a few cases, we had to substitute NO_2 data from nearby sites because NO_2 data were not available for our study locations. Also, in a few cases, we did not have NO_2 data for all the years in the study period.

TABLE 4.1 AVERAGE CONTRIBUTIONS OF NO₂ TO EXTINCTION LEVELS.

SITES*	YEARS OF DATA	ANNUAL MEAN NO ₂ (pphm)	MEAN EXTINCTION DUE TO NO ₂ (10 ⁻⁴ m ⁻¹)
SAN DIEGO AREA			
San Diego	1960-1976	2.9	0.10
San Diego	1976-1979	5.1	0.17
El Cajon	1976-1979	5.4	0.18
LOS ANGELES AREA (Coastal)			
Long Beach	1967-1977	7.2	0.24
Costa Mesa	1976-1979	3.0	0.10
Lennox	1973-1977	6.5	0.21
Downtown L.A.	1973-1977	7.4	0.24
Santa Barbara	1976-1979	3.8	0.13
LOS ANGELES AREA (Inland)			
Burbank	1966-1974	8.5	0.28
La Habra	1976-1979	5.6	0.18
Ontario	1970-1972	4.4	0.15
San Bernardino	1968-1976	4.1	0.14
SOUTHEAST DESERT AREA			
Palm Springs (Indio)	1976-1979	1.9	0.06
Lancaster	1974-1977	1.6	0.05
Victorville	1975-1979	1.8	0.06
El Centro (Indio)	1976-1979	1.9	0.06
CENTRAL COAST AREA			
Salinas	1976-1979	1.5	0.05
Paso Robles (San Luis Obispo)	1977-1979	2.2	0.07
CENTRAL VALLEY AREA			
Bakersfield	1976-1979	4.4	0.15
Fresno	1970-1976	3.1	0.10
Merced	1976-1979	2.6	0.09
Sacramento	1968-1976	2.7	0.09
Sacramento	1976-1979	3.2	0.11
SAN FRANCISCO BAY AREA (Urban)			
Redwood City	1970-1975	3.1	0.10
Oakland	1966-1976	3.6	0.12
San Jose	1970-1975	3.7	0.12
San Jose	1976-1979	4.2	0.14
SAN FRANCISCO BAY AREA (Suburban)			
Livermore	1973-1975	3.1	0.10
Concord	1973-1975	2.8	0.09
Napa	1972-1975	2.5	0.08
Santa Rosa	1972-1975	2.1	0.07
NORTHERN COAST AREA			
Humboldt (Eureka)	1972	1.7	0.06
NORTHERN INLAND AREA			
Red Bluff	1976-1979	1.7	0.06
Yreka (Red Bluff)	1976-1977	1.5	0.05

* Sites in parentheses are NO₂ stations substituted for cities that have no NO₂ data.

4.2 EXTINCTION BUDGETS

Table 3.8 at the end of Chapter 3 lists regional extinction efficiencies "b_i" for sulfates and nitrates. These extinction efficiencies pertain to "dry" conditions (zero relative humidity). As explained in Chapter 3, the average extinction contributions from sulfates and nitrates are simply b₁ times the average value of SULFATE/(1-RH) and b₂ times the average value of NITRATE/(1-RH), respectively. We have calculated these contributions for each of our study sites (note that the nitrate variable is included only at the northern California locations). Also, at each site, we have calculated average extinction from the "remainder of aerosol" simply by subtracting the sulfate, nitrate, air molecule, and NO₂ contributions from total average extinction.

Table 4.2 presents the extinction budgets for the 34 Hi-Vol study locations. The table lists total average extinction levels at each site and the percentage contributions from Rayleigh scatter, NO₂, sulfates, nitrates, and other aerosols.

Because Rayleigh (blue-sky) scatter is essentially constant, the percentage contribution from Rayleigh scatter is inversely proportional to average total extinction (directly proportional to visual range). In the densely populated parts of the Los Angeles basin, where median visibility is less than 10 miles (see Figure 4.1), Rayleigh scatter constitutes only about 4-6% of average extinction. In those areas where median visibility is 10-15 miles, i.e. the San Joaquin Valley and a narrow strip along the coastline, Rayleigh scatter contributes only 7-10% to average extinction. At Red Bluff and Yreka, on the other hand, where median visibility is over 40 miles, Rayleigh scatter accounts for nearly 25% of extinction. Furthermore, simple calculations show that Rayleigh scatter contributes more than 40% of extinction in the area along the Nevada border where median visibility exceeds 70 miles.

The percentage contributions from NO₂ are fairly uniform among the study locations -- typically 7-11%. This reflects the phenomenon that locations with higher pollutant aerosol levels and resulting higher average extinction levels also tend to have higher NO₂ levels.

TABLE 4.2 EXTINCTION BUDGETS FOR THE 34 HI-VOL STUDY LOCATIONS

	AVERAGE EXTINCTION (10^{-4} m^{-1})	PERCENTAGE CONTRIBUTION TO AVERAGE EXTINCTION				
		GASES		PARTICLES		
		Rayleigh Scatter	NO ₂	Sulfates	Nitrates	Other Aerosols
SAN DIEGO AREA						
San Diego (NASN)	1.85	6%	5%	54%	NC	35%
San Diego (ARB)	1.73	7%	10%	62%	NC	21%
El Cajon	1.23	10%	15%	55%	NC	20%
LOS ANGELES AREA (Coastal)						
Long Beach	2.07	6%	12%	51%	NC	31%
Costa Mesa	2.02	6%	5%	43%	NC	46%
Lennox	2.39	5%	9%	75%	NC	11%
Downtown L.A.	3.05	4%	8%	46%	NC	42%
Santa Barbara	1.29	9%	10%	50%	NC	31%
LOS ANGELES AREA (Inland)						
Burbank	2.10	6%	13%	52%	NC	29%
La Habra	1.82	7%	10%	73%	NC	10%
Ontario	2.98	4%	5%	32%	NC	59%
San Bernardino	2.38	5%	6%	44%	NC	35%
SOUTHEAST DESERT AREA						
Palm Springs	0.86	14%	7%	29%	NC	50%
Lancaster	0.77	16%	6%	28%	NC	50%
Victorville	0.74	16%	8%	35%	NC	41%
El Centro	0.74	16%	8%	33%	NC	43%
SOUTHWEST AREA						
Salinas	1.10	11%	5%	29%	NC	55%
Paso Robles	0.86	14%	8%	32%	NC	46%
CENTRAL VALLEY AREA						
Bakersfield	1.81	7%	8%	28%	42%	15%
Fresno	1.49	8%	7%	17%	30%	38%
Merced	1.30	9%	7%	16%	30%	38%
Sacramento (NASN)	1.37	9%	7%	18%	17%	49%
Sacramento (ARB)	1.31	9%	8%	16%	20%	47%
SAN FRANCISCO BAY AREA (Urban)						
Redwood City*	1.49	8%	7%	25%	9%	51%
Oakland	1.63	7%	7%	30%	22%	33%
San Jose* (AQMD)	1.27	9%	9%	23%	11%	48%
San Jose (ARB)	1.35	9%	10%	13%	27%	41%
SAN FRANCISCO BAY AREA (Suburban)						
Livermore*	0.88	14%	11%	25%	13%	37%
Concord*	0.91	13%	10%	32%	12%	33%
Napa*	0.87	14%	9%	32%	12%	33%
Santa Rosa*	0.88	14%	8%	25%	12%	40%
NORTHERN COAST AREA						
Humboldt	1.55	8%	4%	11%	4%	73%
NORTHERN INLAND AREA						
Red Bluff	0.53	23%	11%	24%	36%	6%
Yreka	0.55	22%	9%	31%	13%	25%

* Cellulose filter data

NC Not calculated. Nitrate aerosols are part of the "other" category at locations in southern California.

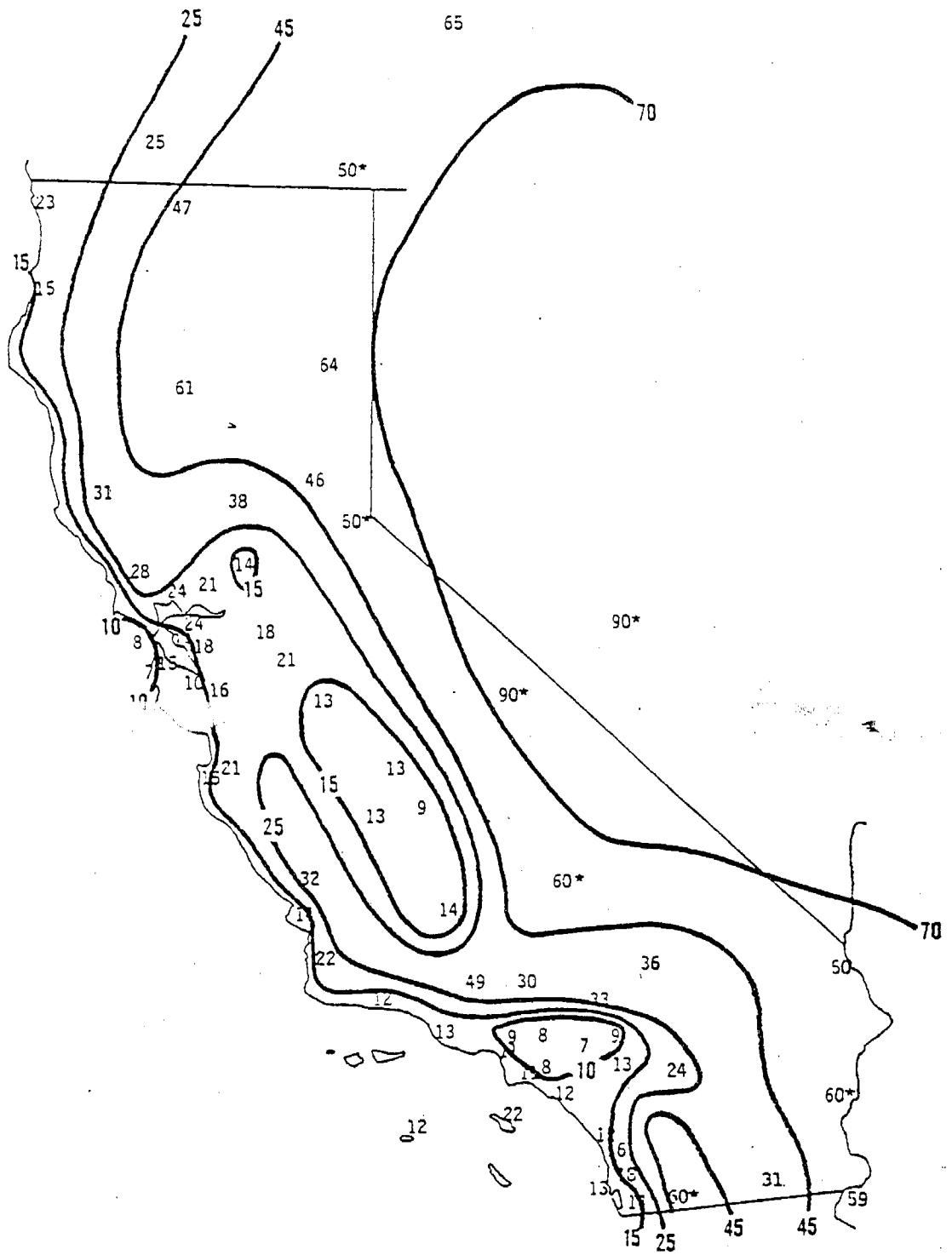


Figure 4.1 Median 1 PM visibilities (in miles) and visibility isopleths for California (Trijonis 1980).

Table 4.2 indicates that sulfate aerosol is the predominant visibility reducing pollutant in the Los Angeles and San Diego areas. In the Los Angeles and San Diego areas, we estimate that sulfates account for about 40-70% of total extinction and about 50-75% of aerosol (non-Rayleigh, non-NO₂) extinction. Sulfates are also significant in the remainder of California, typically contributing about 15-35% of total extinction. As discussed previously in Section 3.2.3, sulfates are critical to visibility not only because they constitute a significant fraction of the fine aerosol but also because they attract a large volume of water into the aerosol phase.

Our methodology indicates that nitrates generally account for about 10-40% of extinction at locations in the northern half of California. The nitrate contributions are especially large, 20-40%, in the Central Valley (including Red Bluff). As noted previously in Section 3.2.5, the visibility/nitrate relationships are very uncertain because of statistical colinearity problems and because of severe measurement difficulties for nitrates. The nitrate variable might best be viewed as a crude representation of nitrate aerosol. ~~As a result, nitrate aerosol~~ ~~is a poor representation of nitrate aerosol~~ ~~and other aerosol~~ ~~pollutants~~ (e.g. NO₂ and secondary organic aerosols). To the extent that nitrate is partially acting as a surrogate for NO₂, there is some double-counting in Table 4.2 (to rectify this, the nitrate contributions might be lessened and the other aerosol contributions might be increased). Also we expect that, at certain locations (especially the Central Valley), the nitrate contributions might be overestimated at the expense of sulfate contributions due to colinearity problems between nitrates and sulfates. A thorough study of the role of nitrates in California visibility must await the development of a reliable sampling procedure for nitrate aerosols.

The extinction contribution from "other aerosols" ranges widely among the locations, from 10 to 70%. Based on other studies using more detailed aerosol data (Hidy et al. 1974; Trijonis et al. 1980; Dzubay 1980; Groblicki et al. 1980; Wolff et al. 1980; Stevens et al. 1980; Pierson et al. 1980; Macias et al. 1980; Herman et al. 1981; Conklin et al. 1981), we know that the important components of this "other" category are light absorption by elemental carbon (soot) and light scattering by various fine aerosols (organics, fine particles at the lower end of the soil dust and sea salt size

distributions, elemental carbon particles, non-carbonaceous primary aerosols from combustion processes, etc.).* It is worthwhile to note that, in urban areas, elemental carbon (soot) is likely to be the most important contributor in the "other aerosol" category. The results of Conklin et al. (1981) and Groblicki et al. (1980) suggest that elemental carbon particles account for approximately 20-40% of extinction in the Los Angeles area.

As a postscript to this chapter, it is interesting to point out the unusual extinction budget at Humboldt. The "pollutant" variables -- nitrogen dioxide, sulfates, and nitrates -- account for only a small fraction of extinction at Humboldt. This finding supports the conclusion of Trijonis (1980) that the low visibilities along the northern California coast (15-20 miles medians) are mostly due to natural factors rather than man-made factors.

4.3 REFERENCES FOR CHAPTER 4

Conklin, M.H., "Wintertime Carbonaceous Aerosols in Los Angeles: An Exploration of the Role of Elemental Carbon", Atmospheric Aerosols: Source/Air Quality Relationships, American Chemical Society, 1981.

Dzubay, T.G., "Chemical Element Balance Method Applied to Dichotomous Sampler Data", Annals of the New York Academy of Science, Volume 338, pp. 126-144, 1980.

Ferman, M.A., G.T. Wolff, and N.A. Kelly, "The Nature and Sources of Haze in the Shenandoah Valley/Blue Ridge Mountains Area", Journal of the Air Pollution Control Association, Volume 31(10), pp. 1074-1081, 1981.

Groblicki, P.J., G.T. Wolff, and R.J. Countess, "Visibility Reducing Species in the Denver 'Brown Cloud': 1. Relationships Between Extinction and Chemical Composition", Atmospheric Environment, 1981.

Hidy, G.M. et al., "Characterization of Aerosols in California", Rockwell International Science Center Report, California Air Resources Board, Contract No. 358, 1974.

*The reader should note that nitrate aerosols are part of the "other" category at the study locations in southern California.

Hodkinson, J.R., "Calculations of Color and Visibility in Urban Atmospheres Polluted by Gaseous NO₂", Air Water Pollution International Journal, Volume 10, pp. 137, 1966.

Macias, E.S., J.O. Zwicker, J.R. Quimette, S.V. Hering, S.K. Friedlander, T.A. Cahill, G.A. Kuhlmeier, L.W. Richards, "Regional Haze Case Studies in the Southwestern U.S. -- Part I. Aerosol Chemical Composition", Atmospheric Environment, Volume 15, pp. 1971-1986, 1981.

Nixon, J.K., "Absorption Coefficient of NO₂ in the Visible Spectrum", Journal of Chemical Physics, Volume 8, pp. 157, 1940.

Pierson, W.R., W.W. Brachaczek, T.J. Truex, J.W. Butler, and T.J. Korinski, "Ambient Sulfate Measurements on Allegheny Mountain and the Question of Atmospheric Sulfate in the Northeastern United States", Annals of the New York Academy of Sciences, 338, pp. 145-173, 1980.

Stevens, R.K., T.G. Dzubay, R.W. Shaw, W.A. McClenny, C.W. Lewis, and W.E. Wilson, "Characterization of the Aerosol in the Great Smoky Mountains", Environmental Science Technology, 14, pp. 1491-1498, 1980.

Trijonis, J., "Visibility in California", prepared for the California Air Resources Board, under Contract 607-10-10-10, April 1980.

Trijonis, J., J. Eldon, J. Gins, and G. Berglund, "Analysis of the St. Louis RAMS Ambient Particulate Data", EPA-450/4-80-006a,b, EPA Office of Air Quality Planning and Standards, Research Triangle Park, North Carolina, 1980.

Wolff, G.T., R.J. Countess, P.J. Groblicki, M.A. Ferman, S.H. Cadle, and J.L. Muhlbaier, "Visibility-Reducing Species in the Denver 'Brown Cloud.' Part II. Sources and Temporal Patterns", for the Symposium at the Grand Canyon, November 1980.

5. FUTURE VISIBILITY MONITORING

To conclude this report, we consider future visibility monitoring requirements. There is an apparent need for two distinct types of visibility-related monitoring in California. The first type (Section 5.1) concerns the collection of precise instrumental data on visibility for quantifying existing conditions, spatial/temporal patterns, and future trends. The second type (Section 5.2) involves collection of detailed particulate data for determining exact extinction budgets in various areas in California.

5.1 VISIBILITY MONITORING NETWORK

A great deal has been learned about the geographical, seasonal, diurnal, and historical patterns of visibility in California through analysis of routine airport visual range data (Trijonis 1980). Nonetheless, it appears that the ARB should consider establishing an instrumental network for collecting more precise data on existing spatial/temporal patterns of visibility. The need for such a network is partly established by the monitoring requirements of the EPA visibility regulations (Federal Register 1980). According to the EPA visibility regulations, State Implementation Plans must include "a strategy for evaluating visibility in any mandatory Class I Federal area" (there are 29 such areas in California). Concomitantly, the ARB might want to collect parallel and equivalent data for non-Class I parts of California (e.g. in the Central Valley, Imperial Valley, Los Angeles area, San Francisco area, coastal towns, etc.).

This section briefly describes available methods for measuring visibility. We also recommend specific methods to be used if the ARB were to establish a visibility monitoring network.

5.1.2 Visibility Monitoring Methods

Measurement techniques for visibility have been thoroughly reviewed in several recent reports and papers (Tombach 1978, 1979; Charlson et al. 1978; EPA 1979; Malm et al. 1979; Malm and Walther 1980). The paragraphs below present a brief synopsis of this literature. For more detailed

discussions of visibility monitoring methods, the reader is directed to the references cited above.

It is important to note that the various monitoring techniques for visibility often measure different specific parameters, e.g. visual range, extinction coefficient, or contrast. The different parameters, however, are closely interrelated. In fact, for a uniform one-dimensional atmosphere, the mathematical expressions relating the parameters are extremely simple. For example, contrast (the relative brightness of various features) is related to extinction coefficient by the formula:

$$C_x = C_0 e^{-Bx} \quad (5-1)$$

where B is the extinction coefficient, C_0 is the inherent contrast or relative brightness of a target and the background (e.g. of a mountain and the sky)*, and C_x is the contrast at a distance x from the target. Assuming that a black target is being viewed against the horizon sky ($C_0 = -1$), and assuming a detectable contrast of 0.02 for the typical observer, Koschmeider (1924) solved Equation (5-1) to derive the "Koschmeider formula" relating visual range (V) to extinction (B),

$$V = \frac{-\ln 0.02}{B} = \frac{3.9}{B} \quad (5-2)$$

Combining Equations (5-1) and (5-2), one can relate contrast and visual range according to the formula

$$C_x = C_0 e^{-3.9x/V} \quad (5-3)$$

It should be noted that, in the case of a nonuniform atmosphere and/or the case of nonuniform illumination of the atmosphere, the above formulae become much more complex, involving integrals of the extinction coefficient over the line of sight.

* If L is the brightness or luminance of the target and L' is the brightness or luminance of the background, then

$$C_0 = \frac{L - L'}{L'}$$

For a black target, L = 0, and $C_0 = -1$.

There are five basic ways of measuring visibility: human observers, telephotometers, photographic photometers, transmissometers, and nephelometers. Human observations of "prevailing visibility" provide a direct measurement of visual range. According to National Weather Service procedures, prevailing visibility is defined as the greatest visual range that is attained or surpassed around at least half of the horizon circle, but not necessarily in continuous sectors (Williamson 1973). Daytime visibility is measured by observing markers (e.g. buildings, mountains, towers, etc.) against the horizon sky. Nighttime visibility measurements are based on unfocused, moderately intense light sources. Advantages of human observations are that they require no instrumentation and that the data tend to be of fair quality for several types of applications (Trijonis 1980). Some disadvantages are that large dark targets (or light sources) are needed at multiple distances in various directions, that the measurement involves subjective judgement, that perception levels may vary among observers, and that observers are often forced to use non-dark targets.*

A telephotometer essentially consists of a photometer combined with a lens. Such a device can be used to measure the contrast between a target and the background sky. If the inherent contrast of the target and sky as well as the distance to the target are known, Equations (5-1) and (5-3) can be used to solve for extinction coefficient and visual range. Advantages of this approach are that commercial equipment are available, that a permanent record is obtained, and that telephotometer measurements correlate better with human perceptions than values derived from other instruments. Some disadvantages are (1) dark targets are needed at several distances, with each distance slightly less than the visual range being measured, (2) scattered light in the optics of the instrument can create problems, (3) a good quality control program is necessary (Tombach 1978), (4) only daytime measurements can be taken, and (5) problems can be created by clouds behind the targets or by variation of illumination conditions on non-black targets.

* As noted previously in Section 3.1.2, human observations typically underestimate true visual range (defined for a black object and for a perception threshold of 0.02). Accordingly, the Koschmieder constant must be adjusted to obtain an unbiased estimate of extinction coefficient from typical human observer data.

Photographic photometry is similar to telephotometry except that contrast changes are measured on photographic film using a densitometer. The contrast measurements can be converted to extinction coefficient or visual range using Equation (5-1) or (5-3). Photographic photometry has the advantages of commercially available equipment and the presence of a permanent record. Some disadvantages are (1) dark targets are needed at several distances, with each distance slightly less than the visual range being measured, (2) careful quality control is needed concerning film density and exposure, (3) there is a significant time delay in making the measurement, and (4) only daytime measurements can be taken (EPA 1979; Tombach 1978).

The transmissometer measures the fractional transmittance (T) of light over a given path length (X). The transmittance can be used to compute the attenuation or extinction coefficient (B) according to

$$B = \frac{-1}{X} \ln T \quad (5-4)$$

Visual range can then be calculated according to the Koschmeider formula, equation (5-2). Advantages of the transmissometer are that it works at night and that commercial equipment are available for short path lengths. A major disadvantage is that the instrument is only accurate for visual ranges up to about 20 path lengths; for the typical 500 feet distance of short-path transmissometers, this implies accuracy only up to 2 miles visual range. For longer path lengths, commercial equipment are not available, and transmissometry is made very difficult due to interference with the light beam by atmospheric turbulence (Malm et al. 1979). Other disadvantages are (1) the choice of light beam size may be critical, (2) careful maintenance is required if a retroreflector is used, (3) the spectral response of the instrument should be matched to the human eye, and (4) visibility is measured only over the light path and not over the full range of view (Tombach 1978).

Integrating nephelometers measure the scattering component of extinction. If it is assumed that light scattering is the dominant part of extinction, the Koschmeider formula can be used to calculate visual range. The advantages of nephelometers are that commercial equipment are available,

that nephelometers work at night, that they are portable and easy to use, and that they can be used even when the sight path is obstructed. The disadvantages are (1) local visibility is measured rather than visibility over the entire sight path, (2) the absorption component of extinction is neglected, and (3) the air may be modified significantly during sampling (losing larger particles and decreasing relative humidity).

5.1.2 Recommended Monitoring Method

If the ARB does create a new visibility monitoring network in California, we recommend that it be a telephotometer network or a nephelometer network (or both). At present, choosing between these two options is somewhat problematical, so that the ARB might want to give the issue further study (e.g. through a seminar or workshop including users and proponents of each instrument).

One important reason for favoring telephotometers is to achieve comparability with the National Park Service telephotometer program operated in the West (and recently expanded to include sites in California). Also, telephotometers are commercially available, yield permanent records, and correlate well with human perceptions. The most significant disadvantage is the difficulty in interpreting data for non-black targets and for conditions with clouds behind the targets.

Nephelometers also are commercially available, yield permanent records, and correlate well with human perceptions. Because nephelometers fail to measure aerosol absorption, a nephelometry network should be combined with instruments for measuring particle absorption (e.g. modified COH paper tape samplers). Other significant disadvantages of the nephelometer are loss of relative humidity and large particles in the sampling train and, possibly, the expense associated with maintaining high quality performance.

It would not be prudent to create an extensive new monitoring program based on human visibility observations because of the high manpower costs and because of the subjectivity involved in human visibility observations. Photographic photometry seems to be inferior to telephotometry because of quality control problems in film densities and exposure. Transmissometry may be the best monitoring technique at some future date (Malm 1981), but

there are no commercial long path transmissometers currently available. Even if the technology for long path transmissometry is significantly improved, it is likely to remain a rather expensive option.

At visibility monitoring sites in mandatory Class I Federal areas, the ARB might want to supplement the telephotometry or nephelometry with photographs and/or human observations. Unlike the continuous (e.g. daily) telephotometry or nephelometry readings, the photographs or human observations could be taken on an intermittent basis. Photographs or human observations are needed in mandatory Class I areas because the current phase (Phase I) of the EPA visibility regulations focuses on visibility degradation that is "reasonably attributable" to "a single source or small group of sources". According to the EPA regulations, direct observations are important in defining "reasonably attributable". Furthermore, photographs would be useful for hearings and presentations as well as for making qualitative assessments of the value of clean versus degraded views.

5.2 EXTINCTION BUDGET

At several scattered locations in California it would be worthwhile for the ARB to conduct field projects that can provide accurate extinction budgets. Based on our knowledge of the potentially important visibility-reducing species and on a review of previous field projects, we think that extremely useful studies can be conducted with a very limited amount of instrumentation. These field projects should be similar to the recent studies conducted by General Motors in Denver and Virginia (Groblicki et al. 1980; Ferman et al. 1981).

Table 5.1 lists the type of instrumentation needed for the extinction budget monitoring projects. The minimum instrumentation required to determine detailed extinction budgets consists of only two nephelometers and two dichotomous samplers. Optional instrumentation includes a third dichotomous sampler, an NO₂ monitor, and measurements of aerosol acidity (e.g. sulfate and nitrate cations).

The data taken in the special field projects can be used to compute average extinction budgets as follows:

- The extinction contribution from Rayleigh scattering by air molecules -- $0.12 \cdot 10^{-4} \text{ m}^{-1}$ at sea level -- is known (see Section 4.1).
- Light absorption by NO_2 can be calculated from average NO_2 concentrations using Equation (4-1) (see Section 4.1). Average NO_2 concentrations can be estimated from the abundant NO_2 data available at numerous locations in California. Optionally, site-specific NO_2 monitoring can be conducted as part of the project.

TABLE 5.1 INSTRUMENTATION FOR DETERMINING DETAILED EXTINCTION BUDGETS.

INSTRUMENT	PARAMETERS MEASURED
NECESSARY INSTRUMENTATION	
Heated Nephelometer	Scattering by "dry" particles.
Ambient Nephelometer	Scattering by ambient "wet" particles.
Dichotomous sampler with teflon filters	Fine and coarse particle mass, fine and coarse sulfate mass, fine and coarse nitrate mass. (Optionally, fine and coarse values for other trace elements: Pb, K, Si, etc.).
Dichotomous sampler with quartz filters	Fine and coarse mass for organics and elemental carbon.
OPTIONAL INSTRUMENTATION	
Dichotomous sampler with nuclepore filters	Light absorption by fine and coarse particles.
NO_2 monitor	NO_2 concentration.
Technique to measure aerosol acidity	Cations (e.g. H and NH_4) associated with sulfates and nitrates.
Cascade impactors	Aerosol size distribution, disaggregated by chemical composition.

- The average contribution of elemental carbon to light absorption can be computed from average fine and coarse elemental carbon concentrations and from published absorption efficiencies for fine and coarse elemental carbon (Groblicki et al. 1980; Conklin

et al. 1981). Optionally, site-specific absorption efficiencies for fine and coarse elemental carbon can be determined by measuring particulate light absorption using dichotomous samplers with nuclepore filters (or, possibly, the ones with teflon filters). This option would also allow one to assess whether aerosols other than elemental carbon -- e.g. soil dust aerosols -- might contribute significantly to light absorption.

- The relative contributions of fine and coarse particles to "dry" aerosol scattering can be determined with bi-variate regression analyses relating the heated nephelometer data to fine and coarse particle concentrations. It is expected that the fine component would predominate over the coarse component, i.e. fine aerosol scattering would be an order of magnitude greater than coarse aerosol scattering. The "dry" scattering from fine aerosols could then be apportioned among various species (e.g. sulfates, nitrates, organics, elemental carbon, and other fine aerosols) using multiple regression techniques similar to those employed in this report.* Light scattering by the water attached to the fine aerosol -- ambient nephelometer data minus heated nephelometer data -- could be apportioned to the fine aerosol electrolytes (e.g. sulfates and nitrates) based on reasonable thermodynamic assumptions (Ferman et al. 1981). Alternatively, the scattering by water could be apportioned to various fine aerosol species based on further regression analysis (Groblicki et al. 1980). This latter regression analysis might be significantly improved if data are available on the acidity of the aerosol electrolytes (Ferman et al. 1981; Wolff 1981).

The final extinction budget at each site would be in the format of Table 5.2. It is remarkable that such a detailed extinction budget can be derived with a rather limited amount of instrumentation.

* It should be noted that the optional monitoring program using cascade impactors would allow Mie theory calculations to supplement or replace many of the regression analyses. Using cascade impactors may be advisable in cases where statistical problems are anticipated in the regression analysis. Cascade impactor data would also allow one to address problems related specifically to aerosol size distribution (such as wavelength-dependent scattering and size-dependent aerosol control options).

Computing extinction budgets from the field study measurements will require a considerable amount of data analysis. If such field studies are undertaken, it is recommended that ample funds also be set aside for the data analysis. A shortcoming of many previous air pollution field studies has been the tendency to devote too few resources to data analysis as compared to data collection.

It may not be cost-effective for extinction budget monitoring stations to be permanently sited. However, in order to avoid seasonal biases and in order to provide robust data sets, such monitoring stations should be operated for one year at each location. A reasonable plan might be to establish five portable monitoring stations that would be relocated every twelve months. In several years, detailed extinction budgets would be available throughout California.

Once the extinction budgets were obtained, a source allocation could

TABLE 5.2 FORMAT FOR EXTINCTION BUDGETS.

RAYLEIGH SCATTER- - - - -	A
NO ₂ ABSORPTION- - - - -	B
PARTICLE ABSORPTION - - - - -	$C = \sum_i C_i$
Fine elemental carbon.	C ₁
Coarse elemental carbon.	C ₂
Other aerosols (optional).	C ₃
PARTICLE SCATTERING - - - - -	$D = d_1 + d_2$
Coarse Particles	d ₁
Fine Particles	$d_2 = \sum_i \delta_i$
Sulfates (plus water).	δ_1
Nitrates (plus water).	δ_2
Organics	δ_3
Elemental carbon	δ_4
Fine crustal	δ_5
Other fine (plus water?)	δ_6
TOTAL EXTINCTION- - - - -	A + B + C + D

be performed by apportioning each component of extinction according to regional emissions (after subtracting background and interregional contributions). This source allocation would require emission inventories for sulfur oxides, nitrogen oxides, hydrocarbons, elemental carbon, organic aerosols, and other primary fine aerosols. Methods or assumptions would also have to be formulated for distinguishing secondary organic aerosols (related to gaseous hydrocarbon emissions) from primary organic aerosols (related to particulate emissions). The source allocation would allow one to calculate the effects on regional haze of increases or decreases in emissions from various source categories.

5.3 REFERENCES FOR CHAPTER 5

Charlson, R.J., A.P. Waggoner, and J.F. Thielke, "Visibility Protection for Class I Areas. The Technical Basis", Report to Council of Environmental Quality, 1978.

Cass, G.R., L.C. Chu, and E.S. Macias, "Wintertime Carbonaceous Aerosols in Los Angeles: An Exploration of the Role of Elemental Atmospheric Aerosols: Source/Air Quality Relationships, 1981.

EPA, Protecting Visibility, EPA-450/5-79-008, EPA Office of Air Quality Planning and Standards, Research Triangle Park, North Carolina.

Federal Register, "Visibility Protection for Federal Class I Areas," Part IV Environmental Protection Agency, December 2, 1980.

Ferman, M.A., G.T. Wolff, and N.A. Kelly (1981), "The Nature and Sources of Haze in the Shenandoah Valley/Blue Ridge Mountains Area", Journal of the Air Pollution Control Association, 1981.

Groblicki, P.J., G.T. Wolff, and R.J. Countess, "Visibility Reducing Species in the Denver 'Brown Cloud': 1. Relationships Between Extinction and Chemical Composition", Atmospheric Environment, 1981.

Koschmieder, H., "Theorie der Horizontalen Sichtweite," Beitr. phys. freien Atm., Volume 12, pp. 33-53, 1924.

Malm, Wm. C., Personal communication, Colorado State University, Fort Collins, Colorado, 1981.

Malm, Wm. C., M.L. Pitchford, and S.F. ...cher, "Comparison of Electro-Optical Measurements Made by Various Visibility Monitoring Instruments", Proceedings of Conference on View on Visibility -- Regulatory and Scientific, Sponsored by APCA, pp. 222-231, 1979.

Malm, Wm. C. and Walther, A Review of Instrument-Measuring Visibility Related Variables, EPA-600/4-80-016, February, 1980.

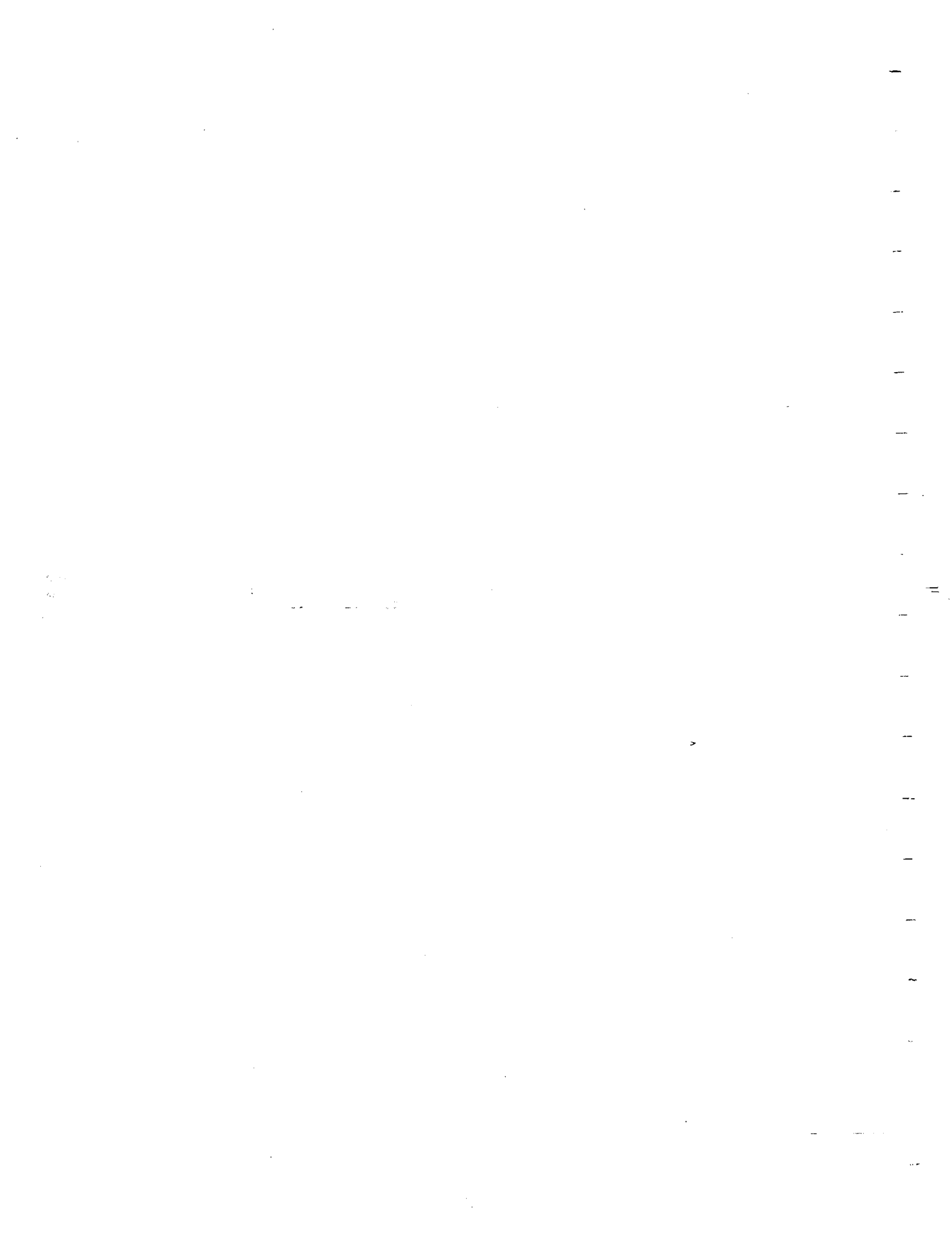
Tombach, I., "A Critical Review of Methods for Defining Visual Range in Pristine and Near-Pristine Areas," Paper No. 78-43.2, Presented at the 71st Annual Meeting of the Air Pollution Control Association, June 25-30, 1978.

Tombach, I., "Intercomparison of Visibility Measurement Methods," Proceedings: View on Visibility - Regulatory and Scientific", Rocky Mountain States Section, Air Pollution Control Association, November 1979.

Trigonis, J., "Visibility in California", prepared for the California Air Resources Board, under Contract No. A7-181-30, April 1980.

Williamson, S.J., Fundamentals of Air Pollution, Addison Wesley, Reading, Massachusetts, 1973.

Wolff, G.T., Personal communication, General Motors Research Laboratories, Warren, Michigan, 1981.



APPENDIX A

VISIBILITY/AEROSOL RELATIONSHIPS BASED ON SIZE/CHEMISTRY PROFILES

The relationships between visibility and Hi-Vol particulate measurements generated in Chapter 3 implicitly include factors central to Mie scattering theory that are not explicitly included in the data set. The most important of these is the strong dependence of extinction on particulate size and the important correlation between particle size and chemical composition. Data exist at a limited number of sites and for limited time periods that can illuminate these relationships more explicitly through detailed size and chemical information. This appendix describes regression studies based on these more detailed data sets at five locations representative of three major air basins - the South Coast Air Basin, the San Francisco Bay Area, and the Sacramento/San Joaquin Valley.

A.1 DESCRIPTION OF THE DATA BASE

The data used in this chapter consist of visibility, relative humidity, temperature, and wind speed readings taken at airports as well as measurements of particulate size and elemental composition taken by the University of California, Davis, under ARB grants and contracts. This section discusses data sources, site selection, and data quality considerations.

A.1.1 Airport Visibility Data

The visibility data used in this chapter are "prevailing visibility" readings made at airport weather stations. The comments made in section 3.1.1 apply, except that the visibility readings were averaged for the entire day, not just the daylight hours.

A.1.2 Study Locations

The sites selected for examination of the size/elemental profiles and subsequent correlation with visibility are chosen so as to be representative of three major California air basins (see Figure A.1). The San Francisco Bay Area is represented by Oakland, with the San Francisco airport providing

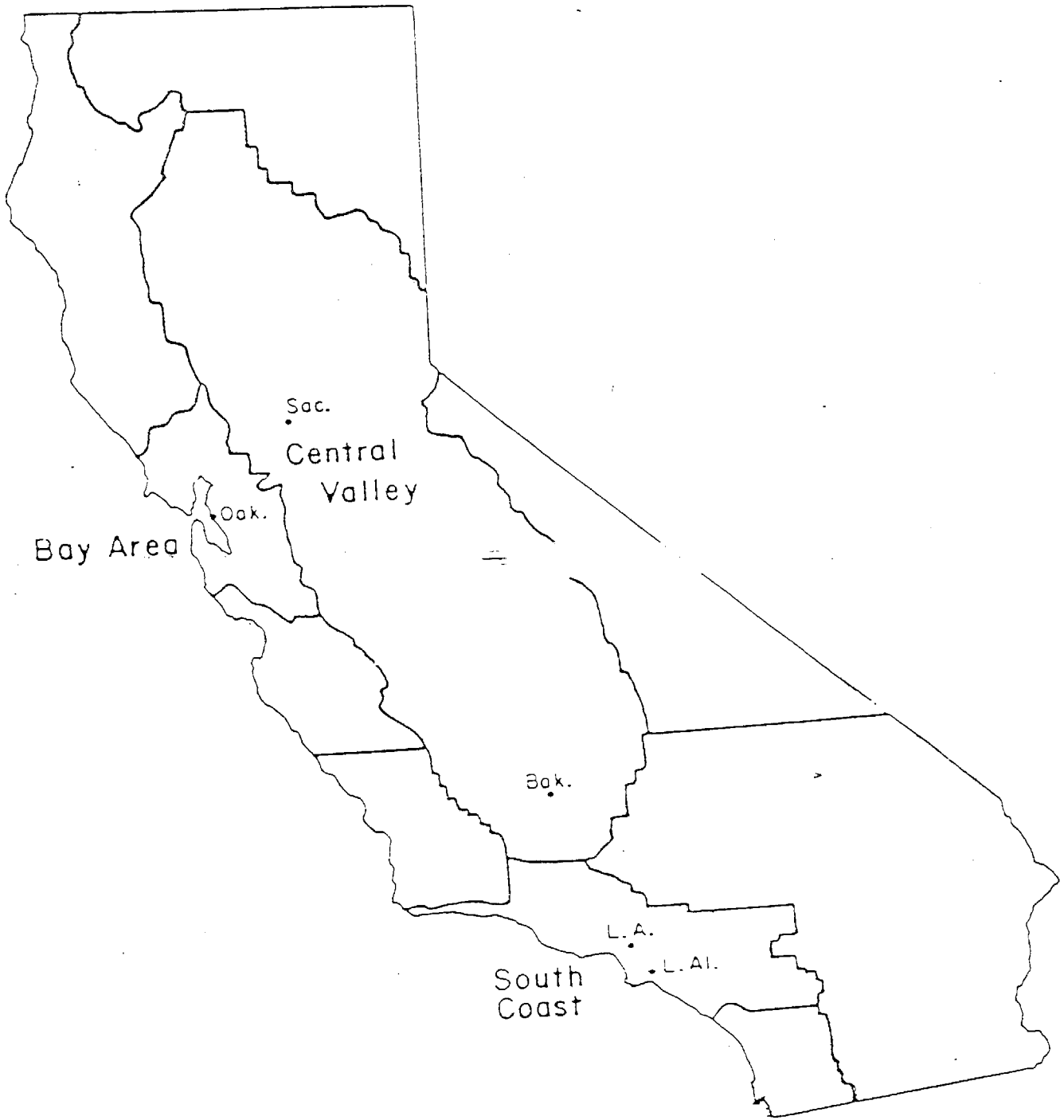


Figure A.1 Location of the study sites.

visibility and weather data. The Central Valley is represented by Sacramento and Bakersfield, with visibility and weather data supplied by their respective airports. In the above cases, the particulate samplers are located at urban air monitoring stations that also supply gaseous pollutant data. Los Angeles (downtown) and Los Alamitos are chosen in the South Coast Air Basin. At Los Angeles, the particulate and gaseous data are from co-located instruments, but weather and visibility come from the Los Angeles International Airport, 15 miles to the west and almost on Santa Monica Bay. The particulate sampler at Los Alamitos is located at the U.S. Naval Air Station. The Long Beach Airport supplies visibility and weather data, while the Long Beach air monitoring station provides data on gaseous pollutants. All data reported herein are for the period June-September, 1973, nominally covering 92 separate 24-hour days at each site. (Flocchini et al. 1976)

A.1.3 Types of Data

Four types of data are used in this chapter - visibility data, weather data, gaseous pollutant data, and particulate data. In all cases, visibility data and weather data (relative humidity, temperature, and mean wind speed) are obtained from the same airport. All represent arithmetic averages of 24-hour values.

The data on gaseous pollutants (oxidant, NO_2 , SO_2 , and hydrocarbons) represent 24-hour mean values. Except for Los Alamitos, these data are collected at the same site as the particulate data.

The particulate data consist of 24-hour mean values for the elements sodium through lead, with the particles collected in 3 size ranges: fine ($\leq 0.65 \mu\text{m}$), intermediate (0.65 to $3.6 \mu\text{m}$), and large (3.6 to about $15 \mu\text{m}$). A restrictive orifice results in a $15 \mu\text{m}$ intake cut, eliminating non-inhalable particles. This orifice eliminates on the average about 30% of the total mass as seen by a Hi-Vol sampler. The samples were collected on coated impactor substrates on a rotating Lundgren-type impactor. Analysis was done through proton induced x-ray emission (PIXE) at the Crocker Nuclear Laboratory, University of California, Davis. On the average, 15 of the 40 elements normally examined were seen in each size range, with sensitivities ranging below 10 ng/m^3 . Summer and winter particulate values in the three size

ranges are shown in Tables A.1 through A.6, along with mean values for gaseous pollutants and weather data.

While detailed examination of these values will be deferred until the statistical studies have been presented, the role of particle size should be mentioned at this time. While particulate mass (or volume) exhibits a bimodal distribution versus size in almost all ambient aerosol data, individual chemical or elemental constituents are rarely bimodal. Mechanically produced aerosols are generally coarse (the "mechanical" mode at above 3 μm diameter), while aerosols from gas-to-particle conversion or from high temperature processes are generally fine (the "accumulation" mode at about 0.3 μm diameter). Our data confirm this tendency, while adding the additional complexity of seasonal size variations of a given species within a mode. Figure A.2 shows results that illustrate these considerations. Silicon, a soil tracer of largely mechanical origin, remains dominantly a coarse mode particle, summer and winter. Likewise, automotive lead remains firmly in the accumulation mode, summer and winter. And to a lesser extent, zinc, show a considerable seasonal variation at Los Alamitos. The winter sulfur size values appear similar to lead, clearly accumulation mode and quite fine. Summer values, however, grow in size up to the very upper edge of the accumulation mode, around 1 micron diameter. During this period, the amount of sulfate more than doubles while the trace elements associated with oil combustion, vanadium and nickel, remain at their winter size profiles. This leads to the hypothesis that primary combustion sulfates have a constant accumulation mode size profile, and that the "new" summer sulfate mode is a secondary aerosol conversion. The summer sulfate aerosol appears hygroscopic, growing in size and accelerating gas to particle conversion via the aqueous state. The consequence of the seasonal size shift on visibility can be very important because particles of 0.3 micron diameter are a little below the size for maximum scattering efficiency. Doubling the size of the particles can increase extinction per particle by factors much larger than the factor of 8 change in volume, yielding increased scattering efficiency per unit mass. Such a model would also predict an important role for relative humidity when gas-to-particle conversion is occurring in the higher oxidant, higher temperature summer periods.

TABLE A.1 ATMOSPHERIC GASES AND PARTICULATES IN CALIFORNIA, 7/1/73 - 9/30/73

SITE	Particulates in ng/m ³ 24-hr averages (1)											Gases in ppm, av. daily max hour (2)									
	Na	Mg	Al	Si	S	Cl	K	Ca	V	Ph	Fe	Cu	Zn	Br	Pb	Ox	CO	NO _x	HC		
Sacramento	617	133	869	3372	1016	336	591	52	94	6	36	1215	8	30	158	704	.06	2.0	.07	2.3	
Richmond (3)	1692	122	134	1058	1181	1948	2296	412	40	22	7	634	4	75	125	557	.03	3.0	.03	3.0	
Livermore (3)	302	92	357	2382	609	244	331	454	64	6	30	934	5	60	65	361	.07	2.3	.05	3.0	
Oakland	1710	137	115	1339	1258	2014	313	528	72	26	36	764	26	132	221	984	.02	2.0	0.10	2.3	
San Jose	732	197	597	3145	869	891	470	836	91	5	30	1182	5	58	288	1058	.05	4.7	.13	4.7	
Salinas	715	89	196	1134	532	1048	219	285	24	7	12	440	2	5	35	179	.04			.06	2.7
Bakersfield	169	77	1420	4566	1507	18	1043	1252	146	19	27	1819	14	47	252	1072	.08	4.7	.16	7.0	
Los Alamitos (4)	825	173	472	2149	3879	366	451	642	79	71	27	973	6	73	115	940	.05	3.7	.17		
Los Angeles	696	98	443	2418	4013	123	473	751	134	25	31	1006	17	183	252	1498	.10	6.7	.20	3.0	
Azusa	478	167	1137	3751	3084	97	913	1063	242	43	49	2009	20	190	217	1407	.18	4.0	.17	4.3	
Riverside	274	94	1024	4019	2884	107	793	1266	143	15	36	1793	7	95	370	1697	.15	4.0	.11	7.7	
Indio	320	182	2434	7864	3409	99	1554	2619	312	35	70	3387	14	108	119	709	.10	3.0	.04	2.7	
San Cajon	899	193	875	3680	2663	296	560	772	139	24	33	1327	7	39	166	1041	.06	2.0	.07	2.0	

(1) Mean number of days/month - 27. Nominal total error, ± 15%.

(2) Data obtained from ARB or A.P.C.D. stations. Oxidant corrected to standard of 6/1/75.

(3) NO₂, not NO_x for Richmond and Livermore.

(4) Gas data from Long Beach station.

TABLE A.2 ELEMENTAL SIZE DISTRIBUTIONS

Stage 3, 0.1 - 0.65 microns
 Stage 2, 0.65 - 3.6 microns
 Stage 1, 3.6 - 20 microns

LOS ALAMITOS

Major Elements, (sets corr. > 0.8)	July, August, September, 1973			January, February, March, 1974						
	Ratios	Mass (ng/m ³)	Median Sizes		Ratios	Mass (ng/m ³)	Median Sizes			
			St.3	St.2			St.3	St.2	St.1	
Aluminum	0.22					0.22				
Silicon	1.00					1.00				
Potassium	0.21					0.23				
Calcium	0.30					0.33				
Titanium	0.035					0.033				
Manganese	0.012					0.007				
Iron	0.41					0.47				
Soil set		4,700	6%	29%	65%		3,400	9%	25%	66%
with oxides (appr.)		9,400					6,800			
Sodium		825	8%	28%	64%		820	2%	36%	62%
Magnesium		175	6%	10%	84%		100	8%	19%	73%
Sulfur		3,900	42%	55%	3%		1,670	73%	24%	3%
S as SO ₄		11,700					5,010			
Chlorine		370	<1%	1%	99%		660	1%	41%	58%
Vanadium		70	70%	18%	12%		20	95%	<5%	<5%
Chromium		1.7		N.D.			1.3		N.D.	
Nickel		59	77%	17%	6%		32	78%	15%	7%
Copper		6	<1%	23%	77%		13	70%	18%	12%
Zinc		75	39%	37%	24%		160	50%	42%	8%
Bromine									0.28	
Lead									1.00	
Soil set		1,000	62%	71%	7%		180			

TABLE A.3 ELEMENTAL SIZE DISTRIBUTIONS

Stage 3, 0.1 - 0.65 microns
 Stage 2, 0.65 - 3.6 microns
 Stage 1, 3.6 - 20 microns

RIVERSIDE (R)

Major Elements, (sets corr. >0.8)	July, August, September, 1973			January, February, March, 1974		
	Ratios	Mass (ng/m ³)	Median Sizes	Ratios	Mass (ng/m ³)	Median Sizes
			St.3 St.2 St.1			St.3 St.2 St.1
Aluminum	0.25			0.23		
Silicon	1.00			1.00		
Potassium	0.20			0.21		
Calcium	0.31			0.32		
Titanium	0.035			0.024		
Manganese	0.009			0.005		
Iron	0.45			0.39		
Soil set		9,100	11% 20% 69%		5,000	10% 24% 66%
with oxides (appr.)		18,000			10,000	
Sodium		270	16% 39% 45%		490	6% 22% 72%
Magnesium		90	12% 24% 64%		90	8% 5% 87%
Sulfur		2,900	41% 57% 2%		1,600	62% 36% 2%
S as SO ₄ (appr.)		8,700			4,800	
Chlorine		110	11% 13% 76%		550	4% 72% 23%
Vanadium		15	26% 49% 26%		10	N.D.
Chromium		6	85% 15% <5%		3	75% 25% <5%
Nickel		10	35% 65% <5%		12	32% 60% 8%
Copper		7	18% 31% 51%		15	88% 12% <5%
Zinc		95	44% 37% 18%		65%	43% 48% 9%
Bromine	0.22			0.28		
Lead	1.00			1.00		
Auto set		2,070	68% 27% 5%		2,400	72% 24% 4%

TABLE A.6 ELEMENTAL SIZE DISTRIBUTIONS

Stage , 0.1 - 0.65 microns
 Stage 2, 0.65- 3.6 microns
 Stage , 3.6 - 20 microns

SACRAMENTO

July, August, September, 1973

January, February, March, 1974

Major Elements, (sets corr. >0.8)	July, August, September, 1973			January, February, March, 1974		
	Ratios	Mass (ng/m ³)	Median Sizes St. 3 St. 2 St. 1	Ratios	Mass (ng/m ³)	Median Sizes St. 3 St. 2 St. 1
Aluminum	0.26			0.21		
Silicon	1.00			1.00		
Potassium	0.18			0.32		
Calcium	0.16			0.47		
Titanium	0.027		1%	0.045		
Manganese	0.015		1%	0.006		
Iron	0.36			0.38		
Soil set		6,700	20% 20% 60%		2,900	14% 37% 49%
with oxides) apprx.)		13,400			5,800	
Sodium		620	23% 68% 9%		390	13% 52% 35%
Magnesium		130	35% 42% 23%		75	7% 48% 45%
Sulfur		1,020	76% 23% 1%		650	62% 35% 3%
S as SO ₄		3,060	" "		~1,950	
Chlorine		340	<1% 30% %		330	N.D.
Vanadium		6	N.D.		2.5	N.D.
Chromium		1	N.D.		4	N.D.
Nickel		< 0.3	N.D.		1	72% 21% 7%
Copper		8	69% 21% %		15	60% 32% 8%
Zinc		30	58% 28% %		80	
Bromine		0.22		0.32		
Lead		1.00		1.00		
Auto set		860	86% 11% 3%		1,090	80% 18% 2%

Percent of Aerosol Particle Size

LOS ALAMITOS, CALIFORNIA

Stage 1, $20\mu - 3.6\mu$
 Stage 2, $3.6\mu - 0.65\mu$
 Stage 3, $0.65\mu - 0.1\mu$

July, 1973
 February, 1974

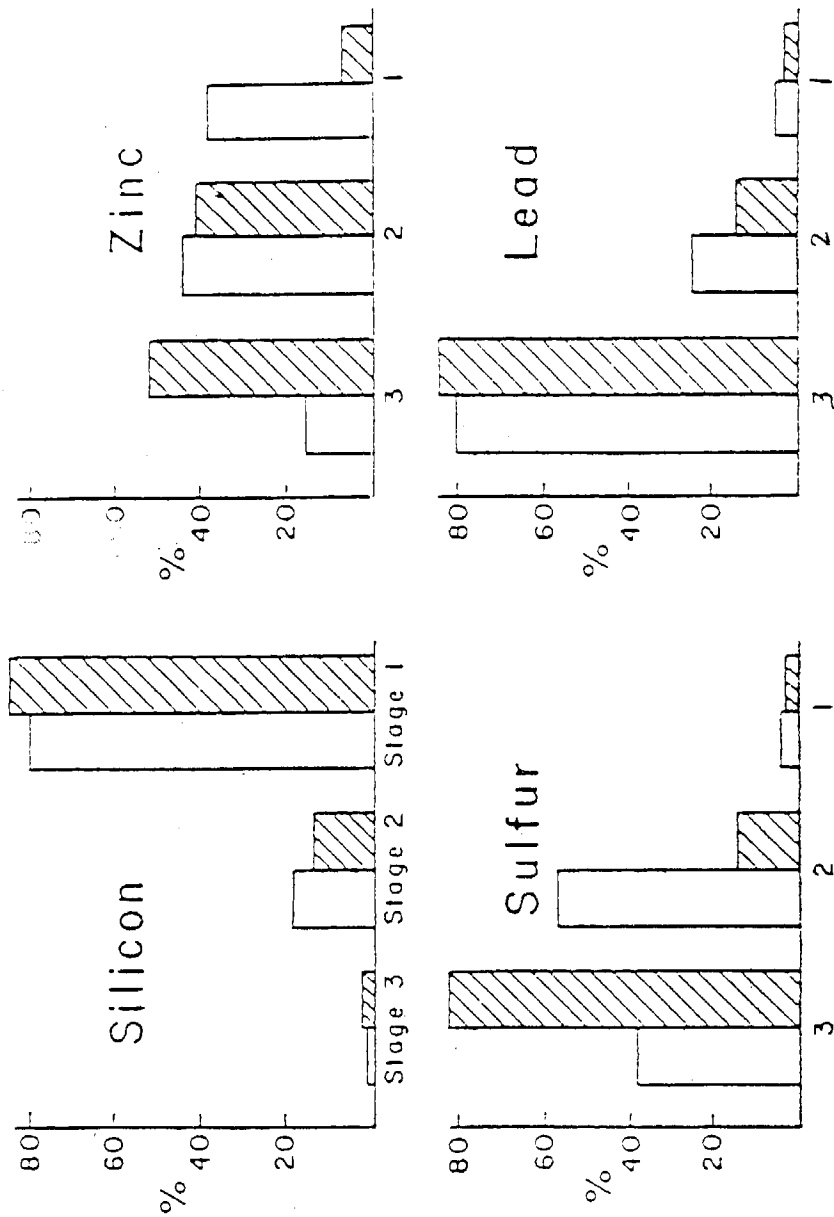


Figure A.2 Seasonal size distributions for various aerosol species.

This seasonal behavior of aerosol sulfur (sulfate) appears closely linked to the meteorology of local air basins. Figure A.3 shows the results for numerous sites in the west. The humid and low oxidant coastal sites, such as in the San Francisco Bay Area, have a very fine sulfur size distribution, summer and winter. High altitude and desert sites are likewise fine summer and winter, despite very different meteorological conditions. All South Coast Basin Area sites behave like Los Alamitos, with coarser sulfate present in summer and finer sulfate present in winter. The California Central Valley, however, behaves in an exactly inverse manner, with finer sulfur in summer and coarser sulfur in the winter. The Imperial Valley maintains relatively constant but coarse profiles for both summer and winter. The remarkable consistency of such behavior for a large number of sites in each air basin is striking, since in some cases, such as Bakersfield and Sacramento, the sites are hundreds of miles apart.

All evidence points to the critical role of water in sulfate aerosol size distributions (see Figure 3.2 in Chapter 3). This effect was studied in detail by Figure A.3, which shows the fraction of sulfur in each size range for given humidity conditions. The regions now appear to be grouped into two classes, those that show a sharp increase in sulfur size versus humidity, and those that don't. In the Bay Area, not only are sulfur particles fine during both summer and winter, but also they do not respond significantly to increasing humidity. Oakland also has the lowest maximum oxidant readings of any site, only 40% of the next lowest site, Los Alamitos. This allows for the hypothesis that the Oakland sulfates are primary fine combustion products, perhaps in a carbon matrix. Since gas-particle conversion is relatively minor, hygroscopic sulfates are not being generated in large amounts. The coarse winter sulfates in the Central Valley can be associated with the high humidity conditions that occur in stagnant winter periods, often resulting in dense fogs. Figure A.4 shows a plot of the fraction of sulfur aerosol in the greater than 0.7 micron size range. The close association with relative humidity is most evident. The fine summer sulfates in that region may then be ascribed to either lack of water content due to dry conditions or lack of SO_2 - sulfate conversion.

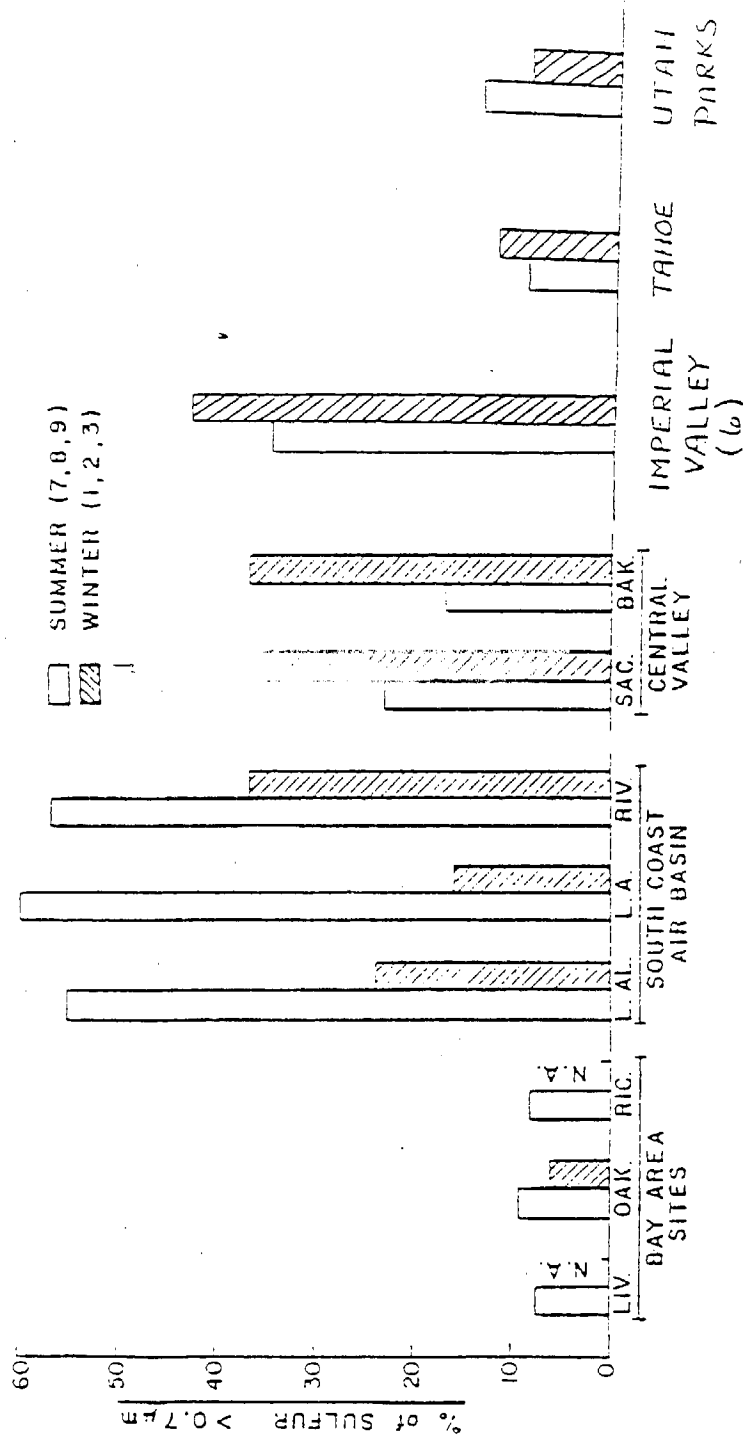


Figure A.3 Seasonal sulfate size distribution information at several locations.

TABLE A.7 EFFECT OF HUMIDITY ON SULFUR SIZE DISTRIBUTION

Humidity	Sacramento	Oakland	Los Alamitos
	<u>Apr73-Dec74</u>	<u>Apr73-Dec74</u>	<u>May73-Nov74</u>
20 - 39%	.023/.110/.867	.020/.049/.930	.054/.142/.804
40 - 59%	.023/.218/.759	.031/.096/.873	.047/.293/.660
60 - 79%	.038/.292/.671	.097/.158/.745	.045/.412/.543
80 - 99%	.042/.453/.504	.074/.148/.778	.050/.488/.462

Humidity	Los Angeles	Bakersfield
	<u>May73-Dec74</u>	<u>Jun73-May74</u>
20 - 39%	.065/.282/.653	.014/.137/.848
40 - 59%	.046/.426/.529	.024/.215/.761
60 - 79%	.038/.469/.	
80 - 99%	.034/.629/.337	.036/.555/.409

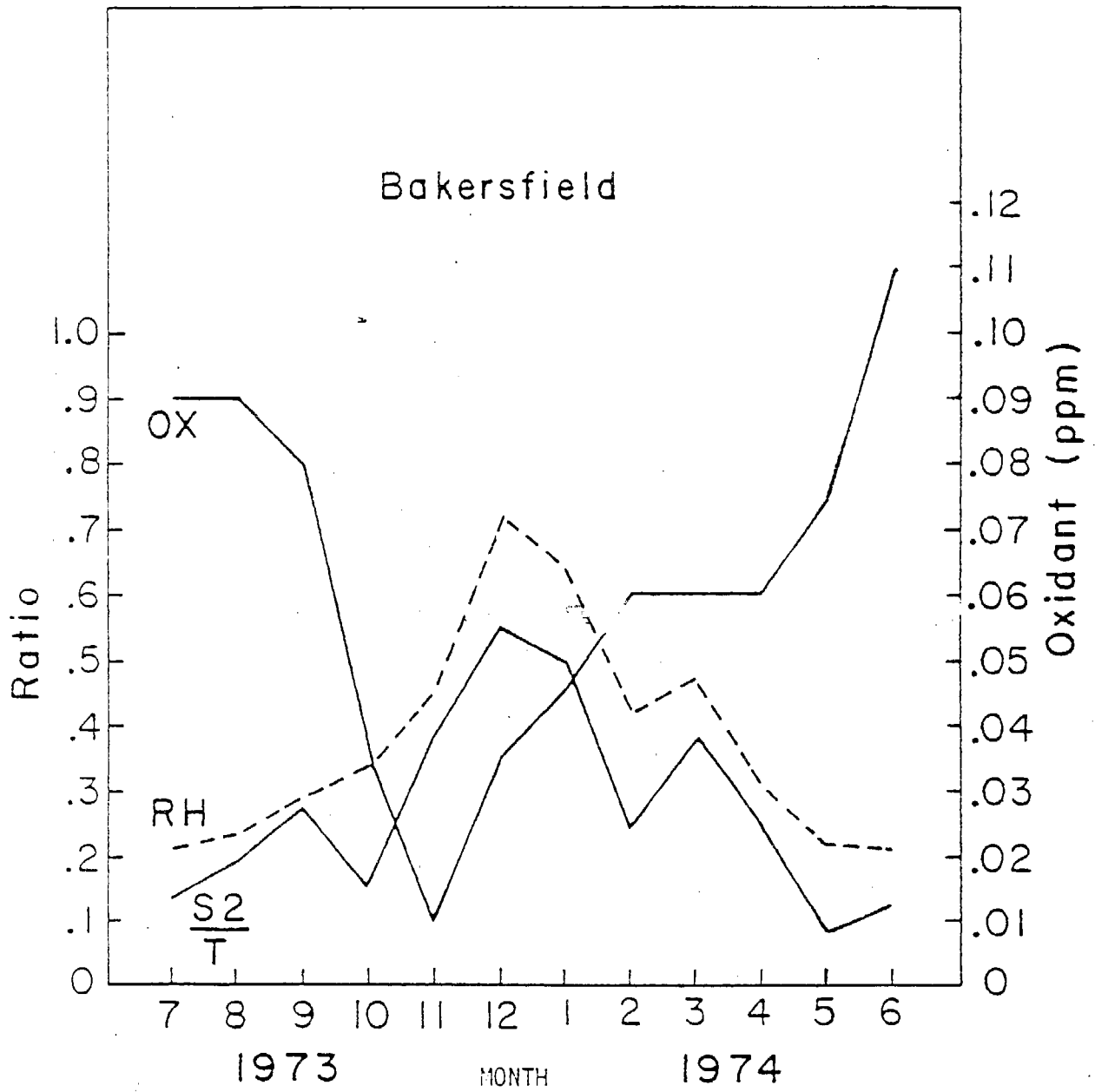


Figure A.4 Seasonal patterns at Bakersfield.

The former appears far more tenable, as conversion processes are known to occur strongly in hot summer conditions in the valley, although not at the rate seen in the cooler, more humid, and more photochemical South Coast Air Basin. The association of such size changes with visibility will be discussed in sections A.3.1, A.3.2, and A.3.3, (also see Figure 3.8).

A.1.4 Data Quality Considerations

Accuracy and precision of the airport visibility data are discussed in section 3.1.4. Gaseous pollutant data is gathered under ARB quality assurance protocols, while weather data is subject to Department of Commerce protocols.

Particulate data are subject to Davis quality assurance tests, which have been validated through interlaboratory intercomparisons, the most extensive of which occurred in Charleston, West Virginia, in 1978 under the EPA and DOE. Data from that test showed that the mean accuracy of fine particulates collected by the Multiday Impactor was 0.94 ± 0.05 , prior to a 4% filter penetration correction which would raise this

Accuracy and precision of the PIXE elemental analysis system at Davis has been verified through formal interlaboratory intercomparisons in 1973, 1975, and 1978. The results of this latter test are shown in table A.8, which is consistent with the long term (1973 - 1980) Davis absolute accuracy of 1.025 ± 0.06 .

A.2 STATISTICAL MODELING APPROACH

The basic statistical approach used in this chapter, multiple log linear regression, differs somewhat from the approach taken in Chapter 3. There are also important differences from Chapter 3 in the data sets and the aims of our program. The major aim of the UC Davis visibility program is to identify the main associative (and, hopefully, causal) factors relating visibility with weather and air quality. The broadest possible primary data set is chosen so as not to overlook any accessible factor. Since log-linear (multiplicative) regressions are used, no mass extinction efficiencies can be generated. There are, in principle, 132 free parameters available at each site to describe the 92 visibility measurements. The following sections

TABLE A.8 COMPARISON OF ANALYTICAL TECHNIQUES

EPA/ERDA AEROSOL
INTERCOMPARISON,
11/3/77 Meeting, RTP, N.C.

Results expressed as the mean value of the ratio of the results obtained by each laboratory to that obtained by R. Giauque, LBL, with the uncertainty representing one standard deviation.

GROUP	METHOD	S	CA	TI	FE	CU	ZN	SE	BR	PB	ALL VALUES	ALL - WORST
UC DAVIS	PIXE	1.01	1.41	1.04	1.01	0.90	1.14	0.93	0.91	0.92	1.03 ± 0.16	0.98 ± 0.08
	XRF	±0.07	±0.26	±0.06	±0.05	±0.05	±0.05	±0.06	±0.05	±0.03		
EPA (res.)	XRF	0.93	0.89	1.14	0.96	1.04	0.95	0.96	0.92	0.93	0.97 ± 0.08	0.95 ± 0.04
		±0.04	±0.06	±0.13	±0.05	±0.13	±0.06	±0.14	±0.05	±0.05		
LBL (Loo)	XRF	0.98	1.27	1.33	0.98	1.02	1.10	0.87	1.16	1.00	1.08 ± 0.15	1.05 ± 0.13
		±0.04	±0.13	±0.19	±0.05	±0.07	±0.06	±0.14	±0.06	±0.06		
FSU	PIXE	0.89	1.06	1.01	0.94	1.33	1.12	0.49	0.92	0.84	0.96 ± 0.23	1.01 ± 0.16
		±0.05	±0.16	±0.05	±0.04	±0.44	±0.20	-	±0.07	±0.05		
EPA (mon.)	Chem, AA	1.06*								1.03		
		±0.10								±0.02		
BNL	Chem.	1.04*										
		±0.13										
Wash. U.	Gamma Rays	0.54**										
		±0.15										

* Results obtained for sulfate, divided by ...; ** Results withdrawn during meeting

describe the statistical techniques used to obtain a unique relationship between visibility and the independent atmospheric variables. (Barone et al 1978).

A.2.1 Extraction of Independent Variable Factors

In order to reduce the set of variables to a number much less than the number of data to be fit, as well as to clarify aerosol sources, the data set was searched for highly correlated sets of parameters. Such sets can arise from either physical or chemical mechanisms, such as the fixed elemental ratios of particulate sources at a given site or the mechanisms dominating the formation of mechanical mode aerosols. A high correlation is exhibited between particles in the coarsest size mode, Stage 1 (3.6 to 15 μm), and chemically similar materials in the next smallest size. At all study locations, no solely coarse mode component existed, so that all Stage 1 data could be eliminated without loss of an "independent" parameter. This also is supported by the greatly reduced impact on visibility per unit mass of aerosol in the greater than 3.6 μm size range (see Figure 3).

Further reduction of the data set was achieved through identification of highly correlated data sets among gaseous and aerosol parameters. One such set consisted of the NO-NO₂-NO_x triad, which exhibited correlations greater than 0.8 at all sites. NO₂ was selected as the representative of this set, as it is physically connected with extinction via its absorption properties. Other sets of elements were seen in aerosols to occur with fixed ratios and high correlations. Table A.9 shows the major such factors so identified. From each set, one factor was retained and the rest eliminated from the search. This procedure not only aids in associating visibility degradation with a specific source, it also reduces multicollinearities in the final regression parameters. Finally, those elements seen less than 50% of the time in the aerosol data were dropped, as they generally occurred at very low levels inadequate to affect visibility seriously in the presence of much stronger factors. Table A.10 lists the remaining parameters, with their mean values for each site. By these procedures, the nominal 132 free parameters have been reduced to 17 free

TABLE A.9 EXAMPLES OF BIVARIATE ELEMENTAL CORRELATIONS
FOR MAJOR PRIMARY AEROSOL SOURCES

	<u>Element</u>	<u>Correlation</u>	<u>Elemental Ratio</u>	<u>Elemental Ratio of Presumed Source (Typical)</u>
<u>Oceanic</u>				<u>Sea Water</u>
3.6 to 20 μ	Na	0.97	1.13	0.56
Oakland	Mg	0.81	0.26	0.07
1/74 - 3/74	S	0.88	0.094	0.047
	Cl	= 1.00	= 1.00	= 1.00
<u>Soil</u>				<u>Crustal Ave.</u>
0.65-20 μ	Al	0.96	0.28 \pm 0.04	0.282
Sacramento	Si	= 1.00	= 1.00	= 1.00
6/73-3/74	K	0.93	0.095 \pm 0.005	0.094
	Ca	0.87	0.20 \pm 0.07	0.131
	Ti	0.89	0.027 \pm 0.005	0.016
	Mn	0.81	0.008 \pm 0.001	0.003
	Fe	0.97	0.285 \pm 0.03	0.181
<u>Fuel Oil</u>				<u>Fuel (x) oil</u>
0.1-0.65 μ	S	= 1.00	= 1.00	= 1.00
Los Alamitos	V	0.95	0.016	0.018
7/73-9/73	Ni	0.97	0.021	0.025
<u>Automotive</u>				<u>PbClBr</u>
0.1-3.6 μ	Br	0.95	0.30	0.355
Sacramento	Pb	= 1.00	= 1.00	= 1.00
7/73-9/73				

TABLE A.10 MEANS OF SELECTED VARIABLES AT FOUR CALIFORNIA SITES (JULY-SEPTEMBER 1973)

PARAMETERS	LOS ALAMITOS	LOS ANGELES	OAKLAND	BAKERSFIELD
WEATHER	MEAN	MEAN	MEAN	MEAN
Humidity (%)	59.1	73.8	79.5	37.5
Wind Speed (mi/hr)	5.8	7.1	8.5	7.3
Temperature (°F)	71.2	68.3	62.0	84.0
AEROSOLS (3.6 to 0.65µm) (ng/m ³)				
Sodium-2	239	224	462	89
Silicon-2	356	447	138	375
Sulfur-2	1985	2109	113	298
Lead-2	208	412	51	123
Total-2	3381	3873	1725	1470
AEROSOLS (<0.65µm) (ng/m ³)				
Sodium-3	56	139	418	57
Sulfur-3	1619	1517	1002	1294
Potassium-3	77	94	132	403
Lead-3	715	1003	923	988
Total-3	3083	3550	3892	4875
GASEOUS POLLUTANTS (ppb)				
Oxidant	19.7	37.3	17.0	44.1
Nitrogen dioxide	53.4	59.2	30.8	36.8
Sulfur dioxide	22.1	*	*	*
Hydrocarbons	*	21.5	23.2	42.8
VISIBILITY				
Miles	4.2	4.0	9.2	9.4
Km	6.7	6.5	14.7	15.1
b _{scat} (km ⁻¹)	0.435	0.448	0.197	0.192
DATA DAYS	78	65	74	85

*Indicates variable not measured

parameters, far less than the 65 to 85 days of data.

In order to check these assumptions, however, the data set was analyzed with all major Stage 1 (coarse particle) aerosols and CO₂ included as well as with the reduced number of variables. No statistically significant variation in R² was seen at any site.

A.2.2 Multivariate Regression

As mentioned in Section 3.2.2, the method of multiple regression is vital when a large number of nominally independent variables affect a dependent variable. The 132 potentially independent variables included in the weather, gas, and size specific aerosol composition data have been reduced to 17 independent factors, each representing a class of variables which, in most cases, arise mainly from a single source. Thus, we have performed a sort of factor analysis before operating on the data set by the method of multiple linear regression, rather than using the entire (and unwieldy) data set in a traditional factor analysis. We feel that this method is both more physical and more robust, as multiple colinearities are handled before the search, yielding solutions unique in parameter space that contain factors easily associated with sources.

The relationship used in our analysis of the California data set (Barone et al 1978) is multiplicative:

$$b_{\text{scat}} = A p_1^{b_1} p_2^{b_2} p_3^{b_3} \dots p_n^{b_n} + E$$

where A, b₁, b₂...b_n are constants, P₁, P₂, P_n are concentrations of pollutants 1, 2,...n, and E is an error term. In retrospect, whatever advantage is gained in terms of improved fit to the visibility data is dissipated by the inability of the method to deliver mass extinction coefficients and by the lack of a physically reasonable (linear) model. The data set is presently being searched via a linear model, and mass coefficients are being extracted. Multiple correlation coefficients are only slightly poorer than the ones presented in this report, and no significant changes in visibility-pollutant relationships occur vis a vis the results presented here.

Table A.11 presents the results of our data analysis. In the search program, all parameters are divided by their mean values to give dimensionless measures. The results of the search yield multivariate beta coefficients. Beta coefficients represent the increment in the dependent variable (b_{scat}) induced by a one standard deviation change in a single independent variable while holding constant all other independent variables in the regression equation. That is, the beta coefficient associated with each variable is a measure of the associative (and hopefully causal) relationship between that variable and visibility, while controlling for all other variables in the equation. The magnitude of the beta coefficient is a measure of the relative importance of that variable in determining visibility, while a positive (negative) sign indicates whether a variable correlates with improving (decreasing) visibility. They can be thought of as the slope in the dependent variable vs. the independent variable in an orthogonal (independent) multifactor space. The actual values of the beta coefficients are not used to extract mass extinction coefficients in this report. However, the rankings of the parameters from the search are indicative of the importance of the factors in influencing visibility, and thus put further light on the Hi-Vol results in Chapter 3. One other point is that the factor with the highest beta coefficient has the greatest impact on visibility, so that a simple plot of that parameter versus visibility can yield the maximum mass extinction coefficient allowed by the data. This approach will be used for the South Coast Air Basin results.

A.3 VISIBILITY RELATIONSHIPS

The results of the previous section illustrate the existence of large areas of California that show similar behavior in response to aerosol loadings and meteorological conditions. In this section, we will discuss the statistical results for these regions - the South Coast Air Basin, the San Francisco Bay Area, and the Central Valley.

A.3.1 Visibility Relationships in the South Coast Air Basin

Two sites were chosen in the Los Angeles area - Los Alamitos/Long Beach and Downtown Los Angeles. Two sites were chosen because of the importance of

TABLE A.11 SIGNIFICANT BETA COEFFICIENTS FOR
SELECTED SITES, SUMMER 1973

	LOS ALAMITOS	LOS ANGELES	OAKLAND	BAKERSFIELD
Sodium 2	-0.189	-0.172	* * * *	* * * *
Silicon 2	* * * *	+0.201	* * * *	* * * *
Sulfur 2	+0.386	+0.283	+0.369	+0.496
Lead 2	* * * *	* * * *	* * * *	* * * *
Sodium 3	* * * *	* * * *	+0.198	* * * *
Sulfur 3	* * * *	* * * *	+0.367	* * * *
Potassium 3	* * * *	* * * *	* * * *	+0.428
Humidity	* * * *	-0.369	* * * *	* * * *
Humidity	+0.644	+0.624	* * * *	* * * *
Wind Speed	* * * *	* * * *	* * * *	* * * *
Temperature	+0.198	* * * *	-0.310	* * * *
Oxidant	+0.240	* * * *	* * * *	+0.499
Nitrogen dioxide	+0.296	+0.282	* * * *	+0.327
Sulfur dioxide	+0.233	* * * * ¹	* * * *	* * * * ¹
Hydrocarbons	* * * * ¹	* * * *	+0.419	* * * *
Multiple R ²	0.848	0.730	0.631	0.645

2 indicates intermediate size particles 0.65-3.6 μ m

3 indicates fine size particles 0.1-0.65 μ m

* * * * indicates that the beta coefficient is not significant at the 0.1 confidence level for the t test.

* * * *¹ indicates that the variable was not measured at that site therefore no beta coefficient could be computed.

visibility degradation in this area, the questions of sulfate source and receptor locations in the basin, and the need to test the stability and robustness of the multivariate solutions. The Los Alamitos/Long Beach site is close to major petrochemical source areas, and has relatively low oxidant values. Los Angeles has twice the mean oxidant level of Long Beach, and represents the central basin receptor area. Unfortunately, visibility data are from the Los Angeles International Airport, 25km from the pollutant monitors and close to Santa Monica Bay. Since monitoring data shows strong pollutant variations between the coast and central areas of the basin, visibility/pollutant relationships will not be quantitatively correct.

The results of the fits between visibility and the independent weather, gas, and aerosol values are shown in Figure A.5, a and b, for Los Alamitos and Los Angeles. The fits are good to very good, with R^2 values of 0.85 (Los Alamitos) and 0.73 (Los Angeles). The similarity of the visibility at the two sites is also quite evident, with a very clean period at both sites in late September.

Examining the beta coefficients at each site (Table A.11), one sees that sodium-2, sulfur-2, humidity, and NO_2 are significant at both Los Alamitos and Los Angeles. The sodium-2 (sea salt) correlation with improving visibility appears to be associated with sea salt in clean marine conditions. The virtually identical beta coefficient for NO_2 , +0.28, Los Angeles is a benefit of using visibility data (which includes absorption) rather than nephelometry data. The physically reasonable associations with oxidant, temperature, and SO_2 at Los Alamitos are absent at Los Angeles, although SO_2 was not measured at Los Angeles. However, the dominant coefficient at both sites is relative humidity (+0.64, Los Alamitos, +0.62 Los Angeles) with a strong sulfur-2 component at both sites (0.39 Los Alamitos, 0.28 Los Angeles). Sulfur-2 reflects the coarse sulfate summer mode characteristic of the South Coast Air Basin, with the seasonal dependence shown in Figure A.6

The lack of a correlation with fine (page 3) sulfur aerosols can be exhibited graphically. This is shown in Figure A.7 which shows the relative importance of fine and intermediate sulfur particles to visibility. If one

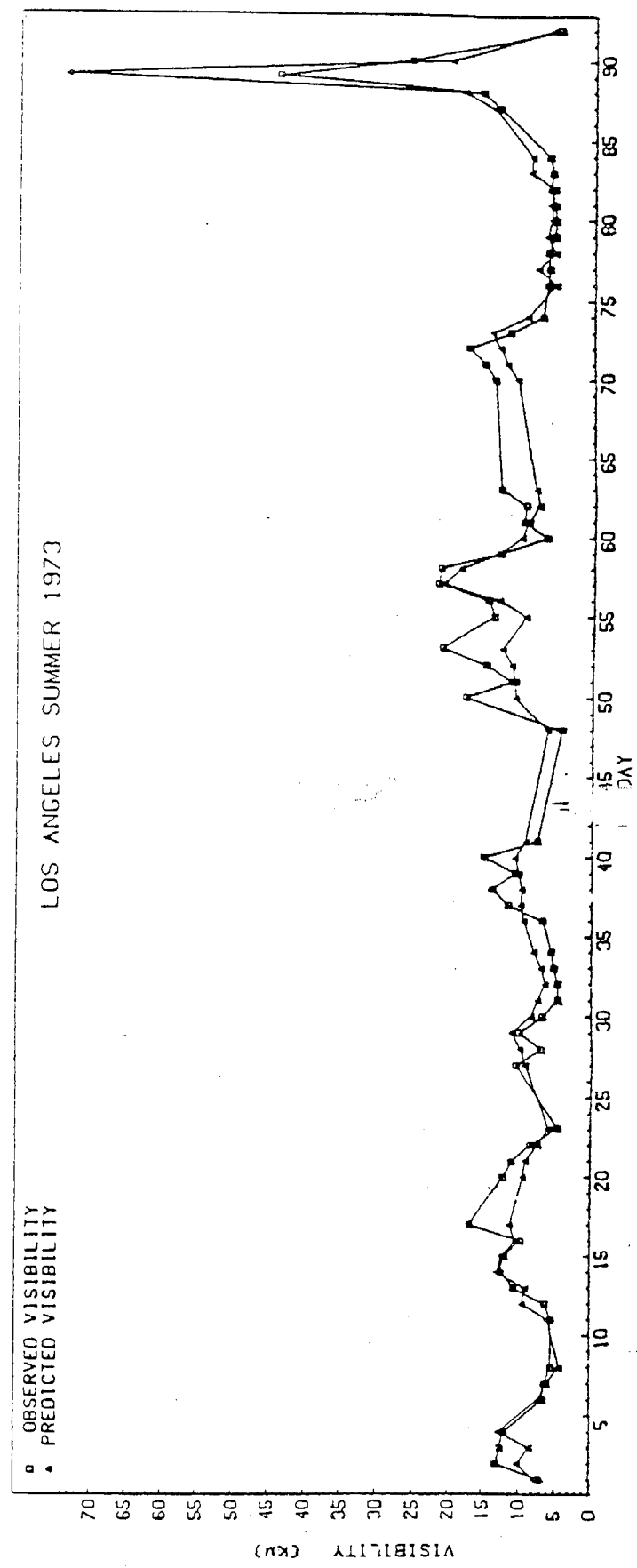
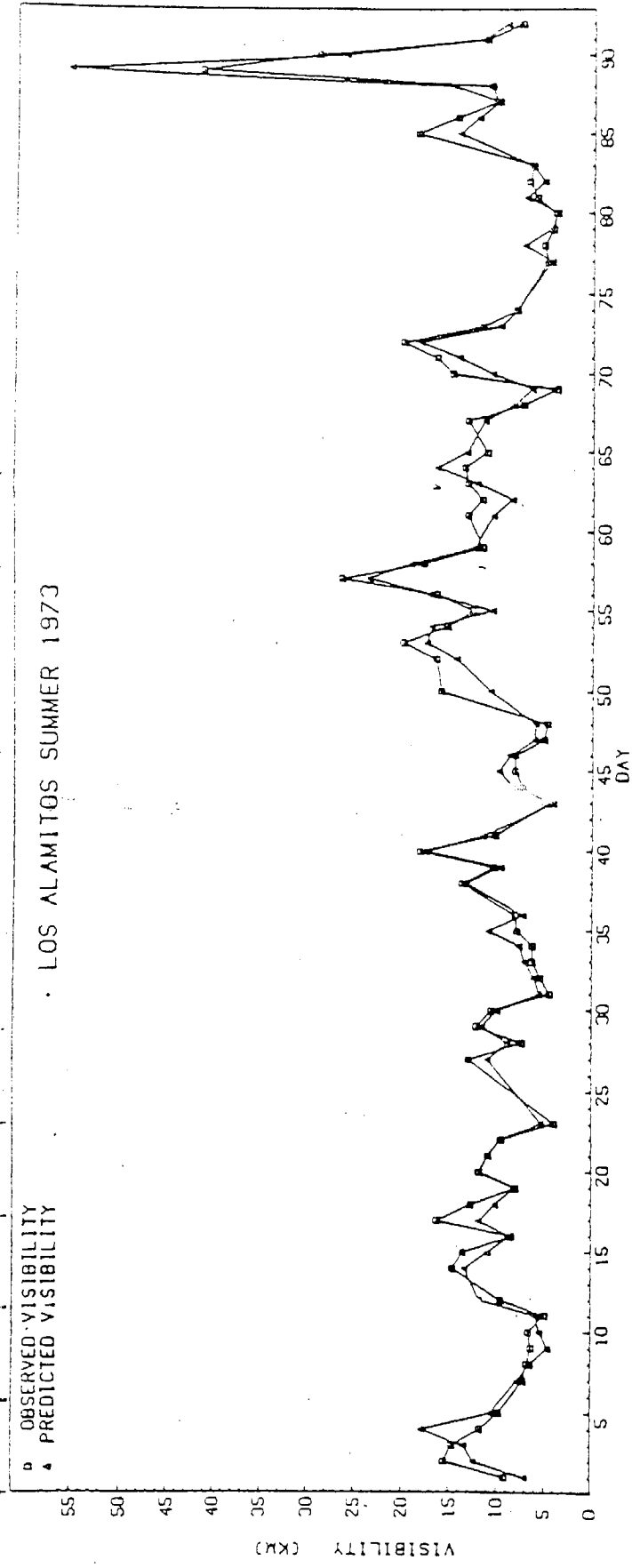


Figure A.5 Predicted versus actual visibility levels in the Los Angeles Area.

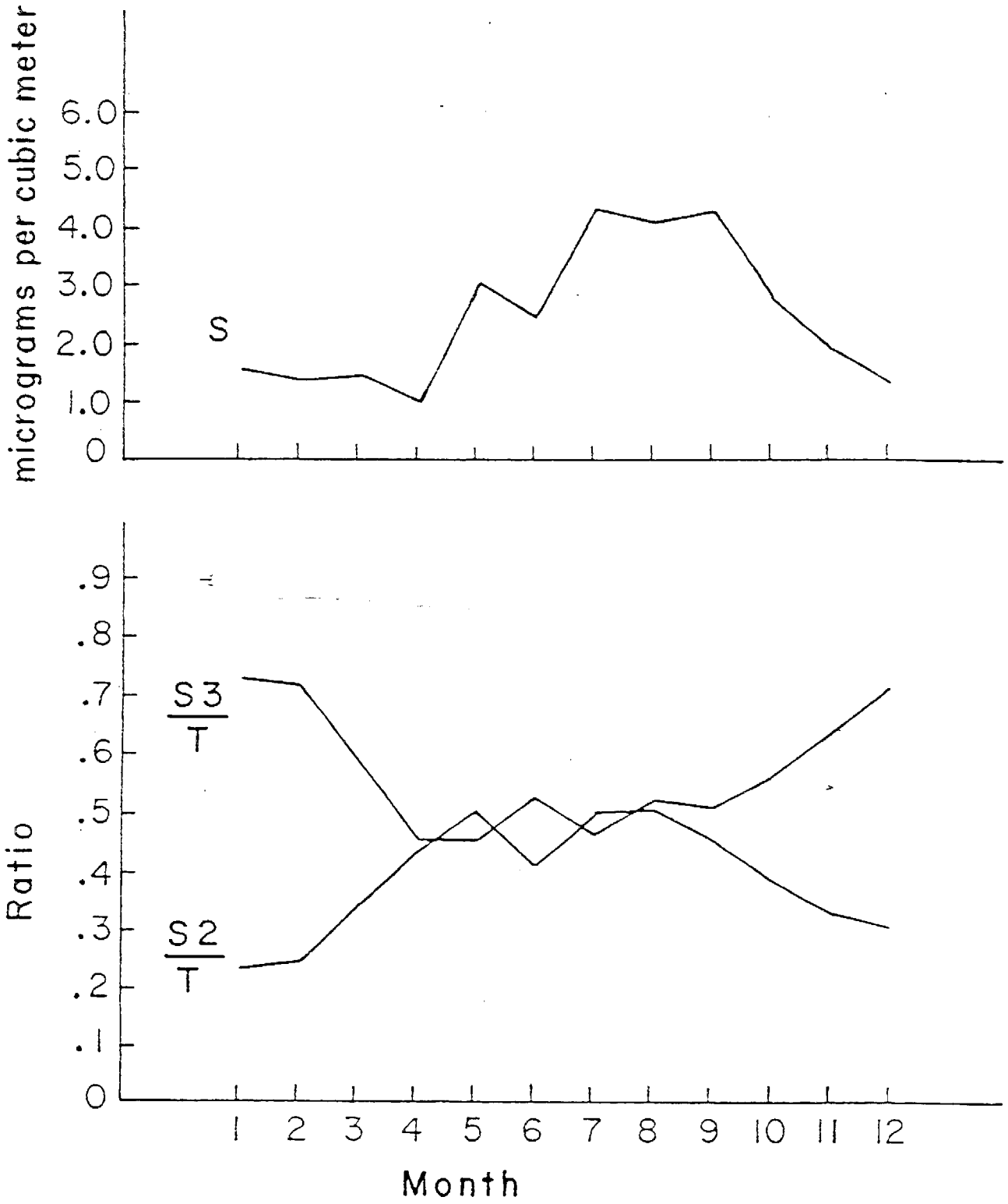


Figure A.6 Seasonal dependence of sulfur aerosol data in Los Angeles.

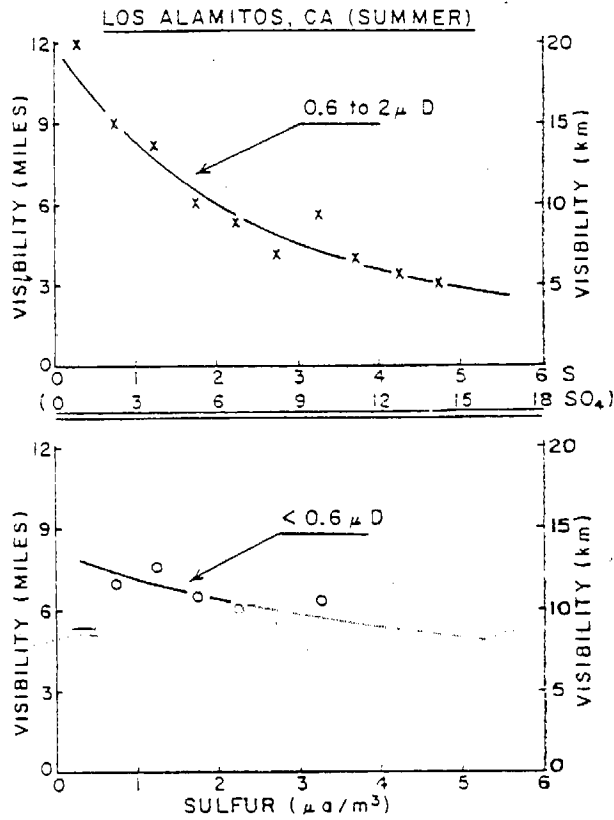


Figure A.7 Visibility at Los Alamitos, California, as a function of coarse sulfur (sulfur 2, 0.6 to about 2 μm diameter) and fine sulfur (sulfur 3, <0.6 μm diameter) particles. Removing the weak correlation between coarse and fine sulfur particles in summer months removes any statistically significant correlation between fine sulfur particles and visibility at both Los Alamitos and Los Angeles, California.

merely associates sulfur-2 with visibility in a bivariate relationship, one obtains a very large value of 0.73 at Los Alamitos. If one eliminates the weak sulfur-2 to sulfur-3 correlation, no association exists between sulfur-3 and visibility. While one can extract mass extinction coefficients from such a graph, this procedure obscures the role of relative humidity. The humidity levels are, of course, far too low to result in particulate water were it not for the presence of hygroscopic sulfate particles. The consequences of this relationship for visibility in the South Coast Air Basin include the simultaneous importance of relative humidity, sulfur sources, and photochemical processes in generating the dominant summer visibility species.

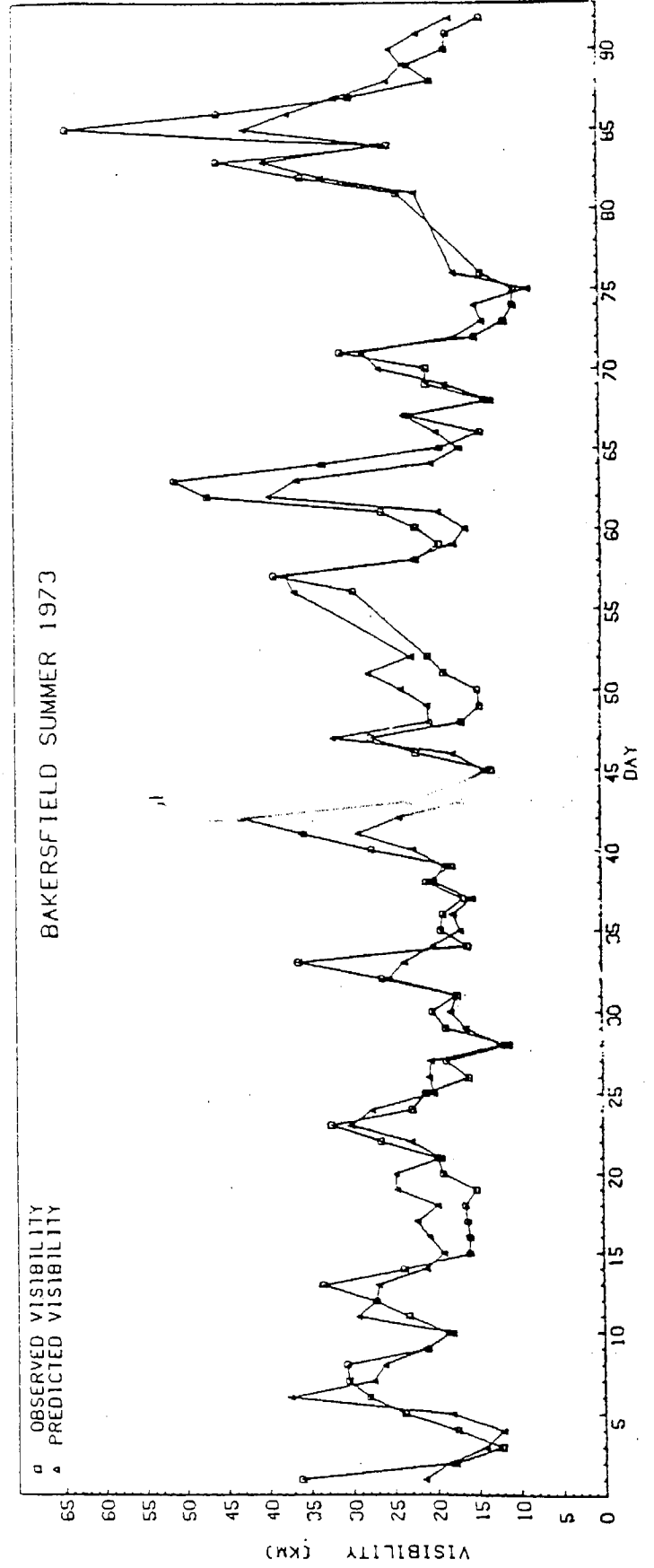
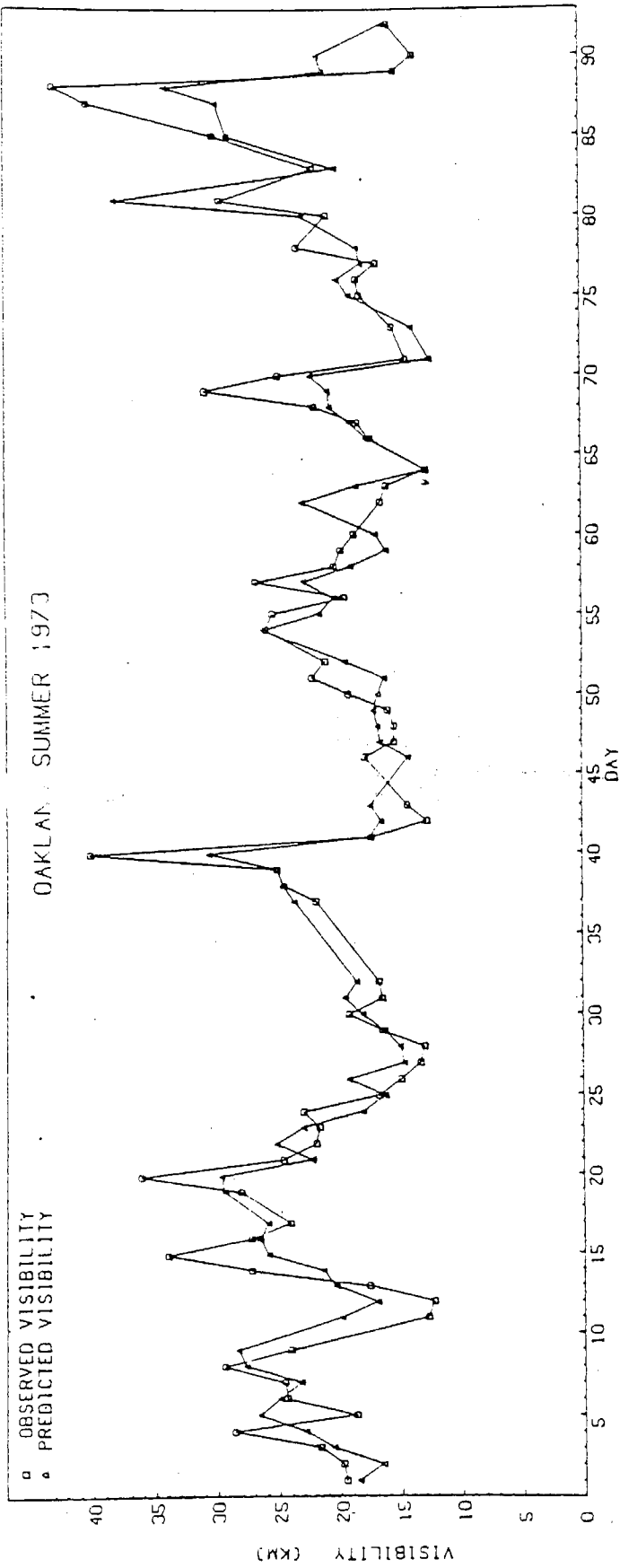
During winter months, NO_2 is the dominant visibility degrading species at Los Alamitos.

A.3.2 Visibility Relationships in the San Francisco Bay Area

The fit to visibility at Oakland, a multiple R^2 of 0.63, is shown in Figure A.8. This is the lowest R^2 of any of the sites. The parameters associated with degrading visibility are sulfur-2, +0.37, sulfur-3, +0.37, hydrocarbons, +0.42, and fine sodium, +0.20. The correlations with sulfur, and especially sulfur-2, are all the more remarkable due to the low sulfur levels at Oakland (Table 4.1). The seasonal size profile for sulfur is shown in Figure A.9, confirming the behavior also shown in Figure A.3 and Table A.8.

A.3.3 Visibility Relationships in the Central Valley

The fit to visibility at Bakersfield is shown in Figure A.8, with a corresponding multiple R^2 of 0.64. Again, about 2/3 of the variance is explained by the five significant parameters. The negative correlation to lead appears to be due to the location of the sampling site directly south of Bakersfield, yielding a correlation with generally clean and vigorous north winds. The highest values are for oxidant (+0.50) and sulfur-2 (+0.50), making sulfur-2 the only parameter significant at all sites. The summer level of sulfur-2 at Bakersfield is also very low compared to Los Angeles area sites, yet it still remains a dominant factor. Again, photochemical factors appear important at Bakersfield, and the hygroscopicity of the sulfate aerosols is similar to that of the Los Angeles area.



Sacramento was also examined for the same period, July through September 1973; it showed significant beta coefficients for sulfur-2 and fine potassium. Thus, a consistent picture emerges of a photochemically derived sulfate aerosol that maintains a smaller summer size profile due to the low humidity conditions present, yet still manages to be a major factor in visibility reduction.

The role of soil particles in visibility reduction is a potentially important one in the Central Valley, since soils contribute a great deal of mass to the aerosol. Strong soil signatures include, in order of mass, silicon, calcium, aluminum, iron, potassium, titanium, and manganese. These ratios are consistent in the coarse Stage 1 and Stage 2 fractions, but they have no significant correlation to visibility despite large mass values, (Tables A.1 to A.6). The major soil elements also appear in the fine Stage 3 size range, but the ratios are now very different. Silicon and potassium share most of the mass, while aluminum, calcium, and iron are sharply depressed in quantity. Studies have been made at Davis on the fine, resuspendable soils, but they do not show such a fine soil component in anything like the ambient air levels. Since the original work of Barone et al. (1978), we have identified the fine potassium as a major tracer of agricultural burning, (Barone, 1980 thesis). Usually, a strong fine silicon component is also present along with massive amounts of carbon, typically 20x the potassium mass. For this reason, agricultural burning must be considered as approximately equivalent in effect to intermediate size sulfate particles in visibility degradation at both Sacramento and Bakersfield, while soils are not implicated in any major sense at either site.

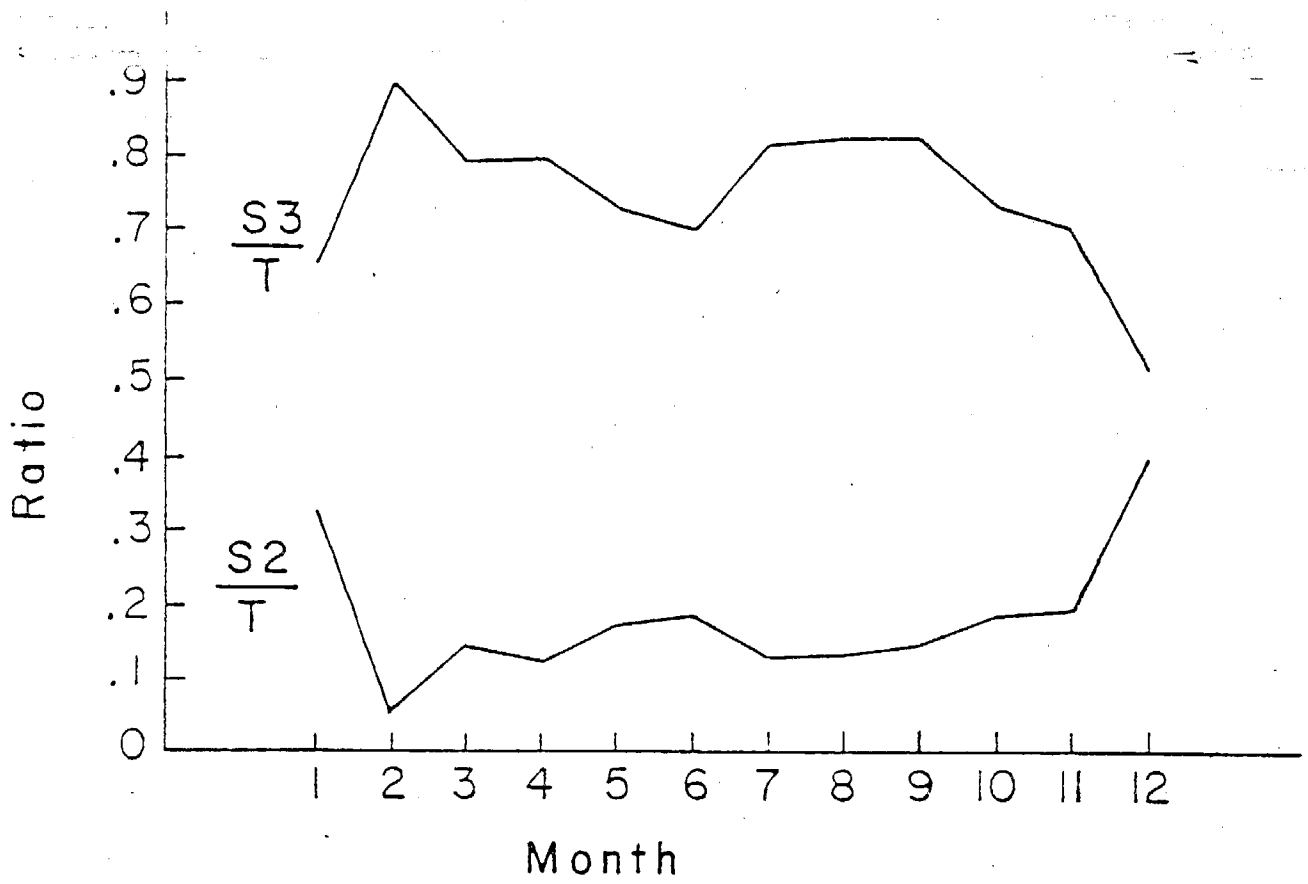
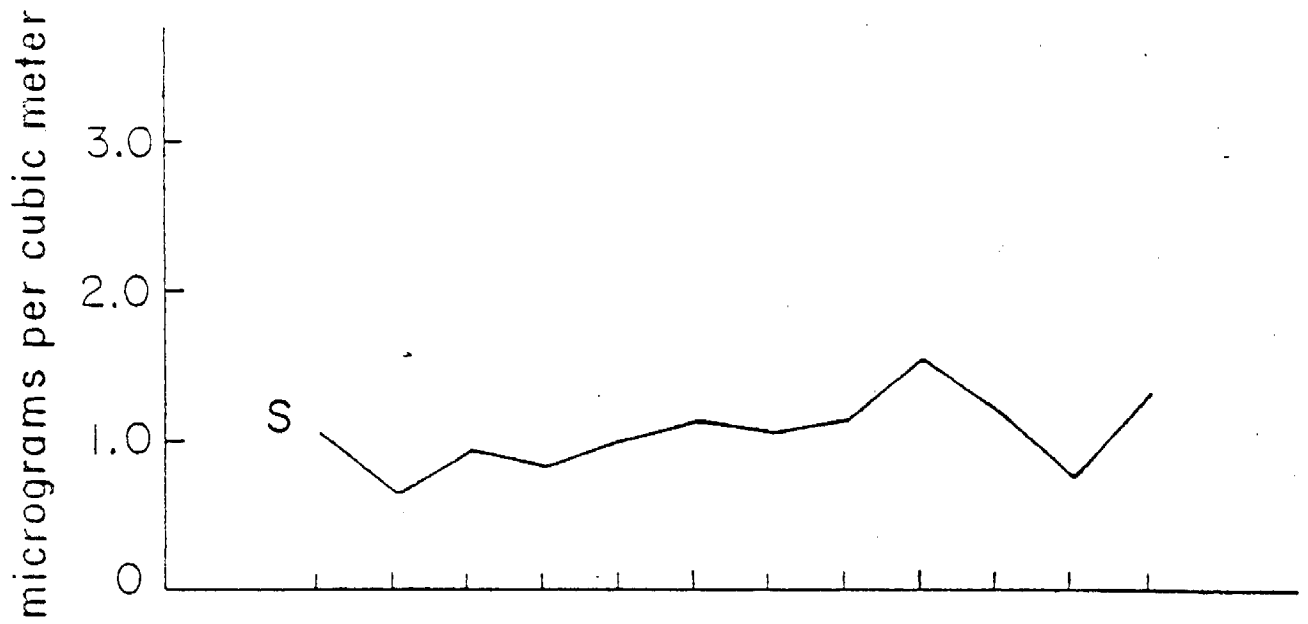


Figure A.9 Seasonal dependence of sulfur aerosol data at Oakland.

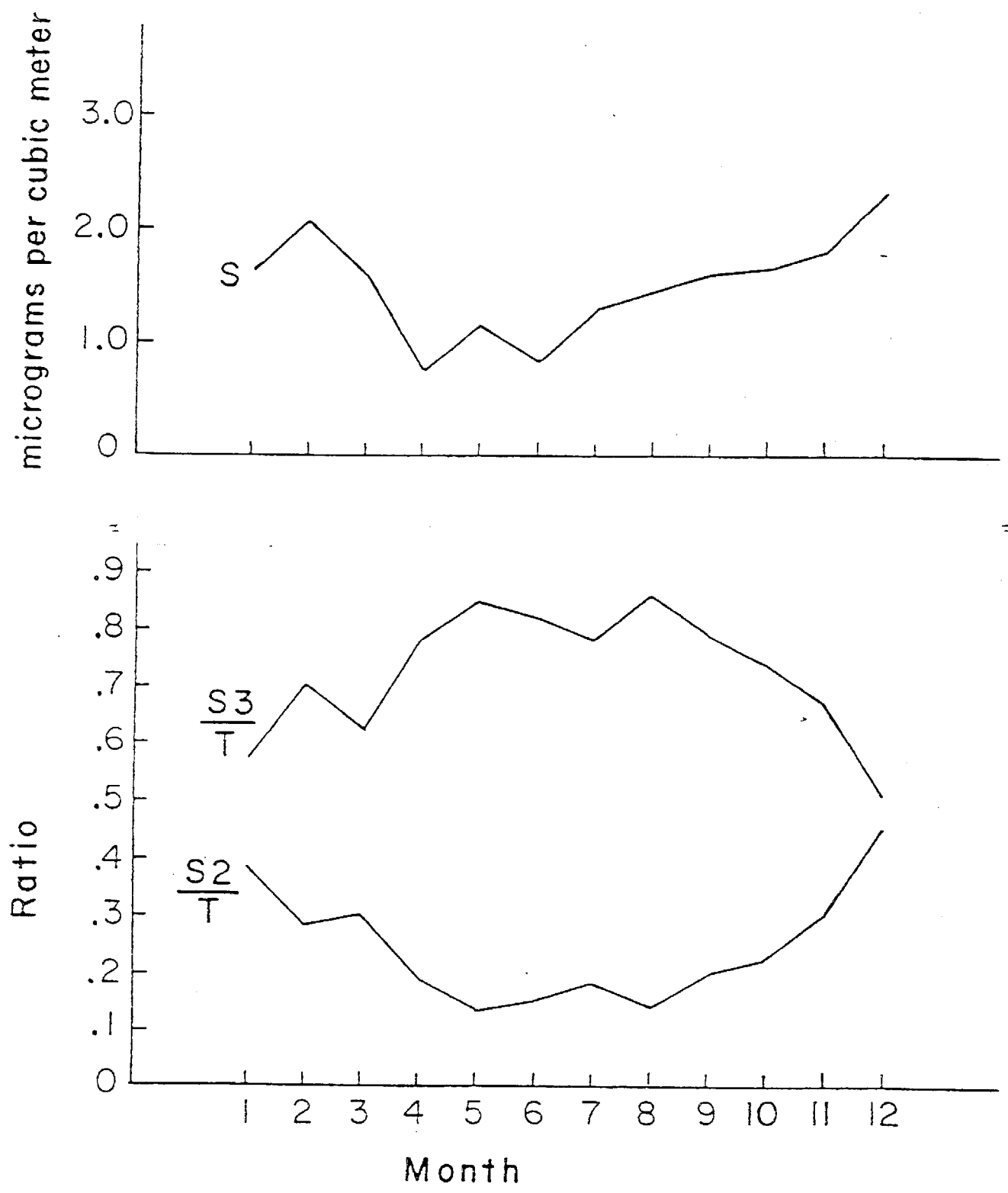


Figure A.10 Seasonal dependence of the sulfur aerosol data at Bakersfield.

A.4 REFERENCES FOR APPENDIX A

Barone, J.B., T.A. Cahill, R.A. Eldred, R.G. Flocchini, D.J. Shadoan, and T.M. Dietz, "A Multivariate Statistical Analysis of Visibility Degradation at Four California Cities," Atmospheric Environment, 12, pp.2213-2221, 1978.

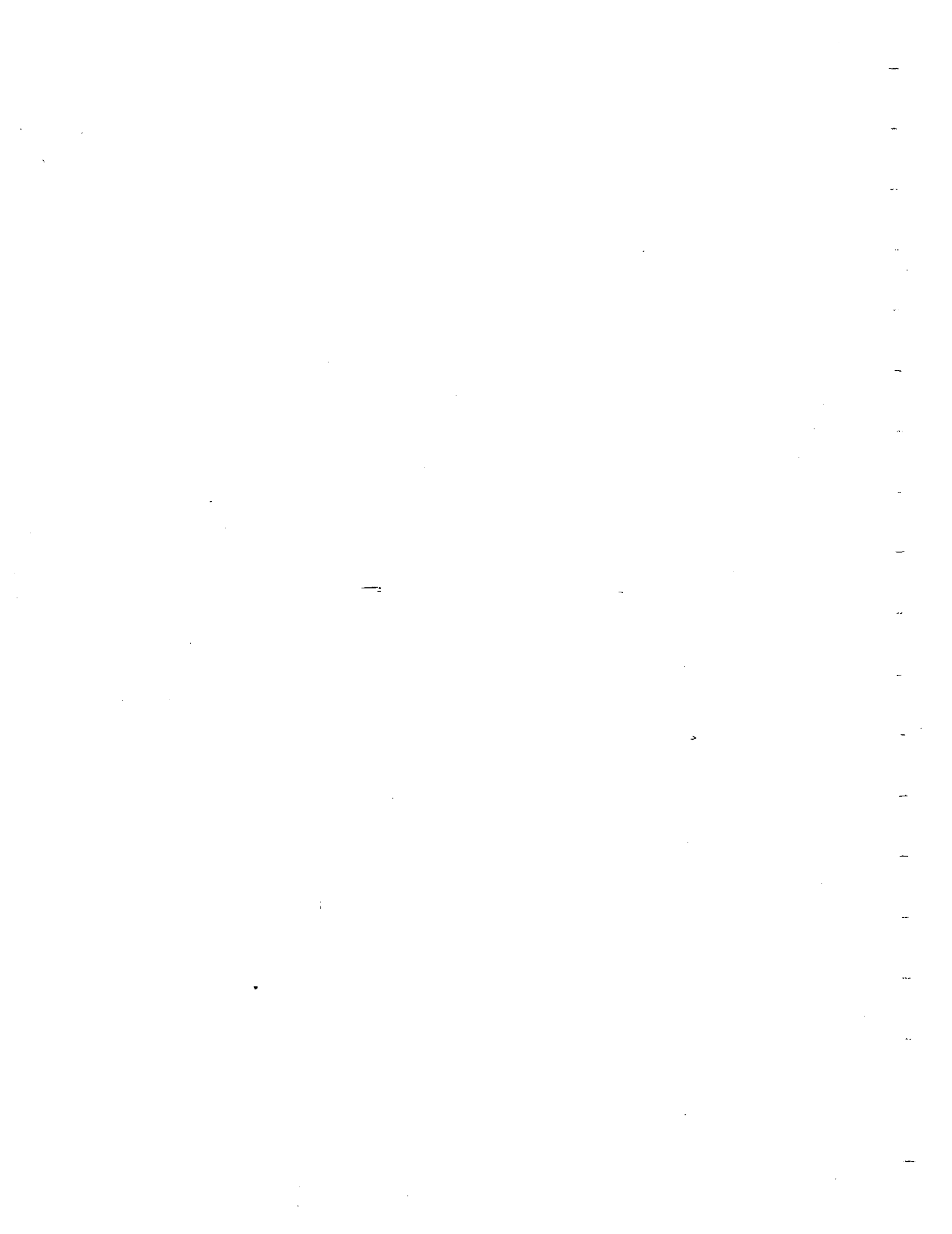
Cahill, T.A., L.L. Ashbaugh, J.B. Barone, P.J. Feeney, "Spatial Distribution of Primary Automotive Pollutants at Lake Tahoe," Proceedings of Conference on Sierra Nevada Meteorology, June 19-21, pp. 29-33, 1978

Cahill, T.A., J. Barone, R.A. Eldred, R.G. Flocchini, D.J. Shadoan, and T.M. Dietz, "Influence of Sulfur Size Distribution on Optical Extinction," Environmental and Climatic Impact of Coal Utilization, J.J. Singh, A. Deepak, Editors, Academic Press, pp. 213-224, 1980.

Flocchini, Robert G., T.A. Cahill, D.J. Shadoan, S.J. Lange, R.A. Eldred, P.J. Feeney, G.W. Wolfe, D.C. Simmeroth, and J.K. Suder, "Monitoring California's Aerosols by Size and Elemental Composition," Environmental Science and Technology, 10, pp. 76-82, 1976.

Flocchini, Robert G., T.A. Cahill, R.A. Eldred, L.L. Ashbaugh, J.B. Barone, "Sulfur Size Distribution by Season and Site in California," Proceedings of the 71st Annual Meeting of the Air Pollution Control Association, June 25-30, 78-39.6, pp. 1-13, 1978.

Flocchini, Robert G., T.A. Cahill, L.L. Ashbaugh, R.A. Eldred, and Marc Pitchford, "Seasonal Behavior of Particulate Matter at Three Rural Utah Sites," Atmospheric Environment, 15, pp. 315-320, 1981.



APPENDIX B

VISIBILITY/AEROSOL REGRESSION STUDIES FOR THE DATA SETS
EXCLUDING DAYS WITH PRECIPITATION OR SEVERE FOG

Tables B.2 through B.7 correspond to Tables 3.2 through 3.7 in Chapter 3.

TABLE B.2 INTERCORRELATIONS AMONG THE INDEPENDENT VARIABLES.
DATA: EXCLUDING DAYS WITH PRECIPITATION OR SEVERE FOG.

	SULFATE versus NITRATE	SULFATE versus OTHERTSP	SULFATE versus RH	NITRATE versus OTHERTSP	NITRATE versus RH	OTHERTSP versus RH	SULFATE/(1-RH) versus NITRATE/(1-RH)	SULFATE/(1-RH) versus OTHERTSP/(1-RH)	NITRATE/(1-RH) versus OTHERTSP/(1-RH)
SAN DIEGO AREA									
San Diego (NASN)	.02*	.14	.43	.24	-.14	-.46	.07*	.55	.21
San Diego (ARB)	.39	.25	.42	.40	.04*	-.41	.51	.56	.45
El Cajon	.30	.05*	.33	.15*	.00*	-.47	.53	.39	.38
LOS ANGELES AREA (Coastal)									
Long Beach	-.15	.25	.30	.33	-.10*	-.35	.07*	.63	.38
Costa Mesa	.25	-.02*	.37	.58	.03*	-.55	.45	.39	.78
Lennox	.07*	-.24	.53	.11*	.04*	-.41	.33	.44	.33
Downtown L.A.	-.03*	.11*	.45	.20*	-.16	-.28	.13*	.49	.21
Santa Barbara	.36	-.04*	.46	.30	.20	-.41	.72	.67	.86
LOS ANGELES AREA (Inland)									
Burbank	-.03*	.20	.33	.45	-.13*	-.20	.08*	.41	.55
La Habra	.49	.11*	.41	.47	.16	-.41	.73	.72	.81
Ontario	.23	.54	.04*	.37	-.24	-.25	.30	.69	.28
San Bernardino	.50	.69	.26	.54	.12*	-.05*	.55	.79	.60
SOUTHEAST DESERT AREA									
Palm Springs	.61	.32	.05*	.28	-.11*	-.05*	.74	.59	.66
Lancaster	.47	.16	-.05*	-.04*	-.15	-.11*	.60	.21	-.02*
Victorville	.56	.13	.03*	.07*	-.12*	-.26	.62	.19	.22
El Centro	.44	.52	-.11*	.17	.17	.02*	.86	.70	.55
SOUTHWEST AREA									
Salinas	.60	.39	.02*	.30	-.04*	-.64	.72	.67	.49
Paso Robles	.44	.31	.08*	.49	.28	-.22	.78	.72	.62
CENTRAL VALLEY AREA									
Bakersfield	.63	.09*	.55	.32	.36	-.33	.80	.81	.82
Fresno	.32	.15*	.12*	.31	.19	-.19	.69	.79	.80
Merced	.70	.22	.25	.26	.33	-.28	.94	.44	.54
Sacramento (NASN)	.33	.20	.09*	.32	.19	-.24	.73	.67	.65
Sacramento (ARB)	.45	.16	.13*	.20	.37	-.36	.86	.77	.80
SAN FRANCISCO BAY AREA (Urban)									
Redwood City*	.65	.42	.11*	.44	-.01*	.01*	.71	.55	.50
Oakland	.33	.52	.11*	.43	-.06*	-.26	.42	.63	.46
San Jose* (AQMD)	.60	.20	.04*	.33	-.03*	-.26	.71	.46	.59
San Jose (ARB)	.25	.02*	-.07*	.49	.02*	-.12*	.38	.33	.65
SAN FRANCISCO BAY AREA (Suburban)									
Livermore*	.72	.46	-.36	.47	-.16*	-.29	.67	.40	.61
Concord*	.71	.49	.05*	.57	-.01*	-.23*	.76	.71	.76
Napa*	.56	.40	-.10*	.39	.56	-.22	.73	.76	.70
Santa Rosa*	.51	.37	-.03*	.41	.29	-.12*	.77	.64	.75
NORTHERN COAST AREA									
Humboldt	.21	.43	.30	.16*	-.05*	.07	.32	.84	.23
NORTHERN INLAND AREA									
Red Bluff	.41	.49	.06*	.34	.45	-.20	.76	.51	.55
Yreka	.54	.47	.46	.34	.33	.24	.68	.68	.61
Average:	.39	.26	.18	.33	.05	-.24	.58	.59	.55

* Cellulose filter data.

* Not statistically significant at a 95% confidence level.

Note that, in this table, OTHERTSP is defined as TSP - SULFATE - NITRATE.

Note that the intercorrelations between VEHICLE or ORG and the other independent variables are also on the order of 0.1 to 0.7.

TABLE B.3 AVERAGE VALUES FOR STUDY VARIABLES.
DATA: EXCLUDING DAYS WITH PRECIPITATION OR SEVERE FOG.

	B versus RH	B versus SULFATE	B versus NITRATE	B versus OTHER TSP	B versus VEHICLE	B versus ORG	B versus SULFATE/(1-RH)	B versus NITRATE/(1-RH)	B versus OTHER TSP/(1-RH)
SAN DIEGO AREA									
San Diego (NASN)	.43	.85	-.01*	.07*			.90	.14	.53
San Diego (ARB)	.48	.78	.04*	.11*	-.00*		.81	.61	.47
El Cajon	.54	.70	.13*	-.27*	-.31	-.29	.88	.45	.19
LOS ANGELES AREA (Coastal)									
Long Beach	.38	.66	-.03*	.34			.81	.14	.77
Costa Mesa	.46	.83	.33	.03*	-.12*		.88	.57	.48
Lennox	.54	.76	.10*	-.03*	-.15		.83	.37	.57
Downtown L.A.	.42	.72	-.14	.19	-.02*		.71	-.02*	.51
Santa Barbara	.61	.73	.33	-.12*	-.14*	.08*	.83	.60	.56
LOS ANGELES AREA (Inland)									
Burbank	.48	.65	-.14*	.15*			.69	-.07*	.45
La Habra	.39	.83	.67	.19	.16		.64	.61	.48
Ontario	.45	.52	-.04*	.32			.80	.20	.70
San Bernardino	.54	.76	.44	.53			.85	.61	.80
SOUTHEAST DESERT AREA									
Palm Springs	.29	.52	.28	.54			.57	.32	.53
Lancaster	.36	.36	.38*	.41	-.14*		.55	.22	.59
Victorville	.37	.09*	.09*	.01*	-.07*		.25	.56	.43
El Centro	.42	.35	.45	.24	.08*	.14*	.78	.68	.65
CENTRAL COAST AREA									
Salinas	.43	.40	.33	-.09*	.05*	.11*	.63	.55	.39
Paso Robles	.38	.80	.66	.24	.40	.49	.80	.90	.80
CENTRAL VALLEY AREA									
Bakersfield	.51	.64	.35	.09*	.06*	.18	.89	.86	.78
Fresno	.59	.31	.33	.05*			.85	.92	.81
Merced	.48	.40	.40	.06*	.27		.61	.61	.55
Sacramento (NASN)	.54	.30	.38	.07*			.73	.73	.74
Sacramento (ARB)	.47	.36	.70	.16	.40		.77	.25	.75
SAN FRANCISCO BAY AREA (Urban)									
Redwood City*	.30	.53	.49	.40	.38	.52	.56	.54	.49
Oakland	.31	.62	.49	.48			.67	.59	.67
San Jose* (AQMD)	.31	.61	.59	.29	.14	.46	.70	.67	.51
San Jose (ARB)	.44	.16	.56	.50	.55		.35	.74	.76
SAN FRANCISCO BAY AREA (Suburban)									
Livermore*	.14*	.56	.47	.06*	.12*	.13*	.63	.43	.08*
Concord*	.38	.64	.52	.22*	.04*	.48	.75	.77	.63
Napa*	.41	.32	.44	.05*	-.00*	.35	.65	.81	.57
Santa Rosa*	.38	.26	.64	.08*	.16*	.35	.73	.91	.61
NORTHERN COAST AREA									
Humboldt	.43	.57	-.06*	.44			.87	.15*	.80
NORTHERN INLAND AREA									
Red Bluff	.54	.25	.75	.18*	.32	.49	.65	.84	.60
Yreka	.54	.27	.15*	.18*	.23	.34	.56	.28	.25
Average:	.44	.52	.32	.19	.10	.27	.71	.53	.57

* Cellulose filter data.

• Not statistically significant at a 95% confidence level.

Note that, in this table, OTHER TSP is defined as TSP - SULFATE - NITRATE.

TABLE B.4 CORRELATION BETWEEN EXTINCTION AND THE INDEPENDENT VARIABLES.
 DATA: EXCLUDING DAYS WITH PRECIPITATION OR SEVERE FOG.

DATA POINTS	AVERAGE VALUE OF VARIABLES						
	$10^{-4}m^{-1}$	RH	SULFATE ($\mu g/m^3$)	NITRATE ($\mu g/m^3$)	OTHER TSP ($\mu g/m^3$)	VEHICLE ($\mu g/m^3$)	ORG. ($\mu g/m^3$)
SAN DIEGO AREA							
San Diego (NASN)	222	2.21	.61	10.85	6.97	56.51	
San Diego (ARB)	195	1.96	.63	10.76	9.98	56.21	14.77
Ei Cajon	157	1.44	.54	9.04	9.75	66.87	19.81 7.43
LOS ANGELES AREA (Coastal)							
Long Beach	234	2.99	.57	15.90	9.65	34.75	
Costa Mesa	163	2.97	.63	12.98	13.96	50.73	16.00
Lennox	299	3.05	.67	18.07	9.98	89.84	29.03
Downtown L.A.	224	3.73	.57	18.81	13.85	91.37	26.36
Santa Barbara	157	2.33	.68	9.10	7.85	54.77	14.65 6.19
LOS ANGELES AREA (Inland)							
Burbank	177	2.85	.51	14.90	9.95	108.52	
La Habra	219	3.22	.67	14.25	21.28	81.76	18.64
Ontario	112	4.10	.48	13.34	12.74	107.92	
San Bernardino	193	3.12	.46	15.73	18.43	99.81	
SOUTHEAST DESERT AREA							
Palm Springs	230	0.86	.35	5.93	10.42	48.09	0.00
Lancaster	191	0.80	.36	5.30	5.64	93.99	6.33
Victorville	257	0.79	.33	6.65	9.50	73.89	5.35
		0.85	.39	5.96	5.38	112.98	5.78 4.29
CENTRAL COAST AREA							
Salinas	162	1.50	.67	5.20	6.28	45.67	5.05 2.51
Paso Robles	158	1.46	.55	7.56	6.96	69.28	7.07 5.07
CENTRAL VALLEY AREA							
Bakersfield	192	4.28	.50	15.16	21.69	126.40	20.34 9.43
Fresno	145	2.39	.52	6.56	11.21	111.76	
Merced	158	2.83	.49	6.51	15.60	81.43	8.12
Sacramento (NASN)	206	2.16	.54	5.93	6.26	60.66	
Sacramento (ARB)	190	2.47	.54	5.04	8.55	66.93	8.56
SAN FRANCISCO BAY AREA (Urban)							
Redwood City*	241	1.66	.67	3.14	4.36	45.53	6.05 30.00
Oakland	226	1.74	.71	8.55	5.17	63.11	
San Jose* (AQMD)	230	1.63	.59	3.35	6.42	65.54	10.55 42.11
San Jose (ARB)	195	2.01	.59	4.58	8.42	61.66	13.63
SAN FRANCISCO BAY AREA (Suburban)							
Livermore*	60	.95	.54	2.83	5.30	71.55	4.75 36.35
Concord*	65	.03	.55	3.69	5.17	38.60	3.77 27.64
Napa*	149	.44	.50	3.32	5.05	55.32	5.20 35.75
Santa Rosa*	102	.65	.62	2.64	3.36	37.29	3.64 25.84
NORTHERN COAST AREA							
Humboldt	97	10	.77	4.47	0.82	43.40	
NORTHERN INLAND AREA							
Red Bluff	121	.65	.42	3.47	5.36	61.26	3.91 4.98
Yreka	76	.53	.49	3.89	1.55	46.62	2.64 3.93

* Cellulose filter data.
 Note that, in this table, O₃

is defined as TSP - SULFATE - NITRATE.

TABLE B.5 REGRESSION COEFFICIENTS FOR THE LINEAR RH MODEL: EQUATION: (3-5).
DATA: EXCLUDING DAYS WITH PRECIPITATION OR SEVERE FOG.

	MULTIPLE CORRELATION COEFFICIENTS	b ₁ SULFATE	b ₂ NITRATE	b ₃ OTHER TSP	b ₄ RH
SAN DIEGO AREA					
San Diego (NASN)	.85	.233	-.007*	.0000*	1.02
San Diego (ARB)	.81	.120	.030	-.0020*	1.59
El Cajon	.79	.107	-.006*	-.0062	1.65
LOS ANGELES AREA (Coastal)					
Long Beach	.75	.155	-.031*	.3186	9.30
Costa Mesa	.86	.245	.010*	.0189	6.54
Lennox	.81	.140	.012*	.0149	4.36
Downtown L.A.	.76	.125	-.029	.0116	2.55
Santa Barbara	.80	.254	.006*	.0046*	6.24
LOS ANGELES AREA (Inland)					
Burbank	.73	.148	-.091	.0116	7.33
La Habra	.89	.196	.077	-.0017*	1.34*
Ontario	.71	.175	-.045*	.0170	10.42
San Bernardino	.85	.115	.010*	.0086	6.74
SOUTHEAST DESERT AREA					
Palm Springs	.71	.040	.003*	.0062	.743
Lancaster	.67	.050	.002*	.0027	1.32
Victorville	.41	-.008*	.021	.0025	2.46
El Centro	.62	.083	.052	.0008*	1.35
CENTRAL COAST AREA					
Salinas	.70	.100	.033	.0025*	4.22
Paso Robles	.78	.090	.124	.0041*	4.24
CENTRAL VALLEY AREA					
Bakersfield	.67	.591	-.028*	-.0117*	10.51
Fresno	.65	.117	.057*	.0027	9.25
Merced	.57	.268	.027*	.0104*	14.66
Sacramento (NASN)	.64	.141	.121	.0077*	9.10
Sacramento (ARB)	.75	.108*	.273	.0172	8.51
SAN FRANCISCO BAY AREA (Urban)					
Redwood City*	.65	.097	.054	.0071	2.11
Oakland	.77	.077	.077	.0088	3.63
San Jose* (AQMD)	.76	.166	.083	.0094	3.71
San Jose (ARB)	.78	.055	.083	.0291	7.41
SAN FRANCISCO BAY AREA (Suburban)					
Livermore*	.70	.107	.011*	-.0022	.781
Concord*	.74	.098	.028*	-.0022*	1.45
Napa*	.61	.193	.184	-.0078*	5.84
Santa Rosa*	.69	-.029*	.524	-.0335	3.09
NORTHERN COAST AREA					
Humboldt	.70	.325	-1.260	.0513	14.66
NORTHERN INLAND AREA					
Red Bluff	.78	-.024*	.093	.0010*	1.27
Yreka	.55	-.007*	.009*	.0002*	1.10

* Cellulose filter data.

• Not statistically significant at a 95% confidence level.

Note that, in this table, OTHER TSP is defined as TSP - SULFATE - NITRATE.

TABLE B.6 REGRESSION COEFFICIENTS FOR THE NONLINEAR RH MODEL: EQUATION (3-6).
 DATA: EXCLUDING DAYS WITH PRECIPITATION OR SEVERE FOG.

		b ₁	b ₂	b ₃
	MULTIPLE CORRELATION COEFFICIENTS	SULFATE (1-RH)	NITRATE (1-RH)	OTHERTSP (1-RH)
SAN DIEGO AREA				
San Diego (NASN)	.90	.053	.011	.0010*
San Diego (ARB)	.84	.030	.015	-.0006*
El Cajon	.81	.043	.005*	-.0025
LOS ANGELES AREA (Coastal)				
Long Beach	.88	.046	-.014	.0127
Costa Mesa	.90	.059	.017	.0007*
Lennox	.88	.025	.003	.0035
Downtown L.A.	.74	.028	-.012	.0047
Santa Barbara	.88	.058	-.003*	-.0003*
LOS ANGELES AREA (Inland)				
Burbank	.72	.050	-.028	.0055
La Habra	.68	.021	.016	-.0035
Ontario	.83	.092	-.016*	.0070
San Bernardino	.88	.047	.014	.0062
SOUTHEAST DESERT AREA				
Palm Springs	.67	.030	-.009	.0027
Lancaster	.74	.036	.001*	.0017
Victorville	.67	-.024	.046	.0041
El Centro	.79	.054	.002*	.0011
CENTRAL COAST AREA				
Salinas	.65	.044	.008	-.0010*
Paso Robles	.91	.023	.036	.0020
CENTRAL VALLEY AREA				
Bakersfield	.92	.058	.036	-.0014*
Fresno	.92	.049	.035	.0009*
Merced	.69	.077	.014*	.0145
Sacramento (NASN)	.85	.050	.020	.0074
Sacramento (ARB)	.86	.019*	.051	.0045
SAN FRANCISCO BAY AREA (Urban)				
Redwood City*	.63	.022	.014	.0021
Oakland	.79	.015	.019	.0024
San Jose* (AQMD)	.75	.054	.021	.0019
San Jose (ARB)	.83	.006*	.034	.0089
SAN FRANCISCO BAY AREA (Suburban)				
Livermore*	.67	.047	.006*	-.0009
Concord*	.83	.020	.018	-.0004*
Napa*	.82	.022	.064	-.0013*
Santa Rosa*	.92	.019*	.071	-.0048
NORTHERN COAST AREA				
Humboldt	.89	.085	-.124	.0026
NORTHERN INLAND AREA				
Red Bluff	.85	-.002*	.028	.0025
Yreka	.60	.032	-.008*	-.0003*

* Cellulose filter data.

* Not statistically significant at a 95% confidence level.

Note that, in this table, OTHERTSP is defined as TSP - SULFATE - NITRATE.

TABLE B.7 REGIONAL REGRESSION COEFFICIENTS FOR THE NONLINEAR RH MODEL:

$$B = a + b_1 \frac{\text{SULFATE}}{(1-\text{RH})} + b_2 \frac{\text{NITRATE}}{(1-\text{RH})} + b_3 \frac{\text{OTHERTSP}}{(1-\text{RH})}$$

DATA: Excluding days with precipitation or severe fog.

	NUMBER OF DATA POINTS	MULTIPLE CORRELATION COEFFICIENT	b ₁ SULFATE (1-RH)	b ₂ NITRATE (1-RH)	b ₃ OTHERTSP (1-RH)
SAN DIEGO AREA	574	.86	.046	.003	-.0004
LOS ANGELES AREA (Coastal)	1082	.76	.031	.001	.0041
LOS ANGELES AREA (Inland)	701	.67	.038	-.011	.0065
SOUTHEAST DESERT AREA	831	.57	.014	.010	.0019
CENTRAL COAST AREA	320	.80	.029	.018	.0033
CENTRAL VALLEY AREA	891	.86	.047	.036	.0026
SAN FRANCISCO BAY AREA (Glass Filters)	421	.75	-.001	.039	.0042
SAN FRANCISCO BAY AREA (Cellulose Filters)	847	.79	.021	.051	-.0001
NORTHERN INLAND AREA	197	.81	.018	.027	-.0001
STATEWIDE	5114	.78	.034	.021	.0041

• Not statistically significant at a 95% confidence level.

